MARTIN MARIETTA ENERGY SYSTEMS LIBRARIES
3 4456 0360713 0

CENTRAL RESEARCH LIBRARY
DOCUMENT COLLECTION

ORNL-1745
Chemistry

cy. 1

THE CRYSTAL STRUCTURES OF OXALIC ACID DIHYDRATE AND ALPHA IODIC ACID AS DETERMINED BY NEUTRON DIFFRACTION

B. S. Garrett

OAK RIDGE NATIONAL LABORATORY
CENTRAL RESEARCH LIBRARY
DOCUMENT COLLECTION
LIBRARY LOAN COPY
DO NOT TRANSFER TO ANOTHER PERSON
If you wish someone else to see this document, send in name with document and the library will arrange a loan.
UCN-7969
(3 3-67)

OAK RIDGE NATIONAL LABORATORY
operated by
UNION CARBIDE CORPORATION
for the
U.S. ATOMIC ENERGY COMMISSION

ORNL 1745

Copy No _____

Contract No W-7405-eng-26

THE CRYSTAL STRUCTURES OF OXALIC ACID DIHYDRATE AND ALPHA IODIC ACID AS DETERMINED BY NEUTRON DIFFRACTION

B S Garrett

DATE ISSUED

JUL 29 1954

OAK RIDGE NATIONAL LABORATORY
Operated by
CARBIDE AND CARBON CHEMICALS COMPANY
A Division of Union Carbide and Carbon Corporation
Post Office Box P
Oak Ridge, Tennessee

ABSTRACT

The crystal structures of oxalic acid dihydrate and alpha iodic acid were determined by neutron diffraction Several modern techniques were utilized in analyzing the data, including Fourier series, structure factor inequalities, statistical intensity distributions, least squares, and Fourier peak shape analysis The positions of all the atoms, including hydrogen, were determined

The structure of oxalic acid dihydrate was found to be consistent in its general features with that deduced from x-ray diffraction data The oxalic acid molecule, including the hydrogen atoms is planar The carbon - carbon bond length is that of a single bond, the carbon - oxygen bonds are nearly equal and are of lengths intermediate between those of single and double bonds The oxygen - hydrogen distance in the acid molecule was found to be 0 10 longer than in gaseous water The oxygen - hydrogen distances, the oxygen bond angles and O - H stretching frequencies of the water molecule in the crystal are very nearly identical with those of gaseous water Strong evidence for libration of the carboxyl groups about the carbon - carbon bond was found in the analysis of the thermal motion of the atoms The acid molecule is bound to the water oxygen atom through the carboxyl hydroxyl group This is a short and apparently strong hydrogen bond, it is nearly linear and is only 2 52 A in length The oxalic acid dihydrate complexes are bound together in a three dimensional network of weaker hydrogen

bonds between water hydrogen atoms and carbonyl oxygen atoms of neighboring acid molecules Two helical chains of hydrogen bonds parallel to each diagonal of the a - c plane appear to be the main elements stabilizing the crystal.

Alpha iodic acid can be described as being composed of two chains of pentagonal rings, tilted at a mutual angle of $64^{\circ}25'$, which are parallel to the crystallographic b axis. The binding between iodic acid molecules within a chain is through a relatively short O - H - O bond and a very short intermolecular iodine - oxygen approach. Binding between chains appears to result from close approaches to iodine by oxygen atoms which project above and below the chains. The earlier description of the IO_3 group in the molecule as an irregular pyramid was confirmed An attempt to correlate structural data with results of nuclear quadrupole spectroscopy led to consistent but not unambiguous assignment of hybridized bonding orbitals to iodine.

3 4456 0360713 0

TABLE OF CONTENTS

Part One

	Page
General Introduction	3
Introduction	8
Experimental Procedure .	13
A Crystallographic Description of Oxalic Acid Dihydrate .	13
B Apparatus and Equipment	14
1 The Neutron Spectrometer .	14
2 Instrumentation . .	17
3 Automatic Programmer	19
C Procedure .	22
1 Preparation of Specimens	22
2 Standardization and Calibration .	23
a Relationship of Experimental Intensities to Structure Factors	23
b Methods of Estimating Absorption Corrections	25
c. Secondary Extinction . .	26
3 Experimental Results . .	28
a Determination of the Absorption Coefficient	28
b Measurement of Powder Reflections	29
c. Comparison of Single Crystal and Powder Measurements . .	30

Page

d (h0l) Zone . . . 32

e (0kl) Zone . . 36

Analysis of Diffraction Data 37

A The General Problem . 37

B. Methods and Procedures Used 39

C Use of the Fourier Series Method 40

D The (h0l) Zone . . . 43

E The (0kl) Zone 57

F Reliability of the Analysis 63

G. Precision of Parameters 65

H. Interatomic Distances and Bond Angles 68

I Compatibility of X-ray and Neutron Diffraction Data 71

Discussion . . 77

A General Results of Structure Determination . 77

B Comparison With Previous Structures 81

C Planarity of the Acid Molecule 84

D Dimensions of the Acid Molecule . . 87

E Dimensions of the Water Molecule 88

F. Hydrogen Bonding . . . 89

G Thermal Motion 93

Part Two

Introduction 97

Page

Procedure and Results 99

A Crystallographic Description of Alpha Iodic Acid . 99

B Procedure . 99

1 Preparation of Specimens . 99

2. Alignment of the Specimens and Preliminary Examination on the Neutron Spectrometer . 100

3 Standardization and Calibration . . 101

4 Absorption Corrections . . . 101

5 Secondary Extinction . . 101

6 (0kl) Data . 104

7. (h0l) Data . . 105

Analysis of Diffraction Data . . 107

A Methods . . . 107

B The (0kl) Zone 108

C The (h0l) Zone . 117

D Reliability of the Structure . . . 124

E Precision of Parameters, Interatomic Distances and Bond Angles . . 126

Discussion 128

A Description of the Structure 128

B. Comparison with X-ray Structure . 133

C. The Iodic Acid Molecule 136

1. General Description 136

2. Electronic Configuration of Iodine . 137

D. Hydrogen Bond Lengths 143

Bibliography 146

FIGURES

		Page
1.	Schematic Diagram of Neutron Diffraction Spectrometer	15
2	Block Diagram of Neutron Spectrometer Instrumentation	18
3	Crystal Rotator - Automatic Programmer	21
4	Modification Function Used to Introduce Additional Convergence into Oxalic Acid Dihydrate Data	48
5.	Fourier Map of the (h0l) Zone of Oxalic Acid Dihydrate	49
6	Comparison of Synthetic and Experimental Peak Shapes	52
7	Fourier Map of the (0kl) Zone of Oxalic Acid Dihydrate	59
8	Comparison of two Sets of X-ray Data as Functions of $(\sin \theta/\lambda)^2$	74
9	Comparison of Two Sets of X-ray Data as Functions of Intensity	75
10.	Dimensions of the Oxalic Acid Dihydrate Complex	85
11.	Illustrative Drawing of the (h0l) Projection of Oxalic Acid Dihydrate	90
12	Illustrative Drawing of the (0kl) Projection of Oxalic Acid Dihydrate	91
13	Modification Function to Introduce Additional Convergence into Alpha Iodic Acid Data	110
14	Fourier Map of the (0kl) Projection of Alpha Iodic Acid	112
15	Fourier Map of the (h0l) Projection of Alpha Iodic Acid	119

Page

16 Views of the Chain of Rings in Alpha Iodic Acid . 129

17. Illustrative Drawing of the (0kl) Projection of Alpha Iodic Acid 130

18 Illustrative Drawing of the (h0l) Projection of Alpha Iodic Acid . . 132

PLATE

1. Photograph of the Neutron Spectrometer . 16

TABLES

		Page
I	Powder Structure Factors of Oxalic Acid Dihydrate	30
II	Dimensions of Small (h0l) Specimen of Oxalic Acid Dihydrate	30
III.	Comparison of Powder and Single Crystal Results	32
IV	Dimensions of Large (h0l) Specimen of Oxalic Acid Dihydrate	32
V	Preliminary Comparison of Structure Factors from Large and Small (h0l) Specimens of Oxalic Acid Dihydrate	33
VI.	Normalization of Structure Factors from Large (h0l) Specimen to Those from Small (h0l) Specimen	34
VII	Dimensions of (0kl) Specimens of Oxalic Acid Dihydrate	36
VIII	Comparison of Structure Factors From Large and Small (0kl) Specimens of Oxalic Acid Dihydrate	37
IX	Preliminary Parameters from (h0l) Fourier Map	50
X.	Results of Back Shift Correction; (h0l) Zone of Oxalic Acid Dihydrate	53
XI.	Results of Least Squares Treatment of H_1 and H_2 Parameters	54
XII	Comparison of Calculated and Observed Structure Factors for the (h0l) Zone of Oxalic Acid Dihydrate	59
XIII	Final y Parameters and Temperature Factors for the (0kl) Zone of Oxalic Acid Dihydrate	61
XIV.	Comparison of Calculated and Observed Structure Factors for the (0kl) Zone of Oxalic Acid Dihydrate	62
XV.	Atomic Parameters and Estimates of Precision, Oxalic Acid Dihydrate	67
XVI	Interatomic Distances and Estimated Precisions, Oxalic Acid Dihydrate	69

		Page
XVII	Bond Angles and Estimated Precisions, Oxalic Acid Dihydrate . .	71
XVIII	Comparison of Atomic Parameters in Oxalic Acid Dihydrate as Determined by Several Investigators . .	79
XIX	Comparison of Interatomic Distances in Oxalic Acid Dihydrate as Determined by Several Investigators	80
XX	Bond Angles in Oxalic Acid Dihydrate as Calculated from X-ray Diffraction Data and from Neutron Diffraction Data .	81
XXI.	Dimensions of the (0kl) Specimens of Alpha Iodic Acid	104
XXII	Comparison of Structure Factors from Large and Small (0kl) Specimens of Alpha Iodic Acid .	105
XXIII	Dimensions of the (h0l) Specimens of Alpha Iodic Acid . .	106
XXIV	Comparison of Structure Factors from Large and Small (h0l) Specimens of Alpha Iodic Acid	106
XXV	Final y and z Parameters from (0kl) Projection of Alpha Iodic Acid .	111
XXVI	Comparison of (0kl) Structure Factors of Alpha Iodic Acid Observed Values Before and After Extinction Corrections and and Calculated Values	113
XXVII	Final x Parameters from (h0l) Projection of Alpha Iodic Acid	120
XXVIII	Comparison of (h0l) Structure Factors of Alpha Iodic Acid, Observed and Calculated Values	121
XXIX	Final Parameters of Atoms in Alpha Iodic Acid . .	126
XXX.	Interatomic Distances in Alpha Iodic Acid	127
XXXI.	Bond Angles in Alpha Iodic Acid	127
XXXII.	Comparison of Parameters of Atoms in Alpha Iodic Acid as Determined by X-ray and Neutron Diffraction	133

Page

XXXIII Comparison of Interatomic Distances in Alpha Iodic Acid as Determined by X-ray and Neutron Diffraction 135

XXXIV Comparison of Bond Angles in Alpha Iodic Acid as Determined by X-ray and Neutron Diffraction 135

XXXV O - H and O - O Distances in Hydrogen Bonds . 144

PART ONE

STRUCTURE OF OXALIC ACID DIHYDRATE

General Introduction

It was first suggested by Elsasser[1] in 1936 that neutrons could be diffracted by solids Halban and Preiswerk[2] and Mitchell and Powers[3] demonstrated in the same year that neutrons were diffracted, using radium-beryllium neutron sources However the technique of neutron diffraction as a method of structural investigation did not begin to develop until more intense neutron sources became available from nuclear reactors

The properties of a neutron which are important in its use in diffraction include its size, mass, velocity, magnetic moment, lack of charge and interactions with nuclei Because of its small size and lack of charge it is highly penetrating, and undergoes appreciable true absorption only in exceptional cases Its diffraction behavior may be described by the de Broglie equation, $\lambda = \underline{h}/mv$, where λ is a wavelength associated with a neutron whose mass is m and velocity is v, $\underline{h}$ is Planck's constant For neutrons in equilibrium with matter at temperature T, somewhat above room temperature, the kinetic energy is $1/2mv^2 = kT$, where k is Boltzmann's constant, and the associated wavelength is of the order 1 A This wavelength is in the range of interatomic distances in crystals and also approximately the same as the x-ray wavelengths ordinarily used in crystal structure determination The magnetic moment of the neutron is useful in determining the magnetic structure of crystals,[4] but will not be further discussed since this investigation was not concerned with magnetic properties of matter

A consequence of the fact that thermal neutrons have associated wavelengths of the order of interatomic distances is that constructive interference occurs when the Bragg condition, $n\lambda = 2d \sin \theta$, is fulfilled Since it is ordinarily convenient to work with essentially monochromatic beams, it is necessary to select a narrow band of wavelengths from the essentially Maxwellian distribution of wavelengths possessed by ordinary thermal neutrons This is accomplished by taking advantage of the fact that Bragg "reflection" occurs from a plane of a single crystal placed at an arbitrary angle to the axis of a beam of thermal neutrons only for narrow bands of wavelengths The intensity of reflections corresponding to high orders of n is attenuated by the low probability of high values in the Maxwell distribution of the incident neutron energies In practice large single crystals of metals such as copper or lead are most frequently used as monochromators

Because of the severe intensity loss suffered in selecting a narrow band out of a broad distribution of wavelengths, the dimensions of the slits in the collimating system must be much larger than is required for the x-ray case where only the intense radiation having the characteristic energy of the target material is used The dimensions of the slit system together with the requirement of a long, well shielded counter result in much more bulky apparatus than is needed in x-ray diffraction

Since both x-rays and neutrons are scattered coherently according to the same geometric conditions, the occurrence of diffraction maxima does not differ in a qualitative way between the two methods It is

rather in the quantitative ways in which the two types of radiation are scattered that important differences arise and make neutron diffraction a useful tool in investigations which are difficult, if not impossible, with other techniques In particular, the differences arise largely from the fact that photons are scattered by the electron cloud around each atom while neutrons are scattered by interaction with the nuclei themselves These processes obey quite different rules as to the amplitudes of scattering by various atoms as well as to the dependence of the amount of coherent scattering on scattering angle The x-ray scattering amplitudes increase smoothly and nearly linearly with atomic number, or the number of extra-nuclear electrons Hence the x-ray scattering from crystals containing both heavy and light atoms is dominated by scattering from the heavy atoms Moreover, elements of nearly equal atomic number are quite difficult to distinguish. The neutron scattering amplitudes of various elements, indeed of various isotopes of the same element, are distinguished by the lack of such large variation in magnitude with atomic size and by their apparently random variation from element to element and from isotope to isotope The magnitude and even the sign of the scattering amplitude is related more directly to the resonance energy of the compound nucleus comprised of the interacting neutron and atom than to the nuclear size[5,6] For most nuclei, the resonance energy of the compound nucleus is so high relative to the neutron energy that ordinary potential scattering, as if by an impenetrable sphere, occurs In this case the phase of the scattered beam undergoes 180° shift in

accordance with the boundary condition that the wave function of the neutron should vanish at the surface of the sphere In a few important cases, however, negative scattering amplitudes, corresponding to 0° phase shift have been noted These are usually found to be associated with known neutron scattering resonances The atomic scattering factor for x-rays falls off rapidly with increasing scattering angle for several reasons The large size of the electron cloud compared to the wavelength of the radiation permits scattered radiation to be completely coherent in only the forward direction Also, the intensity in the scattered beam depends on the degree of polarization, which is a function of scattering angle. In contrast the dimensions of the nucleus ($r = 10^{-13}$ cm) are small compared to the wavelength of thermal neutrons so that nuclei scatter neutrons isotropically There is no polarization factor for this interaction The above statements are rigorous for atoms rigidly fixed in space, but in ordinary crystal lattices the atoms are undergoing thermal vibration It has been shown by Weinstock[7] that the effect of this temperature motion on Bragg-diffracted radiation can be represented in the same way for neutrons as for x-rays For this reason, the scattering of neutrons by actual atoms does have an angular dependence of the form $f_s = f_o e^{-Bs^2}$, where f_s is the scattering amplitude at $s = \sin\theta/\lambda$, f_o is the atomic scattering amplitude, and $B = \overline{\mu^2}/8\pi^2$. The quantity $\overline{\mu^2}$ is the mean square amplitude of the displacement of the atom in the direction of the scattering vector

Neutron diffraction is thus largely a complementary technique to

x-ray diffraction There are two main classes of problems more suitable for neutron diffraction than for x-ray diffraction investigations One of these includes structures containing elements of nearly equal atomic number which happen to have appreciably different neutron scattering amplitudes One example of such a case was the investigation of superstructure in several alloys by Shull and Siegel[8] The second and more common class is the determination of light atom positions in the presence of heavy atoms The most important division of this class is the determination of hydrogen atom positions, which cannot be determined satisfactorily at present by other techniques

Both of the structures described herein fall within this second class of investigation While there were other subsidiary questions in both the oxalic acid dihydrate and iodic acid problems, the central question was the hydrogen atom locations The importance of hydrogen bonding in many fields of chemistry is well known, but until direct determinations of the hydrogen locations in a number of these bonds have been carried out, generalizations concerning the occurrence, strength and dimensions of hydrogen bonds will remain to some extent conjectural The variability of O - H - O bonds described herein is alone sufficient to attest the desirability of obtaining more quantitative structural information about hydrogen bonds

Introduction

Oxalic acid dihydrate has been the subject of several x-ray diffraction investigations, beginning with that of Zachariasen[9] in 1934 The various investigators agree on the general features of the structure as originally proposed by him The C_2O_4 group has been found to be planar and to have a center of symmetry between the carbon atoms Two such groups together with the four associated water molecules make up the unit cell, which is monoclinic with space group symmetry C_{2h}^5 - $P2_1/n$ The crystal is held together by a network of hydrogen bonds linking acid molecules to water molecules It is on the details of the structure, such as bond lengths, bond angles, and actual hydrogen arrangements, that the previous investigators have disagreed, and it is with these features that this investigation has been concerned

Zachariasen determined the dimensions of the unit cell and estimated the parameters of the carbon and oxygen atoms within the unit cell He found the C - C bond length to be 1.59 A, at that time considered to be essentially equal to that of a single bond The two C - O distances within the carboxyl group were reported as both equal to 1 25 ± 0 05 A The co-planarity of the two carboxyl groups was noted to be not immediately explicable since valence forces would not be expected greatly to restrict rotation about a C - C single bond, and from strictly electrostatic considerations, the carboxyl groups would tend to be at right angles to each other. Resonance between two equivalent structures like $\begin{bmatrix} O & & & O \\ O & C & C & O \end{bmatrix}$ was suggested to account

for the observed C - O bond angles and distances He also proposed the existence of the oxonium (OH_3^+) radical in the crystal, and suggested the name oxonium oxalate for the compound

In 1936 Robertson and Woodward[10] reinvestigated the structure using single crystal specimens in a moving film camera with Cu Kα radiation (λ = 1 54 A). The structure factors obtained from the h0l and 0kl zones were used to construct Fourier series representations of the projections of the scattering density functions This represented one of the earliest applications of this analytical technique to a complex structure Atomic coordinates were determined by locating the maxima of the peaks in the scattering density function They found the C - C distance to be probably 1 43 and not more than 1.48 A, showing some double bond character, hence some resistance to rotation In support of the reasonableness of this result they pointed to the planar nature of the molecule and to the fact that oxalic acid is quantitatively oxidized by potassium permanganate This latter observation was presumably in analogy with the oxidation of olefins They reported C - O distances of 1 24 A and 1 30 A, the shorter distance being associated with the close approach (2 52 A) of the water oxygen This carboxyl oxygen was identified as the carbonyl oxygen.

A later investigation by Brill, Hermann and Peters[11] yielded different results Using Mo Kα radiation (λ = 0 707 A), they collected the experimental data to a larger sin θ/λ limit, thus potentially increasing the resolution and the natural convergence of the Fourier series representation of the scattering density function.

They found the C - C distance to be 1 53 A, almost identically that of C - C in diamond (1 54 A) They also found two distinct carboxyl C - O distances, 1 17 A and 1 28 A respectively In this case, however, the longer distance (1 28 A) was associated with the close approach of water oxygen Accordingly, this was identified as the hydroxyl oxygen and the other (1 17 A C - O) distance as the carbonyl oxygen The planarity of the oxalate radical was again noted

In an effort to resolve these obvious discrepancies, Dunitz and Robertson[12] reconsidered the experimental data of Robertson and Woodward[10] and also of Brill, Hermann and Peters[11] After trying numerous combinations of parameters, they concluded that best agreement between calculated and observed structure factors was obtained by combining the x and z parameters of Brill et al with the y parameters of Robertson and Woodward They found several other arbitrary combinations which gave essentially equal agreement The set of parameters finally chosen corresponded to a C - C distance of 1 46 A and two essentially equal C - O distances of 1 24 A for the O involved in the close approach of water and 1 25 A for the other

While the present neutron diffraction investigation was in progress, Ahmed and Cruickshank[13] carried out a new analysis of the two apparently non-concordant sets of data of Robertson and Woodward[10] and of Brill, Hermann and Peters[11] Their objective was to show that concordant results could be obtained from the two sets of data, or, if not, to find the source of the incompatibility. Their procedure consisted of analyzing each set of h0l data separately and analyzing

each set of h0l data separately and analyzing a set of data obtained by combining the h0l data into mean values In the case of the 0kl zone, the data of Robertson and Woodward were analyzed and the results compared with those obtained by combining their data with those of Brill, Hermann and Peters This was necessary because the latter did not remeasure all of the reflections common to the two sets of observations In obtaining parameters they applied Booth's[14] method of correcting for termination of series errors This was found to be particularly important in obtaining correct parameters from the data of Robertson and Woodward because of the poorer convergence resulting from the smaller sin θ/λ limit of the observation The "equal slopes" method of Cruickshank[15] was utilized in resolving the 0kl projection of the carbonyl group Using statistical methods to estimate accuracy and compatibility, they concluded that concordant results could be obtained from the two sets of data Their final structure was generally close to that of Brill, Hermann and Peters The molecule was found to be planar and the C - C distance to be 1.529 A The C - O distances were found to be 1 285 A for the O associated with the close water approach and 1 187 A for the other carboxyl C - O bond They also redetermined the unit cell dimensions by the Straumanis technique.

Richards and Smith[16] examined the nuclear magnetic resonance spectrum of oxalic acid dihydrate and found the proton resonance absorption curve to be compatible with a structure consisting of water molecules and oxalic acid molecules. It could not be fitted with a structure consisting of oxonium ions and oxalate ions This was

consistent with the interpretation by Marignan[17] of the Raman spectra of the solid, but inconsistent with the suggestion of Zachariasen that the compound is oxonium oxalate The suggestion of Brill et al that the structure involves resonance between these two extremes and Peters that the structure involves resonance between these two extremes seems to require the carboxyl hydrogen to be centered between the water and acid oxygen atoms for electronic resonance to occur, or a disordered structure involving OH_3^+ and H_2O groups

This neutron diffraction investigation was intended to provide direct information concerning the hydrogen locations in order to answer the question of the existence of OH_3^+ and to delineate the hydrogen bond network which has been presumed to hold the crystal together Because of the apparent non-concordance of the results of early x-ray workers, it was also hoped that improvement in the precision of the overall structure determination might be achieved The recent study by Ahmed and Cruickshank[13] has in some measure obviated the necessity for this, but these new experimental determinations may be considered an essentially independent check of many of their conclusions, with in addition more extensive analysis of the thermal motion of the atoms and a suggestion concerning possible sources of error in the x-ray data themselves

Experimental Procedure

A Crystallographic Description of Oxalic Acid Dihydrate

Oxalic acid dihydrate has the chemical formula $(COOH)_2 \quad 2H_2O$ The solid is a soft, colorless crystal whose morphological characteristics have been described by Groth[18] The crystal is monoclinic with space group symmetry $C_{2h}^5 - P2_1/n$ The asymmetric unit is one half of a molecule, the molecule lying across a center of symmetry in the crystal A description of the unit cell, whose dimensions were recently redetermined by Ahmed and Cruickshank[13], is summarized below

The axial lengths are: $a_o = 6\ 12$ A, $b_o = 3\ 60$ A, $c_o = 12\ 05$ A, the monoclinic angle, $\beta = 106^o\ 16'$ There are two molecules per unit cell and the unit cell volume is 254 5 A^3 The calculated density is 1 63, compared to an observed density of 1 653

Space group absences for h00, 0k0, 00l are h, k, or l $\neq$ 2n and for h0l are h + l $\neq$ 2n. All atoms lie in general four-fold positions: $\pm$ (x, y, z), $\pm$ (1/2 + x, 1/2 - y, 1/2 + z).

B. Apparatus and Equipment

1. The Neutron Spectrometer

The design of the spectrometer used in this investigation is similar to that described by Wollan and Shull[19] The arrangement of the components is illustrated in a schematic drawing Figure 1 and by a photograph Plate I The source of neutrons is the graphite reactor of the Oak Ridge National Laboratory The flux available is approximately 3×10^{11} neutrons sec^{-1} cm^{-2} A beam of neutrons emerges from a 2 in x 2 in square hole in a 1 foot long shielding block with an angular divergence of about 1 degree The monochromating crystal, located on a turntable outside the pile face, is a single crystal of copper with a reflecting face about 2 in by 4 in cut nearly parallel to the (111) plane The reflecting face is cut at an angle to the (111) plane equal to about one half the Bragg angle, in the manner suggested by Fankuchen, in order to concentrate the diffracted beam The monochromator is heavily shielded with borated paraffin and lead bricks to reduce background radiation at the spectrometer counter By selecting the angle between the face of the monochromating crystal and the beam from the reactor the desired wave lengths can be diffracted The collimating slits fit into a channel in a plug which bolts into the front face of the monochromator shield This channel is fixed, so that it is necessary to change plugs when the wave length is changed The beam defined by these slits is 3/8 in wide by 1 1/2 in tall, with a neutron current of approximately 10^7 neutrons per minute

The spectrometer table and counter arm rotate about a vertical

UNCLASSIFIED
DWG 21992

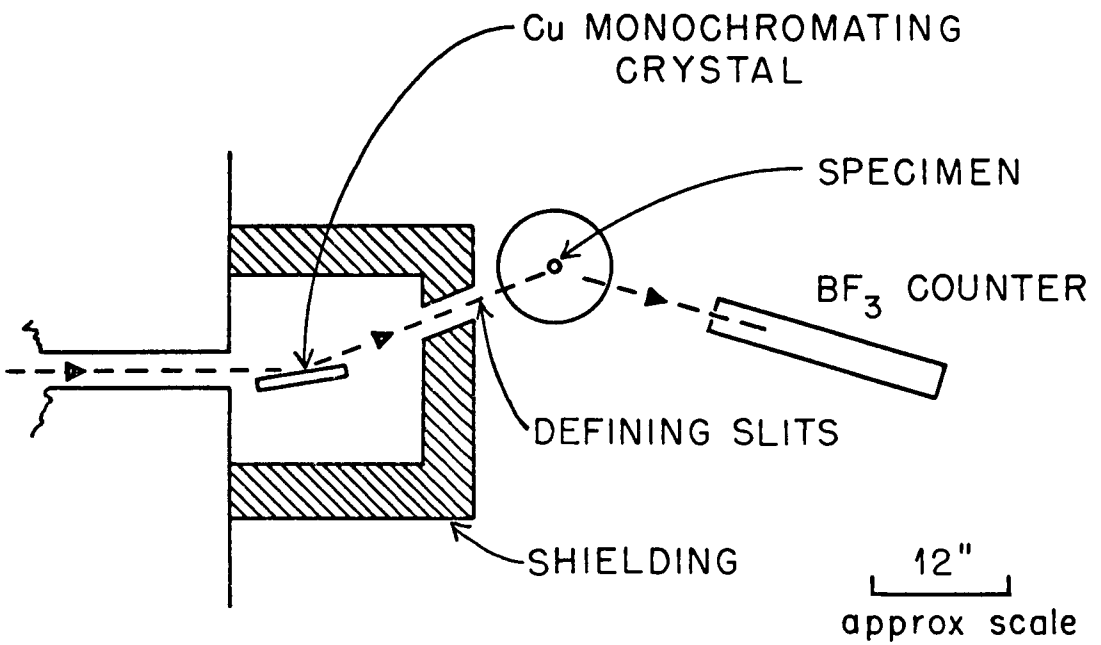

FIG 1
SCHEMATIC DIAGRAM OF NEUTRON DIFFRACTION SPECTROMETER

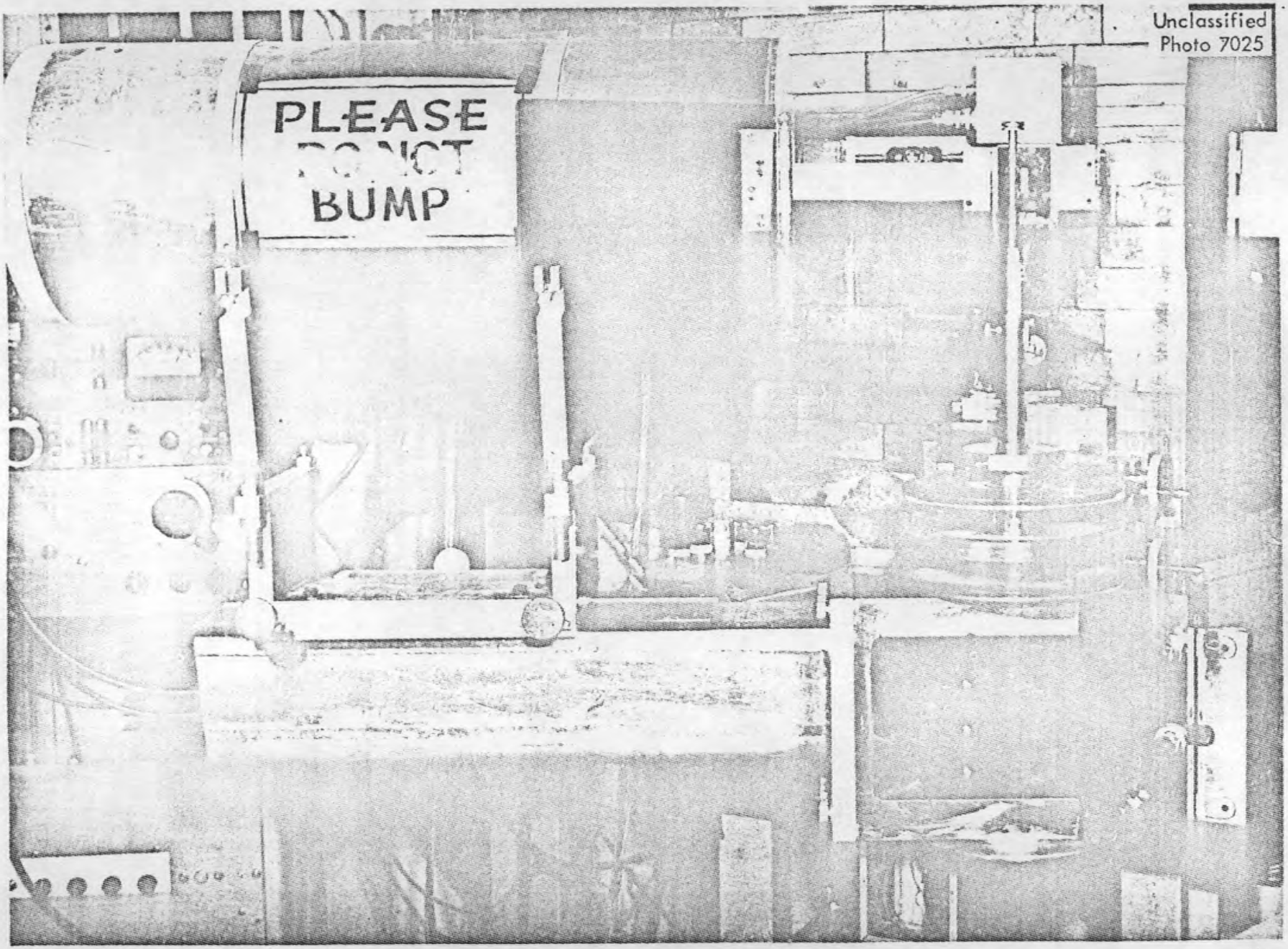

Plate 1. Photograph of the Neutron Spectrometer.

axis which intersects the center of the monochromatic beam The table and counter are driven at relative angular velocities of one to two by a three speed synchronous motor through a gear train Six angular velocities from 1/2 to 16 degrees per hour of counter angle are available. Clutches are provided for disengaging the table and counter independently from the gear train

The detector of scattered neutrons is a proportional counter filled with B^{10} enriched BF_3 It has an active length of 20 in and is shielded with 0 020 in Cd foil, 1/2 in boron carbide powder surrounded by 2 in of borated paraffin, all enclosed in ar iron tube. The entrance slit of the counter is 1/2 in wide by 1 1/2 in tall

2. Instrumentation

A block diagram of the instrumentation is shown in Figure 2 To minimize the effect of power fluctuations of the reactor, automatic compensation for flux changes is used A thin counter inserted in the monochromatic beam indicates the beam intensity on a linear count rate meter through an associated preamplifier and amplifier The rate meter output is recorded and also actuates a semi control Deviations in flux from the level at which the servo-control is set cause the servo-motor to open or close the magnesium wedges in the beam until balance is restored

Two records of the diffracted beam are obtained Amplified pulses from the counter are fed to a linear count rate meter The output of the rate meter is recorded so that intensity as a function of counter angle may be measured The amplified pulses also feed into

UNCLASSIFIED
DWG 21995

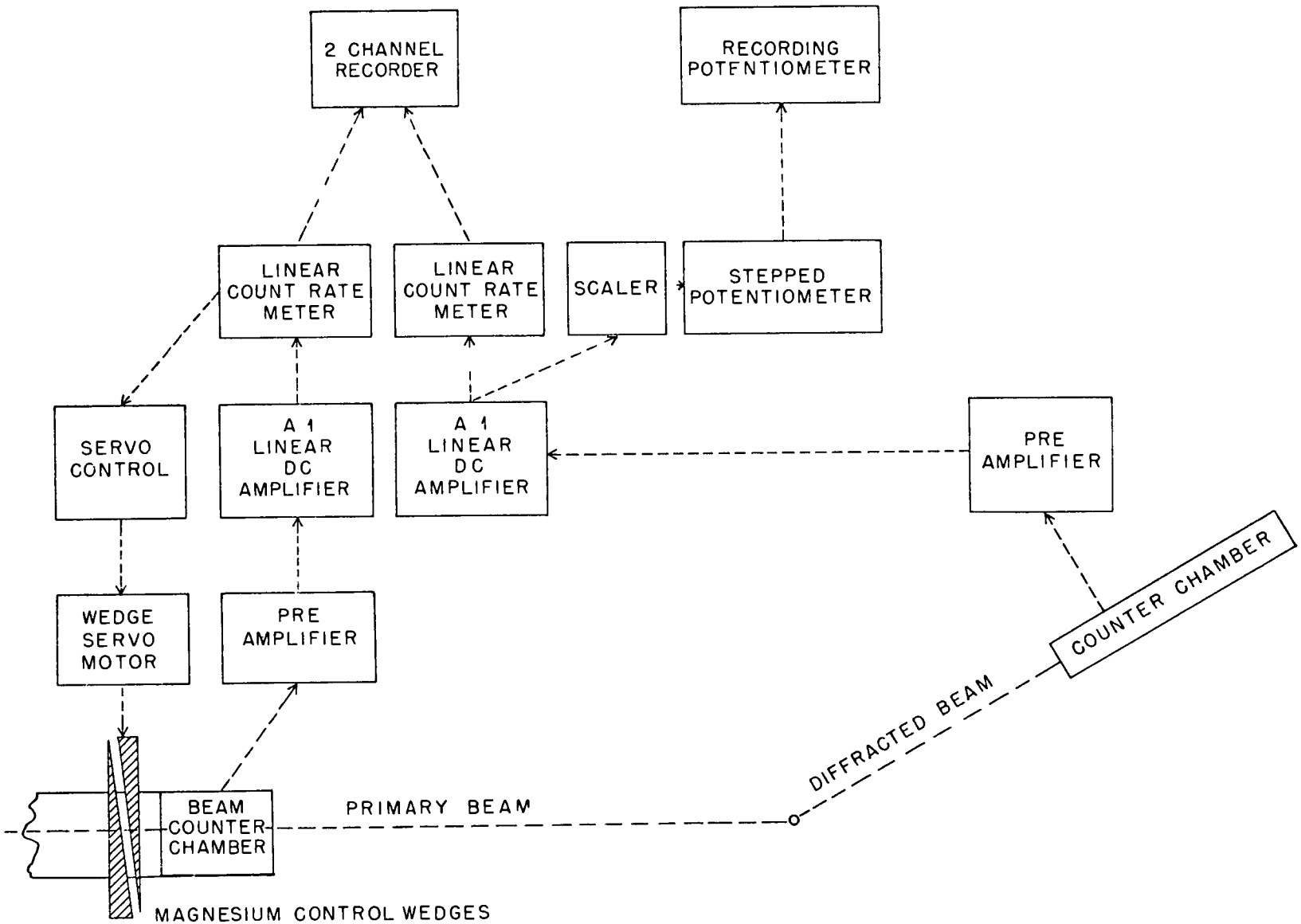

FIG 2
BLOCK DIAGRAM
NEUTRON SPECTROMETER INSTRUMENTATION

a scaler The output of the scaler operates a step-motor which is geared to a precision potentiometer The gearing is arranged so that the potentiometer makes a complete revolution after 200 pulses from the scaler Full potential across the potentiometer corresponds to full scale reading on a recorder, hence each pulse from the scaler causes a 1/2 per cent increase in recorder scale reading between 0 and 99% of full scale The circuit opens on 99 1/2% and the potentiometer and recorder pen return to zero when a cycle is complete This provides a record of the integral number of counts in any interval of angle

Because intensities encountered experimentally vary by a factor of about 10^4, several scales are provided on both the linear count rate meter and the scaler As intensity available is reduced, it is necessary to reduce angular velocity in order to obtain reasonably good counting statistics Because of the relatively high incoherent scattering from hydrogenous materials, it is not usually profitable to operate below 1/hr counter angle or 50 counts/minute full scale rate meter settings

3. Automatic Programmer

For automatic operation in taking data on single crystals, an automatic programming device to be described by Levy and Peterson[20] was utilized A diagram of the crystal rotator is shown in Figure 3 The function of the device is to bring successive crystal planes into reflecting orientation in proper time relation as the counter scans through 2 θ at constant angular velocity A program of twenty reflections can be run in a period of approximately twenty hours without

UNCLASSIFIED
DWG 21851

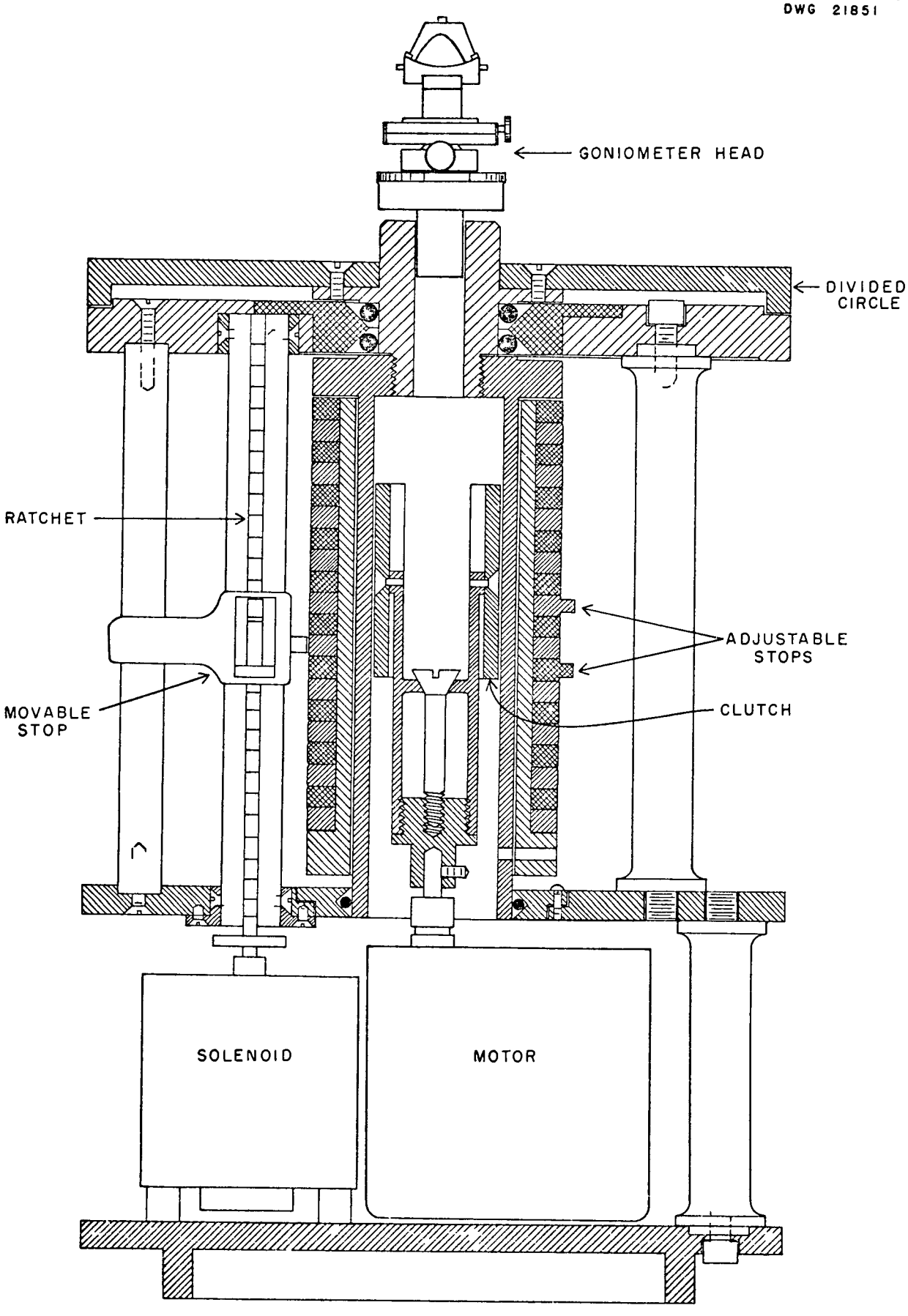

FIG 3
CRYSTAL ROTATOR – AUTOMATIC PROGRAMMER

attention from an operator

From the list of reflections to be measured, all of whose θ values have been calculated, a set of twenty or less is arranged in order of θ The values of θ between consecutive reflections must differ by 3° to 4° in order that their rate meter traces will be resolved. The angles these planes make in the crystal with some reference plane are also calculated Since the counter scans at a constant angular velocity, the time at which the θ of a particular reflection will be reached can be calculated The function of the automatic programmer is to rotate the crystal to compensate for the different angles at which the various planes lie in the crystal This is accomplished by having a battery of clocks set to provide a single electrical impulse to the crystal rotator at the end of each reflection Stops have been set on the crystal rotator at each of the interplanar angles which were previously calculated These stops are located one above the other around a central shaft in the sequence of the program of reflections. When a reflection is completed, a clock controlled pulse causes a rider to rise one notch, releasing the central shaft, which is driven through a friction clutch, and permitting it to rotate until the stop for the next reflection engages the rider. The reflection is scanned and the process repeats. Ordinarily, half of the reflections are run with increasing θ, and, after reversal of the spectrometer motor by a limit switch, the remainder are run with decreasing θ

C Procedure

1 Preparation of Specimens

Large crystals of oxalic acid dihydrate were supplied by Dr S W Peterson of the Oak Ridge National Laboratory. They were grown from a saturated aqueous solution of oxalic acid in which seeds of oxalic acid dihydrate were slowly moved to and fro in a thermostated saturated solution The temperature of the solution was continuously reduced by means of a motor-driven control on the thermostat setting After morphological examination following Groth[18] and identification of faces and axial directions, specimens suitable for diffraction were prepared. The crystals were sliced parallel to the desired axis with a wet cuttyhunk string saw Abrasive paper was used to reduce the slab to an approximately square column, about 5 x 5 x 10 mm in dimensions, taking proper precautions to keep the proper axis of the crystal accurately parallel to the long axis of the pillar One square end of the specimen was ground to a flat surface normal to the pillar axis The specimen was cemented to a metal pin so that it could be rapidly revolved in a drill press. It was reduced to cylindrical form by grinding against abrasive paper, reducing the coarseness of the abrasive as the cylinder diameter reduced Final polishing was done with wet emery paper

Two specimens were prepared for each of the two zones under investigation A small crystal about 1 mm in diameter and a larger one about 3 5 mm in diameter, both about 10 mm long, were prepared These were cemented to glass fibers and immersed in diluted Duco

cement The cement coating was required to prevent spalling when the crystals were treated to increase mosaic spread by immersion in liquid nitrogen The glass fiber was then cemented to a pin suitable for mounting on a goniometer head Alignment of the zone axis of the crystal with the rotation axis of the crystal was accomplished with an x-ray precession camera Patterns were taken from various portions of the crystal and the films examined for evidence of imperfections such as twinning or polycrystallinity No such irregularities were noted

2 Standardization and Calibration

a Relationship of Experimental Intensities to Structure Factors

The quantity measured experimentally is the total number of neutrons scattered in a given Bragg diffraction maximum The quantity desired for use in deducing the structure is the magnitude of the structure factor, which is calculated from this experimental quantity Intensities may be measured on single crystals or on powders, each method has its special advantages The more powerful method for structural investigations is the single crystal method introduced by Levy and Peterson[21] to neutron diffraction The advantages of this method are the complete resolution of most reflections and the relatively high ratio of Bragg scattering to background The method suffers from the disadvantage that secondary extinction may occur This point is discussed in some detail below The powder method has been found to be of value for relatively simple structure determinations, but of little value for complex structures because of insufficient

resolution It is still generally useful, however, in evaluating extinction effects in single crystal measurements

In the case of single crystal measurements the following expression adapted from x-ray relationships has been found to hold for an ideal crystal

$$E = (I_0 \lambda^3 N^2 V |F|^2) / (\omega \sin 2\theta)$$

E being the number of neutrons scattered in a Bragg reflection, I_0 the incident intensity, λ the wave length, ω the angular velocity of rotation of the crystal, N the number of unit cells per unit volume, V the volume of the specimen, θ the Bragg angle and F the structure factor For an actual crystal with an appreciable absorption coefficient, a correction to the measured intensity must be made in order to place the measured structure factors on an absolute scale Absorption is defined as attenuation of the beam by processes other than Bragg scattering Determination of the absorption correction is discussed below The method of evaluating the instrumental constant, I_0, is beyond the scope of this investigation, but I_0 is implicitly determined by comparing all experimental measurements of integrated intensity to measurements made under duplicate conditions on a carefully evaluated NaCl crystal

A similar relationship between integrated intensity and the square of the structure factor holds for powders

$$E = \left[(I_0 \lambda^3 l w V') / (8\pi r^2 \omega \rho)\right] \left[(N^2 J |F|^2) / (\sin\theta \sin 2\theta)\right]$$

E, λ, I_0, θ, N and F having the same meaning as before, ρ' being the powder bulk density, ρ the crystal density, V the sample volume, l,

w, ω, and r the height, width, angular velocity and radius of travel, of the sensitive aperture of the detector, and j the multiplicity of the plane The instrumental constants are determined as before by comparison with a standard sample, in this case powdered nickel An absorption correction to be discussed below must be made to the experimental integrated intensity in the powder case also

b Methods of Estimating Absorption Corrections

Because cylindrical samples are used for both single crystal and powder measurements, absorption corrections are isotropic with respect to directions of the scattered beam normal to the cylindrical axis The quantities necessary to determine the absorption correction for a cylindrical sample are the linear absorption coefficient, μ_ℓ, and the radius of the sample The value of the absorption correction, A, is read from a tabulation of A as a function of $\mu_\ell R$[22]

There are several ways of determining μ_ℓ for a single crystal. The most satisfactory is to measure the neutron transmission directly on the slab from which the single crystal specimens are to be cut. The absorption coefficient follows directly from the relationship

$$I_s = I_0 e^{-\mu_\ell t},$$

where I_s is the intensity transmitted through the sample, I_0 the incident intensity, μ_ℓ the absorption coefficient, and t the thickness of the slab Measurements may sometimes be made on the actual specimens on which diffraction data are taken It is necessary that the diameter of the specimen be large compared to that of the pinhole defining the beam so that the average path length through the crystal

can be approximated by the crystal diameter

An alternative method of estimating the absorption coefficient is to calculate the total cross-section per molecule corresponding to the attenuation measured on a powder sample and to make the assumption that the single crystal absorption correction is equal to the total powder absorption cross-section less the total coherent cross-section per molecule Another method sometimes used is to assume that the absorption is altogether accounted for by the large incoherent cross-section of hydrogen, effectively about 38 barns The absorption coefficient by either method follows from the relationship

$$\mu_{\ell} = (\sigma N \rho) / \mu \quad MW$$

where σ is the cross-section per molecule in cm^2, N is Avogadro's No , ρ is the sample density and μ MW is the molecular weight of the sample material

The average radius of a single crystal specimen is conveniently calculated from the height, weight and density, all of which can be measured with considerably greater precision than can the average radius

The absorption coefficient of a powder sample is calculated from the total cross-section, measured on the powder and the bulk density of the diffraction sample The radius of the powder sample is that of the standard aluminum sample cell, 0 5 cm.

c Secondary Extinction

Secondary extinction refers to loss of intensity in the diffracted beam relative to that from an ideal crystal element, by Bragg scattering For the relationships between intensity and struc-

ture factors discussed above to hold, the whole crystal must be bathed in a uniform flux of neutrons If, however, the crystal is of finite size, Bragg scattering will attenuate the incident beam as it passes through the crystal, so that, for intense reflections, the flux is no longer uniform, but is a function of position in the crystal and of intensity of the reflection The severity of the effect is very sensitive to the mosaic imperfection of a particular specimen Bacon and Lowde[23] have established criteria for maximum permissible thickness in terms of Q, the reflectivity per centimeter thickness, of a plane and ν_0, the mosaic spread of the crystal The mosaic spread is a measure of the random misalignment of the micro-crystalline blocks of which a macro-crystal is composed

The problem of obtaining single crystal specimens for neutron diffraction which are free from extinction is a major one. In order to reduce the effect of extinction, the radius of a specimen may be reduced The ultimate practical limit in this direction is the resulting low diffracted intensity In practice, at least two sizes of specimens are needed, a small one with a radius near 1 mm on which very intense reflections are measured, and a larger one on which the remaining reflections are measured After specimens have been prepared, it is then necessary to demonstrate that extinction is indeed absent This is done, when possible, by comparison with data obtained on powder samples. The diffraction samples are usually treated to reduce extinction by immersion in liquid nitrogen Presumably this thermal shock causes an increase in the mosaic spread of the crystal.

Levy and Peterson[21] have shown experimentally that extinction is not important in many crystals for thickness of 1 to 3 mm From

this it may be inferred that secondary extinction is not important in measurements on powder samples Usually not more than one or two powder reflections from a complex structure can be resolved The assumption is usually made, however, that extinction is absent in all single crystal measurements if agreement is found between powder and single crystal measurements on one or two intense reflections.

The problem of detecting the presence of extinction and correcting intensities for extinction is much more indirect if no resolved powder peak can be measured This problem is treated in Part Two in connection with iodic acid

3. Experimental Results

a Determination of the Absorption Coefficient

At the time the diffraction specimens were prepared, the importance of determining the absorption coefficient on the blank from which the specimens are to be made was not appreciated It has subsequently been observed that there is sometimes a significant variation in transmission by different specimens of the same substance This effect was observed in specimens of oxalic acid dihydrate, among others

The absorption coefficient was originally estimated by the method of determining the total cross-sections of of a powder specimen, 261 barns, and subtracting the coherent cross-sections of the atoms in the molecule, 46 barns, giving an absorption cross-section of 215 barns, or a linear absorption coefficient of 1 65 cm^{-1}.

The incoherent cross-section of 38 barns for hydrogen yields an absorption cross-section of 228 barns for six hydrogen atoms per molecule or an absorption coefficient of 1 81 cm^{-1}

Determination of the transmission of the larger (h0l) diffraction specimen gave an absorption coefficient of 1 80 cm^{-1}. Since the approximation of the path length of the beam as the diameter of the cylinder cannot lead to high values of the absorption coefficient, the value of 1 81 cm^{-1} was accepted.

The absorption coefficient of the powder was calculated directly from the total powder cross-section and the bulk density of the powder sample in the diffraction cell.

b. Measurement of Powder Reflections

It was found that in the oxalic acid dihydrate powder pattern only (101) was resolved, while $(10\bar{1})$ and (002) were almost exactly superposed, since at the experimental wave length of 1 42 A, $\theta(10\bar{1})$ is $5^{\circ}31'$ and $\theta(002)$ is $5^{\circ}40'$. These were treated as a single peak by assuming the intensities to be additive

Intensities were measured for (101) and the compound peak by the following procedure Powdered oxalic acid was packed to a standard depth in a standard cylindrical aluminum sample cell The weight of the sample was noted The cell was placed on the spectrometer table in a special cell holder which revolved the cell while the counter was scanning This rotation of the sample served to reduce preferred orientation effects After centering the sample in the beam and installing Soller slits on the entrance slit of the counter to improve collimation, the counter was started scanning through the reflections. The rate meter trace of intensity was recorded Integrated intensity was estimated by measuring the area under the rate meter trace of the

reflection with a planimeter The background level was estimated by measuring integral counts per degree in portions of the pattern adjacent to the peak on each side, making a smooth interpolation under the peak Standardization was against Ni (111) which was measured in a similar way. Values of jF^2 were calculated from the relationship with integrated intensity given above (Section 2-a) Results of the measurements are given in Table I

Table I

Powder Structure Factors Oxalic Acid Dihydrate

Form	E (Counts)	ω (Degrees per hour)	jF^2
(101)	3010 ± 116	1	31 5 ± 1.2
(002 10$\bar{1}$)	8085 ± 221	1	56.2 ± 1.7

c. Comparison of Single Crystal and Powder Measurements

A small crystal with the crystallographic b axis in its long dimension was prepared in the manner previously described The dimensions of this crystal were as follows

Table II

Dimensions of Small (h0l) Specimen of Oxalic Acid Dihydrate

Height (mm)	9.0
Weight (mg)	8 9
Radius (mm)	0 44
$\mu_\ell R$	0 079
A (%)	87 0

The specimen was mounted in a goniometer head and aligned in an x-ray

precession camera The scattering angles and interplanar angles referred to (h00) as 0° were calculated for the h0l zone at $\lambda = 1.142$ A, out to the experimental $\sin \theta/\lambda$ limit of about 0.67. The crystal was then mounted on a spindle on the spectrometer table and centered in the beam. The counter was set at the 2θ angle characteristic of a low index reflection, such as (002), and the table was slowly rotated by hand until the rate meter indicated a diffraction peak was being observed By locating several such peaks and comparing with the calculated orientations relative to (h00) it was possible to index the peaks unambiguously and to fix a precise reference setting of the spectrometer table

The confirmation of space group absences for $h + l \neq 2n$ indicated no revision of previously determined symmetry because of hydrogen scattering

The next step was to measure F^2 for (101) and $(10\bar{1})$ plus (002) in order to establish the presence or absence of secondary extinction The crystal and counter were set in proper correlation and each reflection was scanned The total number of counts from each reflection was estimated from the integral count record, estimating background as for the powder by interpolating under the peak On the integral count record the slope of the trace was proportional to the counting rate, the product of the average slope of the background and the duration of the peak equals the background correction to the integrated intensity. Standardization determinations were made on the reference NaCl crystal Values of F^2 were calculated with the equation

relating E and F^2 for single crystals given above (Section 2-a) The results of the determination are compared with those obtained on the powder in Table III.

Table III

Reflection	Single Crystal		Powder
	$\|F\|^2$	jF^2	jF^2
002	12 2	51 2	56 2
$10\bar{1}$	13 4		
101	16 4	32.8	31.5

The agreement was excellent for the resolved reflection (101) and fairly good for the composite peak Extinction did not appear to be appreciable in this single crystal specimen.

d. (h0l) Zone

Complete data were first obtained on the (h0l) zone of reflections A large specimen with the b axis vertical was prepared and oriented in the same way as above Its dimensions were as follows:

Table IV

Dimensions of Large (h0l) Specimen of Oxalic Acid Dihydrate

Height (mm)	10.0
Weight (mg)	164 0
Radius (mm.)	1.8
$\mu_\ell R$	0.32
A (%)	59.0

Values of F_{hkl} were determined on both the small and large specimens for reflections (303), $(30\bar{3})$ and (200) The comparison is

presented below

Table V

Preliminary Comparison of Structure Factors From Large and Small (h0l) Specimens of Oxalic Acid Dihydrate

Reflection	$\lvert F \rvert$ from Small Crystal	$\lvert F \rvert$ from Large Crystal
303	2 17	1.89
$30\bar{3}$	3.07	2.90
200	1 10	1.00

Although the values of $|F_{hkl}|$ were about 10% smaller for the large than the small specimen, there was no trend with intensity and the effect was not ascribed to extinction This discrepancy is discussed below in more detail

Intensities of all but a few of the most intense reflections were measured for the large crystal The automatic programmer was used since the total number of reflections was ninety-eight. Determinations of the integrated intensity from the standard NaCl crystal were made at intervals and whenever a change in operating conditions occurred Twenty-two of the more intense reflections were then remeasured on the small crystal When the values of $|F_{hkl}|$ were calculated comparison of the values for the eighteen reflections measured on both specimens confirmed the earlier observation that values from the large specimen were lower than those from the small specimen Systematic analysis uncovered no trend with direction in the crystal, with scattering angle, with intensity, or with any other obvious parameter It was found empirically that division of $|F_{hkl}|$

from the large crystal by 0 890 normalized the data remarkably well. The comparison of the data before and after normalization is given in Table VI

Table VI

Normalization of Structure Factors From Large (h0l) Specimen to Those From Small (h0l) Specimen

Reflection	$\lvert F_{obs} \rvert$ (large)	$\lvert F_{corr} \rvert$ (large)	$\lvert F_{obs} \rvert$ (small)
008	3.94	4 42	4.26
107	3.68	4.13	4 28
$10\bar{11}$	5.34	6 00	6 30
200	1 00	1 12	1.10
206	4.13	4 64	4.70
$20\bar{4}$	4.18	4 69	4 70
303	1.78	2.00	2 18
$30\bar{3}$	2 92	3 28	3 07
$30\bar{5}$	3.80	4.27	4.19
$30\bar{9}$	3 15	3 54	3.66
$30\bar{15}$	3.85	4 32	4.32
$40\bar{2}$	4.68	5.26	5.24
$40\bar{4}$	2.80	3 14	3.11
503	3.89	4 37	4 53
$50\bar{1}$	3 02	3 39	3 27
$50\bar{7}$	4 30	4.83	4.69
$60\bar{6}$	4.19	4.70	4.60
$70\bar{1}$	3.52	3.95	3.93

The average deviation of the corrected values from the values observed directly on the small crystal is 2 55% This would have been well within acceptable limits if a reasonable explanation for the constant error had been found. Precession camera x-ray photographs were made of ten different portions of the large crystal in an effort to find mis-oriented material Examination was made under polarized light No evidence of polycrystallinity or imperfection was noted by either technique It was then postulated that a mistake had been made in weighing or in making the absorption correction The latter point was checked immediately and the former at the conclusion of the structure analysis when destruction of the sample could be risked No error was found Finally in the latter stages of structure analysis a test was made of the possibility that the discrepancy was in reality an extinction effect For this purpose a normalizing factor which was a function of intensity was estimated Since extinction is a monotonic function of intensity, even a partially correct extinction correction should have led to improved agreement in the structure analysis. Actually, the peaks on the Fourier series synthesis map became distorted and the agreement between observed and calculated structure factors materially worsened A least squares treatment at this latter time confirmed the original choice of 0 890 as the best constant normalizing factor Accordingly, this normalization was used throughout the data analysis The successful analysis of the structure provides strong empirical evidence that this procedure is not seriously in error One is forced to conclude that some 20% of the mass of the

large specimen is not crystallographically coherent with the remainder

e. (0kl) Zone

Data in the (0kl) zone were then collected on specimens of similar dimensions prepared with the crystallographic a axis parallel to the cylinder axis The same procedure of preparation and alignment as for the (h0l) specimens was followed The dimensions of the (0kl) specimens are given in Table VII

Table VII

Dimensions of (0kl) Specimens of Oxalic Acid Dihydrate

Specimen	Small	Large
Height (mm)	9 0	10 0
Weight (mg)	14 7	132
Radius (mm)	0 56	1 6
$\mu_{\ell}R$	0 101	0 29
A (%)	84 5	62

Data were collected for all reflections with the large specimen and for ten of the most intense reflections with the smaller specimen In Table VII the common data for both specimens are presented together with values of $|F|$ for the (00l) reflections from all four specimens from both zones

Table VIII

Comparison of Structure Factors From Large and Small (0kl) Specimens of Oxalic Acid Dihydrate

Reflection	h0l Specimen		0kl Specimen	
	(Large)	(Small)	(Large)	(Small)
002		3 88	3 65	3 67
004	1 37		1 22	
006	3 20		3 03	3 15
008	4 42	4 26	4 51	4 54
0 0 10	4 48		4 64	4 67
0 0 12	89		67	
0 0 14	1 88		2.02	
011			3.45	3.74
014			4 44	4 71
015			2.61	2.86
0 1 11			3.36	3 37
024			2 37	2 53

Agreement between zones and among specimens was satisfactory. There was no indication of extinction or other serious disagreement between the large and small specimens

Analysis of Diffraction Data

A The General Problem

The analysis of diffraction data to obtain structural information may be an involved and indirect procedure even for relatively simple structures The problem is one of finding the best values for many

parameters from the values of a large set of experimental numbers whose magnitudes are observed, but whose signs are unknown For each atom in a structure the parameters to be determined are generally three coordinates in space and at least one parameter for thermal motion

The first step in the analytical procedure in the case of a centro-symmetric structure, is usually the determination of signs for the experimentally observed structure factor magnitudes After the signs have been at least partially determined, the structure factors are used to obtain the desired structural parameters There are two different approaches to each of these steps The simplest and in some ways most direct is essentially to compare the magnitudes of the observed quantities with those of structure factors calculated from an approximate structure, and to estimate systematically the parameter changes to the calculated structure required to improve the agreement to the desired level It is assumed that the calculated signs are correct if the two sets of magnitudes agree. More powerful methods are available, however, which utilize the experimental data directly to yield the desired information For sign determination, such a method is use of structure factor inequality relationships, for atomic coordinate determination, the Fourier synthesis of the scattering density function is an example These methods are especially satisfactory in cases such as the present ones where part of the structure is known with confidence, being less sensitive to incorrect assumptions concerning the unknown part of the structure than are

direct methods such as least squares

A feature of structural investigat ons is the large number of stages of approximation often required In practice many signs cannot be determined immediately until approximate parameters are determined because of limited applicability of the inequality relationships Conversely, the structural parameters cannot be accurately determined until all the signs are known Because it is a multiparameter problem, several steps are usually required to bring the refining process to the point of convergence

B Methods and Procedures Used

At one point or another in the analysis of the oxalic acid dihydrate data almost every important method of analysis was employed. As an example, an outline of the procedure of analyzing the (h01) data was the following.

In estimating signs of the structure factors, elements of several methods were combined in a novel way so that signs were determined without making any assumption regarding hydrogen locations To accomplish this, however, it was necessary to make assumptions concerning the rest of the structure Since the positions of the carbon and oxygen atoms were known with good precision from x-ray data, the necessary assumptions could be made with confidence The other information which was required in order to permit use of the inequalities was the average temperature factor of the carbon and oxygen atoms This information was obtained directly from the experimental data by statistical methods largely developed by Wilson[24].

The signs obtained by the above procedure made possible the computation of a Fourier synthesis of the scattering density function from which approximate atomic coordinates were determined The temperature factors for all the atoms were refined by analysis of the shapes of atomic peaks in the Fourier map The atomic coordinates were refined by two procedures Termination-of-series errors were corrected systematically in resolved atoms The least squares method, which is applicable even to partially resolved atoms, was employed to refine the coordinates of such atoms in the structure. The structure was a sufficiently good approximation to the true structure at this stage that the least square method should have converged to the true structure

Although many detailed and repeated steps were omitted from the foregoing, the nature of the method as a series of successive approximation, the various steps of which are not independent, is evident

C Use of the Fourier Series Method

The structure factor of a plane is related to the atomic coordinates and temperature factors by the relation

$$F_h = \sum_i f_i \exp\left\{-B_i(\sin\theta/\lambda)^2\right\}\cos 2\pi(\underline{h}\ \underline{r_i})$$

where F_h is the structure factor, f_i the scattering factor and B_i the temperature factor of the ith atom, $\underline{r_i}$ the position vector of that atom, and $\underline{h}$ the reciprocal lattice vector of the plane The Fourier series method inverts the structure factors to obtain the scattering density function, $\rho(r)$ or $\rho(x, y, z)$ in unit cell coordinates, by using them as coefficients in a Fourier series whose general form for a

centrosymmetric structure is

$$\rho(x, y, z) = V^{-1} \sum_h \sum_k \sum_l F_{hkl} \cos 2\pi(hx + ky + lz),$$

where V is the unit cell volume, (x, y, z) the coordinates of a point in the unit cell, hkl are the indices of a plane and F_{hkl} must have been previously determined The theoretical limits of summation over h, k and l are $-\infty$ to ∞

In the case of a centrosymmetric projection the expression for the series becomes

$$\rho(x,z) = A^{-1} \sum_h \sum_l F_{h0l} \cos 2\pi(hx + lz)$$

where A is the area of the projection In evaluating the function for a set of experimental structure factors, it is not possible to extend the summation beyond the highest values of the indices observed experimentally The summation is then from -h to h and -l to l rather than $-\infty$ to ∞ for h and l The effect of breaking off the series in this way is to introduce false features into the function which have the same form as optical diffraction rings from a circular stop. The effect of these satellite rings around the atomic peaks is to disturb the shapes of the main peaks of neighboring atoms It is possible both to minimize this effect and to allow systematically for the errors

If the series were completely convergent within the $\sin\theta/\lambda$ limit of the experimental observation, no termination-of-series error would result from breaking off the series In neutron diffraction data, however, there is much less natural convergence than in x-ray data, since the neutron atomic form factor is isotropic The only nautral convergence is that resulting from the thermal motion of the

atoms, with the result that diffraction effects in maps prepared directly from observed neutron structure factors may be quite serious If the observed structure factors are modified by multiplying with a function of sin θ/λ which converges smoothly to small values at the limit of observation, the series is made convergent and diffraction errors are reduced This question has been treated in detail by Waser and Schomaker[25] who discussed its mathematical significance and introduced the term modification function for this type of multiplier. The qualitative effects of a useful modification function on the Fourier peak shape are decreased peak height and curvature, increased peak width, and reduction or elimination of diffraction rings. The increase in ease of interpreting the Fourier map because of the reduction of complex overlap effects usually more than compensates for a small loss in resolution

The interpretation of the Fourier function involves estimating the coordinates of the maxima, which are taken to represent the atomic locations, and analysis of the peak shapes for temperature factor estimation One method of estimation of atomic coordinates is to interpolate the function as though it were Gaussean near the maximum, using the method described by Donohue[26]. Temperature factors may be estimated by comparison of observed peak shapes with peak shapes calculated for various values of the temperature factor B A peak shape is defined as a graph of scattering density versus displacement from the point of maximum density. In this method synthetic peak shape functions for comparison are calculated for a hypothetical

unit cell containing one atom at the origin with a scattering factor equal to that of the atom in question The same convergence factor used in obtaining the experimental map is used in modifying the synthetic structure factors calculated for various values of B The value of B chosen is that which gives the best fit of peak height and width (Figure 6). In practice, the limit to the precision of the experimental peak shape is drawn

After determining the maxima on the experimental map and estimating temperature factors, it is possible to correct systematically for any residual termination-of-series errors by the backshift method[14]. For this purpose a set of structure factors is calculated from the tentative observed atomic coordinates and temperature factors A synthetic map, with the same convergence factor and term omissions as in the experimental map, is prepared and the peak coordinates are estimated If termination-of-series errors are small and if the interpretation of the experimental map was essentially correct, the termination-of-series errors will be equal in the two maps Accordingly, if a parameter determined as x from the experimental map is read $x + \Delta x$ on the synthetic backshift map, the true parameter is $x - \Delta x$

D <u>The (h0l) Zone.</u>

The Fourier series method as outlined above was used to obtain the main features of the atomic arrangement from the (h0l) zone data Preliminary to computing the series, however, it was necessary to establish the signs of a large fraction of the structure factors.

The procedure for determining the signs made use of the fact that a part of the structure, namely the carbon and oxygen positions, was well known For about two-thirds of the reflections, the signs were determined directly by the contributions of carbon and oxygen The condition for direct determination of a sign was that the temperature corrected structure factor contribution from carbon and oxygen be larger than the maximum possible hydrogen contribution, when all hydrogen atoms scatter in phase The problem at this stage was to estimate temperature factors.

An attack on the estimation of an average temperature factor, B, for carbon and oxygen was made by means of statistical methods largely developed by Wilson[24] He has shown that the mean value of the intensity, $\langle I \rangle$, in a small range of $\sin \theta/\lambda$ can be represented by the relations

$$\langle I \rangle = S \sum_{j=1}^{N} f_j^2 \exp\left\{-2B_j(\overline{\sin \theta/\lambda})^2\right\}$$

where the index j designates the atoms in a unit cell This expression was expanded for application to oxalic acid dihydrate to

$$(2n)^{-1} \sum_{i=1}^{n} F_i^2 = (4f_C^2 + 12f_O^2)\exp\left\{-2B(\sin \theta/\lambda)^2\right\} + 12f_H^2 \exp\left\{-6(\sin \theta/\lambda)^2\right\}$$

where n is the number of structure factors F_i in a small range of $\sin \theta/\lambda$, $f_C = 0\ 659$, $f_O = 0\ 58$, and $f_H = -0\ 38$, are scattering amplitudes and B is the average temperature factor for carbon and oxygen The parameter S has the value 2 for a centered net. A value of 3 was assigned to B_H by analogy with previously determined structures Since the thermal motion of hydrogen is usually greater than that of

heavier atoms, the expression was evaluated for 18 reflections of largest sin θ/λ where hydrogen scattering was relatively less important A value of 1 8 was found for the average B of carbon and oxygen

Applying this value of B to structure factor contributions for carbon and oxygen calculated from x-ray parameters, it was found that the net structure factor contribution exceeded the maximum possible hydrogen contribution in about two-thirds of the cases, thus determining the sign of those observed structure factors

The signs of the remaining structure factors were determined by application of structure factor inequalities originally discussed by Harker and Kasper[27]. They and others have shown that inequality relationships among structure factors exist for structures composed of point scatterers with scattering amplitudes of uniform sign Scattering by real structures can be made to approximate that from point scatterer by removing the dependence on sin θ/λ. This can be done for neutron diffraction data by multiplying each observed structure factor by the reciprocal of the average temperature factor for the corresponding sin θ/λ While x-ray scattering amplitudes are all of one sign, neutron scattering amplitudes may be both positive and negative in a given structure In this case, the inequalities apply separately to the contributions from positive and negative scatterers, respectively.

In applying inequalities to oxalic acid dihydrate data, it was therefore necessary to separate the structure factor contributions of hydrogen from those of carbon and oxygen This was accomplished by

means of the following relationships

$$\left|F_{obs}\right| = \left|F_{C,O}\exp\left\{-B_{av}(\sin\theta/\lambda)^2\right\} + F_H\exp\left\{-B_H(\sin\theta/\lambda)^2\right\}\right|$$

where $B_{av} = 1\ 8$, $F_{C,O}$ is the calculated contribution of carbon and oxygen, F_H is the unknown contribution of hydrogen, and B_H is assigned a value of 3 as before Noting that the sign and magnitude of the temperature corrected carbon and oxygen contribution are known,

$$F_H = \left[F_{C,O}\exp\left\{-B_{av}(\sin\theta/\lambda)^2\right\} \pm \left|F_{obs}\right|\right] / \exp\left\{-3(\sin\theta/\lambda)^2\right\}$$

From this equation are obtained two possible values of F_H, with signs. The following inequality relationship[28] was used to choose the correct value

$$(F_K + F_L)^2 \leq (F_{000} \pm F_{K+L})\ (F_{000} \pm F_{K-L})$$

The letters K and L refer to the indices hkl of the reflections The inequality was applied to data from four reflections with indices having the indicated relationship and for three of which signs and therefore the hydrogen contributions were already determined Substitution into the inequality of the three known values of the hydrogen contribution with each of the two possible values of the unknown hydrogen contribution led in some cases to satisfaction of the inequality by one value and not by the other value of the unknown. At times the inequality was satisfied by both values, an ambiguous result, and it was then necessary to try another set of structure factors whose signs were known. In this way, signs were determined for all but three or four of the remaining (h0l) structure factors

It was now possible to prepare a Fourier series with only a few weak terms omitted in which no assumptions regarding hydrogen positions

had been made in determining signs of the coefficients Coefficients were prepared, using the empirical modification function, M ($\sin \theta/\lambda$) shown in Figure 4, putting them in a form suitable for machine computation All Fourier series in this investigation were computed on IBM machines by the Numerical Analysis Laboratory of the K-25 plant at Oak Ridge

The resulting values of $\rho(x,z)$ were plotted on a scaled grid representing the "b" face of the crystal It was observed that one hydrogen atom was closely associated with a carboxyl oxygen and two hydrogens were closely associated with the water oxygen Hydrogen parameters were estimated by locating the centers of the upper peak contours with a compass A set of hydrogen structure factor contributions was calculated from these parameters with B equal to 3 0. The remaining signs were determined and the final Fourier map Figure 5 was eventually prepared There were several intermediate steps before the final map was obtained which were all concerned with elimination of errors and did not otherwise contribute to refinement of the structure

The following parameters were obtained by Gaussian interpolation along sections near the top of the various peaks parallel to the axes[26]

UNCLASSIFIED
ORNL-LR-DWG 1036

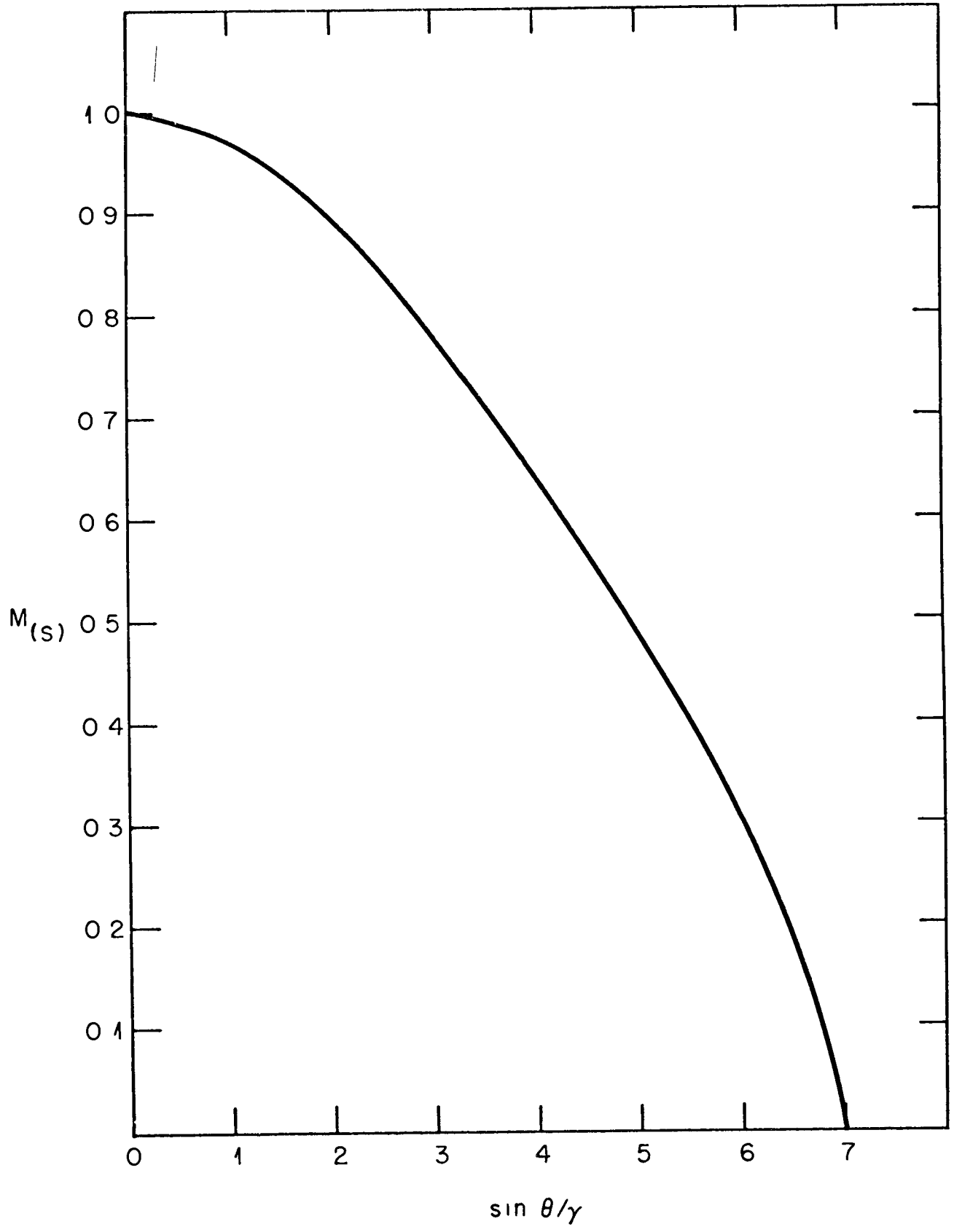

FIG 4
MODIFICATION FUNCTION USED TO INTRODUCE ADDITIONAL CONVERGENCE INTO OXALIC ACID DIHYDRATE DATA

UNCLASSIFIED
ORNL LR DWG 104

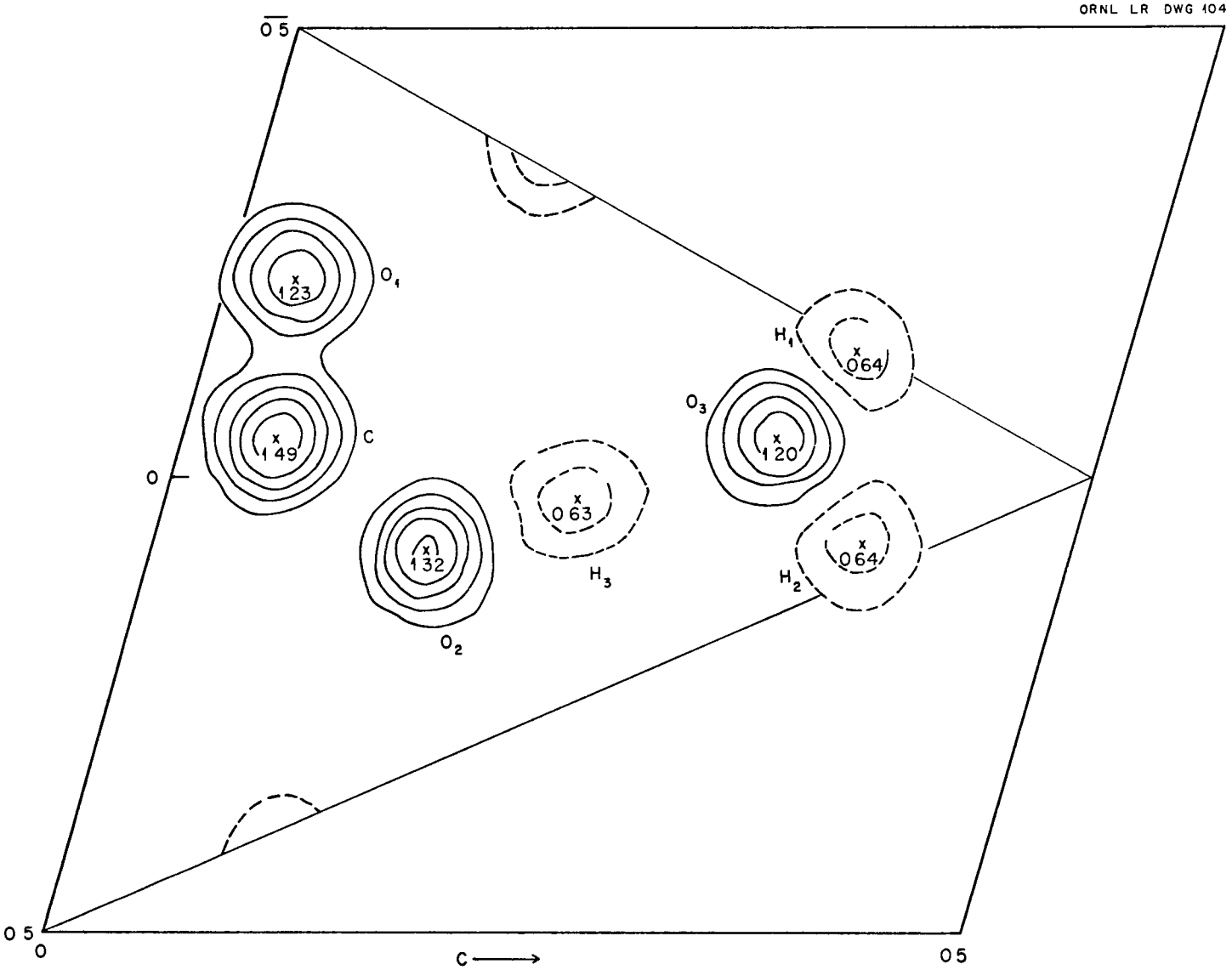

FIG 5

FOURIER MAP OF (hOl) ZONE OF OXALIC ACID DIHYDRATE

Contours at Intervals of 0 25 x 10^{12} cm/A^2
Zero Contour Omitted
Negative Contours Dashed
Numbers (x 10^{2}) Indicate Maximum Values of the Scattering Density
Crosses Locate Atomic Positions

Table IX

Preliminary Parameters from (h0l) Fourier Map

Atom	Parameter	
	x	z
C	-0 0435	0 0500
O_1	0 0825	0 1483
O_2	-0 2232	0 0365
C_3	-0 0445	0 3217
H_1	-0 1340	0 3530
H_2	0 0720	0 3800
H_3	0.0235	0 2197

The agreement factor, defined as

$$R = 100(\Sigma \left| F_{obs} - F_{calc} \right|)/\Sigma \left| F_{obs} \right|$$

was 12 2% for this set of parameters

Comparison between experimental and synthetic peak shapes (Figure 6) showed best agreement was obtained with B equal to 1 8 for atoms C and O_1 and equal to 2 0 for atoms O_2 and O_3 A value of 4 to 5 was indicated for the H atoms, but this result was not accepted at that time because it was so much larger than had been observed on other structures, and because data in this and other structures seemed to indicate a possible anomaly in the coherent scattering of hydrogen A set of structure factors was calculated from these parameters, the revised values of B for O_2 and O_3, and with B for hydrogen equal to 3 0 The agreement factor between calculated and observed structure factors, R, was 11 4%

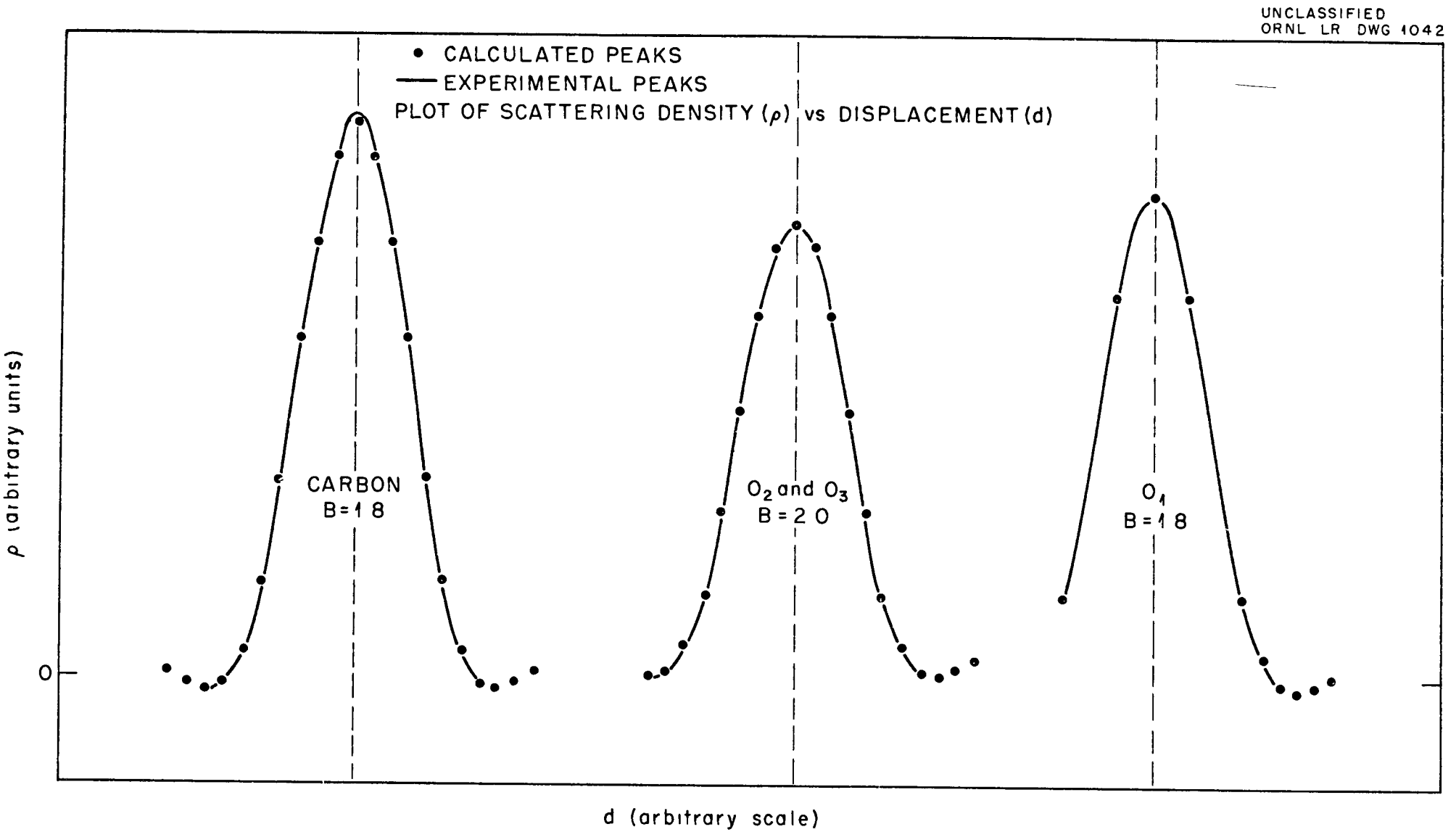

FIG 6

COMPARISON OF SYNTHETIC AND EXPERIMENTAL PEAK SHAPES

A backshift map was prepared with the revised temperature factors for atoms O_2 and O_3 and with B of 3 0 for hydrogen Revised parameters, corrected by the backshift, gave an agreement factor of 12 4%, indicating that an incorrect step had been made By this time information from other structures together with the conclusions of a theoretical consideration of coherent scattering by hydrogen by Dr G T Trammel of the Physics Division of the Oak Ridge National Laboratory had ruled out the possibility of an anomaly.

The indications of the peak shape analysis were therefore accepted Trial calculations showed a value of 4 0 for B_H to give the best agreement factor, 11 3%, using the backshifted parameters A Fourier synthesis with these calculated structure factors confirmed the previous backshift corrections for all atoms except H_2 Quite different corrections were obtained for B_H = 3 0 and B_H = 4 0, indicating that the method was unreliable for this atom, probably because of incomplete resolution from the water oxygen atom It was felt that the same argument should apply to H_1, since it was also incompletely resolved, even though the backshift corrections were not very different for the two different hydrogen temperature factors That the method had led to an erroneous position for H_2 was indicated by the improved agreement factor, 9 8%, obtained with a new parameter for H_1 chosen by trial. The final backshifted parameters for all atoms except H_1 and H_2 are given in Table X

Table X

Results of Back Shift Correction (h0l) Zone of Oxalic Acid Dihydrate

		Trial Parameter	Correction	Final Parameter
C	x	-0 0435	-0 0015	-0 0450
	z	0 0500	0 0001	0.0501
O_1	x	0.0825	-0 0008	0 0817
	z	0 1483	-0 0016	0.1467
O_2	x	-0.2232	-0 0003	-0.2235
	z	0.0365	0 0010	0 0375
O_3	x	-0 0445	-0 0007	-0.0452
	z	0 3217	0.0005	0 3222
H_3	x	0 0235	-0 0028	0.0207
	z	0 2197	-0 0017	0.2180

Because H_1 and H_2 were not fully resolved in this projection and because the back shift procedure did not lead to consistent results for H_2, the method of least squares was applied to determining the parameters of these atoms

The basis of the method is to minimize the sum of the squares of the differences between a set of quantities and their true values, about which they are assumed to be normally distributed[29] It can be shown that minimizing such a function yields the most probable values of the quantities consistent with the observations The quantity to be minimized in the present case was $(F_{calc} - F_{obs})^2$ The expressions for the structure factors was linearized by expanding

about an initial set of parameter values in a Taylor series and retaining only the linear terms Substitution of this expanded expression and application of conditions for minimizing $(F_{calc} - F_{obs})^2$ leads to a set of normal equations

$$\sum_i \left\{ \sum_{rj} \left(\frac{\partial F}{\partial x_{rj}}\right)^o \Delta x_{rj} - \Delta F_i^o \right\} \left(\frac{\partial F}{\partial x_{sk}}\right)^o = 0$$

where x_{rj} is the jth parameter of the rth atom, the index i designates the various structure factors, the superscript zero refers to values calculated from initial parameters, and the index (sk) covers the same range as (rj) There is thus one equation for each parameter being adjusted Solution of this set of normal equations gives correction, Δx_{rj}, to the starting values of the parameters whose most probable value is sought

Choosing starting parameters for H_1 and H_2 as the best previous set and using the set in Table X for the rest of the structure, a least squares procedure led to the following final x and z parameters for those atoms. Reflection (10$\bar{5}$) was omitted because it was felt that its large discrepancy could be assigned more probably to extinction.

Table XI

Results of Least Squares Treatment of H_1 and H_2 Parameters

		Starting Parameters	Correction	Final Parameters
H_1	x	-0.1340	-0 0021	-0.1361
	z	0 3530	-0 0024	0.3506
H_2	x	0.0720	0 0009	0.0729
	z	0.3900	-0.0030	0 3870

The agreement factor was 9 9%, but the value of $\Sigma (\Delta F)^2$ was reduced from 6 8155 to 6 5200 when these new parameters were used to calculate structure factors

In Table XII the calculated and the normalized observed structure factors for the (h0l) zone are listed

Table XII

Comparison of Calculated and Observed Structure Factors for the (h0l) Zone of Oxalic Acid Dihydrate

h 0 l	F_{calc}	$\lvert F_{obs}\rvert$	h 0 l	F_{calc}	$\lvert F_{obs}\rvert$
0 0 2	3 71	3.88	1 0 $\bar{1}$	4 13	3 66
0 0 4	1.15	1.37	1 0 $\bar{3}$	-0.23	0.33
0 0 6	3 00	3 20	1 0 $\bar{5}$	-7 86	6.63
0 0 8	-4 10	4.26	1 0 $\bar{7}$	0.25	0 60
0 0 10	-4 40	4 48	1 0 $\bar{9}$	-1 78	1 46
0 0 12	-0 99	0.89	1 0 $\overline{11}$	-5 83	6.30
0 0 14	-1 86	1 88	1 0 $\overline{13}$	-0 58	0 49
1 0 1	4 37	4.06	1 0 $\overline{15}$	2 39	2.57
1 0 3	2 68	2.77	2 0 0	1.08	1.10
1 0 5	0.40	0.33	2 0 2	-1 83	1 86
1 0 7	4 14	4 28	2 0 4	0 51	0 93
1 0 9	-1 52	1 92	2 0 6	4 58	4 67
1 0 11	-2 12	1 88	2 0 8	-2.33	2 43
1 0 13	61	1.06	2 0 10	-0 89	1 02
1 0 15	-1 12	1.24	2 0 12	0 83	0

h.0 l	F_{calc}	$\lvert F_{obs}\rvert$	h 0 l	F_{calc}	$\lvert F_{obs}\rvert$
2 0 14	-0 51	0 62	4.0 0	2 61	2.39
2 0.$\bar{2}$	0.72	0 80	4 0 2	-0 85	0 76
2 0 $\bar{4}$	-4 74	4 70	4 0 4	3.04	3.19
2 0.$\bar{6}$	-0 75	1.18	4.0 6	2.47	2 54
2.0.$\bar{8}$	-2.72	3.27	4 0 8	-2 93	2.95
2 0 $\overline{10}$	-2.67	2.94	4 0 10	-0.80	0 52
2 0.$\overline{12}$	2 25	2.10	4 0 $\bar{2}$	5.70	5.25
2 0 $\overline{14}$	1 04	1 04	4 0 $\bar{4}$	-2 73	3.11
3 0.1	-0 10	0.25	4 0 $\bar{6}$	-1 61	1.58
3 0.3	2 18	2 18	4 0.$\bar{8}$	0.55	0.98
3 0 5	-0 64	0 72	4.0.$\overline{10}$	-1.75	1.77
3.0 7	-0.73	0 83	4 0.$\overline{12}$	0 33	1.10
3.0 9	-2 87	3.22	4 0 $\overline{14}$	-0 78	1.00
3.0.11	-0.39	0	5 0.1	2 61	3.12
3.0.13	0.30	0 34	5.0 3	4 85	4.53
3.0.$\bar{1}$	-1 20	1 36	5 0.5	2.20	2.31
3.0 $\bar{3}$	3 28	3 07	5.0.7	-1.59	1.29
3.0.$\bar{5}$	-3.97	4.19	5.0.9	-0.30	0.52
3.0 $\bar{7}$	-0.24	0.45	5 0.$\bar{1}$	-3 20	3.32
3.0.$\bar{9}$	3.30	3.60	5 0 $\bar{3}$	1.70	1.73
3.0.$\overline{11}$	-1.32	1.00	5.0.$\bar{5}$	-1 77	1 53
3 0 $\overline{13}$	-0 85	0 76	5.0 $\bar{7}$	-5.22	4.69
3 0.$\overline{15}$	3.59	4 32	5 0 $\bar{9}$	-1 21	1 18

h 0 l	F_{calc}	$\lvert F_{obs}\rvert$	h 0 l	F_{calc}	$\lvert F_{obs}\rvert$
5 0 $\overline{11}$	-0.06	0	6 0.$\overline{10}$	0.16	0
5 0.$\overline{13}$	-1 89	1.76	6 0.$\overline{12}$	1 43	1 61
5 0 $\overline{15}$	1 78	1.82	7 0 1	0 02	0
6.0 0	-2.70	2 64	7 0 3	-0.02	0
6.0 2	-0.14	0.19	7.0 $\overline{1}$	-4 26	3.94
6.0 4	3.54	3.00	7 0.$\overline{3}$	-1 08	1 06
6 0.6	-1 26	1.01	7 0.$\overline{5}$	0.52	0
6 0.$\overline{2}$	-0 37	0 19	7 0 $\overline{7}$	-1 96	1.56
6 0.$\overline{4}$	-3.71	3.80	7.0.$\overline{9}$	0.53	0 31
6 0 $\overline{6}$	-4.63	4.60	7 0 $\overline{11}$	3.36	3 38
6 0.$\overline{8}$	-0 48	0	8.0.0	-1 75	1.62

E The (0kl) Zone.

The problem of determining signs of the set of (0kl) structure factors appeared to be less involved since one parameter was already determined for the hydrogen atoms A preliminary set of signs was calculated by assuming that the hydrogen atoms were located on the lines joining the water oxygen and the three nearest-neighbor oxygens. The same temperature factors were those used in the intermediate stages of the (h0l) refinement, B for C and O, being 1.8, for O_2 and O_3, 2.0, and for H, 3.0. A Fourier synthesis was made, employing the same modification function (Figure 4) as for the (h0l) zone.

The resulting map contained some unusual features, particularly a low value of the H_1 peak and an inequality in height of the three

hydrogen peaks The peaks for H_1 and H_2 were decidedly off the lines joining O_3 to neighboring oxygens and it was felt that incorrect phases might account for the appearance of the map After reading the maxima of all the resolved peaks and estimation of parameters for C and O_2, structure factors were calculated, but no important structure factors changed sign At this time the new treatment of the x-ray data by Ahmed and Cruickshank[13] appeared Their y and z parameters for the carbon and oxygen atoms and y parameter for hydrogen from the neutron diffraction map were then combined with the z parameters for hydrogen previously obtained. Structure factors were again calculated, but no important signs were changed As a last step to preclude the possibility of converging on a wrong structure, a map was made using only those experimental structure factors whose signs were completely determined by the C and O contributions Again the procedure yielded the same final set of signs. The final Fourier map of this projection is illustrated in Figure 7

At this stage, the agreement factor, using an intermediate set of z parameters and temperature factors from the (h0l) zone was about 25%, varying from about 10% for seven (00l) reflections to 40% for eight (04l) reflections Inspection of the manner of deviation of the calculated structure factors led to the speculation that a large anisotropic temperature motion might account for a large part of the discrepancy. A rather extensive exploration of the possibility that uncertainty in the y parameters was responsible led to the conclusion that no reasonable variation of the y parameters could account for the

UNCLASSIFIED
ORNL LR-DWG 1041

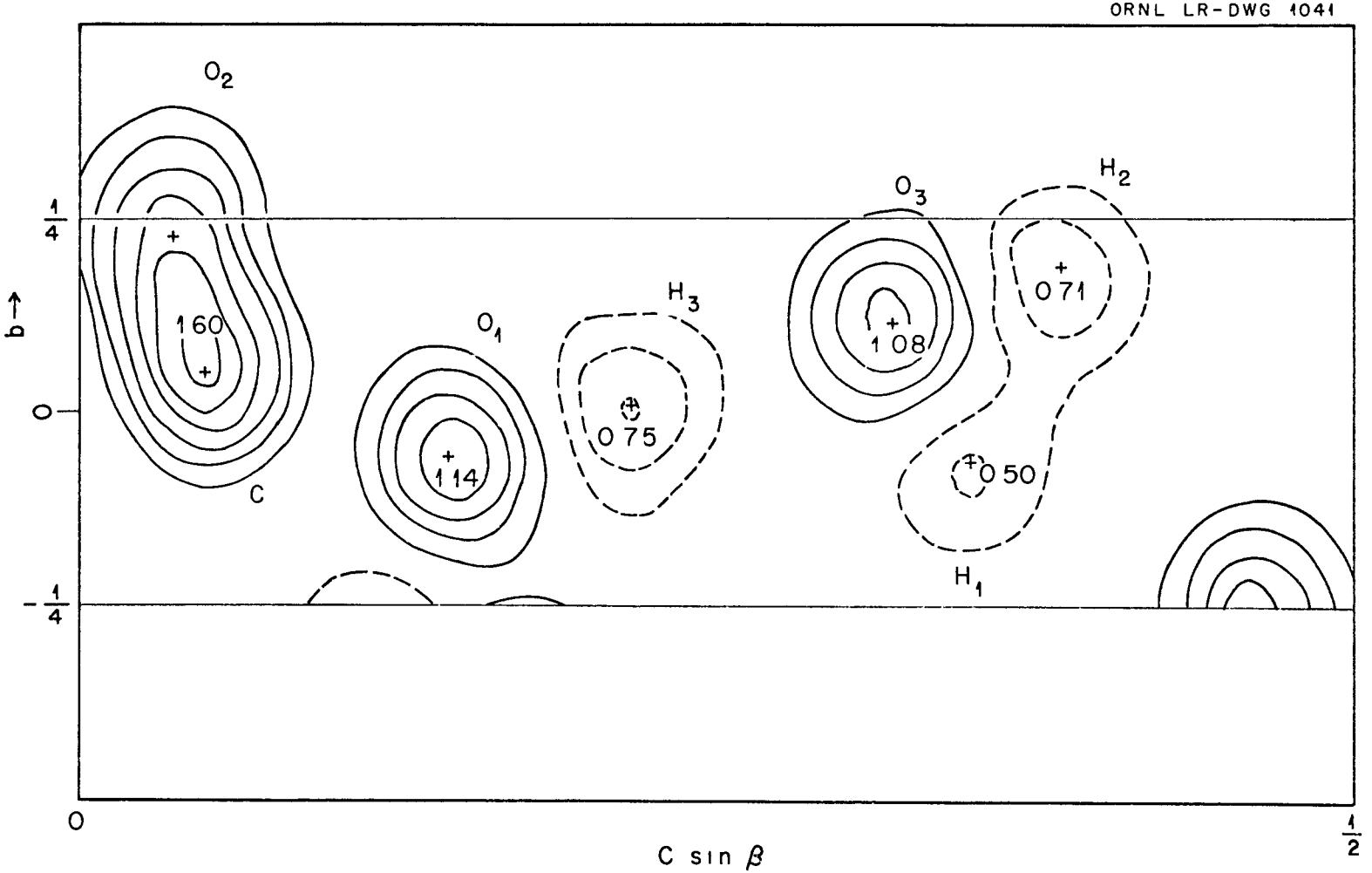

FIG 7

FOURIER MAP OF THE (0kl) ZONE OF OXALIC ACID DIHYDRATE

Contours at Intervals of 0 25 x 10^{-12} cm/A^2
Zero Contour Omitted
Negative Numbers Dashed
Numbers (x 10^{-12}) Indicate Maximum Values of the Scattering Density
Crosses Locate Atomic Positions

differences Particular attention was paid to the unresolved carbonyl group and to the poorly defined H_1 peak. Returning to the idea that unusual thermal motion was responsible, it was found for k equal to 3 or 4 that calculated structure factors deviated greatly from observed structure factors when the calculated contributions from H_1, O_2, or O_3 were particularly large The first step was to assign asymmetric temperature factors to H_1 and O_2 Because of the sensitivity to the k index, the asymmetric component was taken to be along b as an approximation The form of the total temperature factor for an atom then became

$$\exp\{-B(\sin\theta/\lambda)^2\}\exp\{-B'(k/2b)^2\}$$

where B' is the asymmetric component of the temperature factor. Assigning B' values of 3 0 to H_1 and 2 5 to O_3, the agreement factor was reduced to about 15% The procedure after this stage was to refine the structure by successive least squares treatments of the water molecule and carbonyl group Successive least squares involving first the y parameters and B' values of H_1 and O_3, then those of C and O reduced the agreement factor to 13% It was found that an increase in observed structure factors by a scale factor of 1 02 improved the agreement to 12 2% It was then found that a B' of 1 3 for O_1 reduced the agreement factor to 10 9% and assignment of an isotropic temperature factor coefficient of 5 0 to H_1 and a B' of 1 3 to H_2 reduced the agreement factor to 9 9% These values were suggested by the appearance of an $(F_o - F_c)$ Fourier map A final least squares on the y parameters of C_1, O_2, O_3, H_1 and H_2 together with backshifted parameters for O_1

and H_3 gave a final agreement factor of 9 5% The backshift corrections were 0 020 A for H_3 and 0 008 A for O_1 An agreement factor of 8 9% was obtained with an intermediate set of z parameters from the (h0l) zone, but the improved agreement is of questionable significance, since they were clearly not the best set of z parameters for the other zone No effort was made to determine z parameters from the (0kl) data, so that the above discrepancy may in a sense represent the degree of discordance between the two sets of data The following y parameters and temperature factors were finally obtained for this zone.

Table XIII

Final y Parameters and Temperature Factors for the (0kl) Zone of Oxalic Acid Dihydrate

	y	B	B'
C	0.054	1.8	0
O_1	0.943	1.8	1.3
O_2	0.227	2.0	2.3
O_3	0.114	2.0	2.3
H_1	-0 062	5 0	1 3
H_2	0 188	3 0	1.3
H_3	0 015	3 0	0

The observed and calculated structure factors for this zone are given in Table XIV The signs of the reflections for which k + l = 2n + 1 are reversed from those reported by Brill, Hermann and Peters presumably because of a different convention employed

Table XIV

Comparison of Calculated and Observed Structure Factors for the (0kl) Zone of Oxalic Acid Dihydrate

0 k l	F_{calc}	F_{obs}	0 k l	F_{calc}	F_{obs}
0 0 2	3 72	3.67	0 1 14	0.97	1 06
0 0 4	1 14	1 22	0 1 15	-0 28	0.39
0 0 6	3 12	3 09	0 2 0	0 60	0 55
0 0 8	-4 16	4.53	0 2 1	-0 89	0.92
0 0 10	-4 66	4 65	0 2 2	0.77	0.60
0 0 12	-0.74	0 67	0 2 3	-0 09	0
0 0 14	-1 77	2 02	0 2 4	-2.57	2.37
0 1 1	3 96	3 74	0 2 5	-1.53	1 49
0 1 2	-0.36	0.46	0 2 6	0 02	0
0 1 3	0 69	0 61	0 2 7	-3 31	3.18
0 1 4	-4 74	4.57	0 2 8	-0 10	0
0 1 5	-2.70	2.71	0 2 9	0.64	0.81
0 1 6	-1.69	1.59	0 2 10	-1 12	1 26
0 1 7	2.39	2.45	0 0 11	0.46	0.12
0 1 8	-0 29	0 36	0 2 12	0 36	0.35
0 1 9	-2.51	2.91	0 2 13	-0 50	0 12
0 1 10	-2.38	2.66	0 2 14	0 40	0.38
0 1 11	-3 34	3 34	0 3 1	0 52	0.51
0 1 12	-0 60	0 63	0 3 2	2 22	2.00
0 1 13	0 11	0 14	0 3 3	-0 35	0.31

0 k l	F_{calc}	F_{obs}	0 k l	F_{calc}	F_{obs}
0 3 4	-2.34	2.47	0 4 0	0 07	0
0 3 5	0 05	0	0 4 1	0 01	0
0 3 6	-0 96	0 68	0 4 2	1.72	1.46
0 3 7	0.71	0 24	0 4 3	-1 07	1.32
0.3 8	1 25	1 48	0 4 4	0.20	0.36
0.3.9	-2.13	2 12	0 4 5	-1.28	1 01
0.3.10	0 45	0	0 4 6	-0.19	0.36
0 3.11	-0.01	0	0 4 7	-0.33	0.27
0 3 12	0 42	0 40	0 4.8	0.12	0 23

F. Reliability of the Analysis

The sources of error in the experimental determination are believed to arise from three principal sources Counting statistics and instrumental inaccuracies contribute to absolute errors which increase with the magnitude of the measured intensity At least partially counterbalancing this tendency is the increased difficulty and uncertainty of making the background correction for weak reflections The result is that the absolute error in structure factor magnitudes is more nearly constant than the relative error A third source of error is essentially a scale factor uncertainty caused principally by errors in intensity measurements on the standard samples and in the estimated absorption correction It is believed that the cumulative effect of these three sources of error should make the average error in sets of zonal data equal to no more than two or three per cent

If the analysis of the structure were optimum, the residual error should be that inherent in the data, whether it be from statistical or external sources Since the agreement factor in both zones is three or four times the expected error in the data, it follows that the analysis is not optimum; that it is not was recognized, not only because of the occasional large discrepancies between calculated and observed structure factors, but because the model of the thermal motion was known to be a crude one Refining the treatment of the thermal motion is an enormously complicated procedure which can be carried out in reasonable time only after the problem has been adapted for solution on high speed computing engines.

Some remarks concerning some of the larger discrepancies may be made In the (h0l) zone, the large discrepancy for $(10\bar{5})$ is thought to result from extinction The intensity of this reflection was several times that of the next highest, and the calculated value was not sensitive to parameter changes The explanations for the large calculated value of $(20\bar{12})$, observed zero, and the low value of $(40\bar{12})$ are not known, but it is suggested that these represent extreme consequences of the incompleteness of the analysis of thermal motion Increased scatter in the data with larger values of the l index appear common to both zones. Reflections whose magnitudes were observed 0 50 or below are quite poorly determined ever at intermediate values of $\sin \theta/\lambda$.

In the (0kl) zone no particular discrepancy stands out among the well determined reflections Several weak reflections such as (0211),

(0213), (046) and others are in poor agreement, but these largely represent measurements made at the limit of observability. Increasing scatter is observed with both increasing k and increasing l, again a probable consequence of the incomplete treatment of thermal data The two per cent scale factor correction to the observed structure factors was not inconsistent with the precision with which the scale was established

It should be emphasized that the interaction of temperature factors and atomic position parameters is almost negligible, once they each have been approximately determined The similarity of the structures obtained by neutron diffraction and x-ray diffraction despite large differences in the analyses of thermal motion is a striking example of this For this reason it is felt that the reliability of the parameters, distances and angles obtained in this investigation may be measured with some confidence by the statistically determined precisions given for them

G Precision of Parameters

Statistical methods were applied in determining the precision with which the atomic parameters were estimated in the present analysis Two methods were used, both of which give measures of the standard error expected from random errors in the data Possible systematic errors are not taken into account in these methods.

The first method is applicable to parameters obtained from resolved peaks in a Fourier map, and was described by Cruickshank[30]. The expression is the following:

$$\sigma(X_{rj}) = A^{-1}a_j^{-1}2\pi\left\{\sum_2 h_j^2 W_{hk}^2 \Delta F_{hk}^2\right\}^{1/2}/(\partial^2\rho/\partial X_j^2)_r$$

where X_{rj} is the coordinate in angstrom units of the rth atom in the jth direction, A is the area of the cell projection and a_j the length of the cell edge, h_j the index of the reflections referred to, a_j, $W_{hk}\Delta F_{hk}$ is the weighted residual $|F_{calc} - F_{obs}|$, and $(\partial^2\rho/\partial X_j^2)_r$ is the curvature of the peak of the rth atom along the jth direction The symbol $\sum_2$ indicates summation over both indices of the reflections employed in the projection The weight, W_{hk} in this case was the value of the modification function, $M_{(s)}$, by which each F_{obs} was multiplied in obtaining the Fourier map This method was used for all atoms except H_1 and H_2 in the (h0l) projection and for O_1, H_2 and H_3 in the (0kl) projection. The curvatures were estimated by treating each peak as though it were a parabola near the maximum

$$\rho(X) = \rho_0 - a(X - X_0)^2$$

where ρ is the scattering density and X the coordinate of that point. X_0 and ρ_0 are the values at the maximum of the peak Differentiating twice with respect to X and eliminating ρ_0 between equations for different values of X, it follows that

$$\partial^2\rho/\partial X^2 = -2a = 2(\rho_1 - \rho_2)/\left[(X_1 - X_0)^2\ (X_2 - X_0)^2\right]$$

The second method, which was used for parameters of unresolved atoms, was derived from the least squares treatment. If the normal equations used in determining the parameters of best fit are written in the form

$$\sum_i A_{ij}X_i = Y_j, \quad Y = 1, 2 \ldots$$

the solution may be carried out by inversion of the matrix whose

elements are A_{ij} It can be shown that the variance of the quantity X_1 is

$$Var(X_1) = (A_{11}^{-1}\sum\Delta F^2)/(N - n)$$

where A_{11}^{-1} is the diagonal term corresponding to X_1 in the inverse matrix, N is the number of independent observations and n the number of parameters determined, $\sigma(X_1)$ is, of course, the square root of this quantity

The atomic parameters and their estimated precisions are listed in Table XV

Table XV

Atomic Parameters and Estimates of Precision Oxalic Acid Dihydrate

Atom	x		y		z	
C	-0 0450	0 0013	0 054	0 003	0 0501	0 0003
O_1	0.0817	0 0009	-0 057	0 002	0 1467	0 0004
O_2	-0.2235	0 0010	0.227	0.005	0.0375	0.0005
O_3	-0.0452	0 0013	0.114	0 006	0.3222	0.0003
H_1	-0 1361	0 0032	-0.062	0 009	0.3506	0.0016
H_2	0 0729	0 0032	0.118	0 005	0 3870	0.0016
H_3	0 0227	0 0020	0.015	0 004	0.2180	0 0013

The precision with which parameters of carbon and the oxygen atoms were estimated was about 0 01 A or slightly less except for the y parameters of O_2 and O_3, which were not completely resolved The average precision of estimating parameters of hydrogen atoms was nearer 0 02 A, primarily because of the combined effects of hydrogen's smaller scattering amplitude and relatively large amplitude of thermal motion

H Interatomic Distances and Bond Angles

Calculation of interatomic distances was straightforward The monoclinic axes of the crystal were transformed to a Cartesian set scaled in Angstroms by the following transformation

$$X = x \quad a \sin \beta$$

$$Y = y \quad b$$

$$Z = z \quad c - x \quad a \cos \beta$$

X Y, and Z are the transformed coordinates of the point x, y, z in the space defined by the crystal axes a, b, c and the monoclinic angle β Transforming the parameters for any pair of atoms 1 and 2, the distance between them becomes

$$d_{12} = \left[(X_2 - X_1)^2 + (Y_2 - Y_1)^2 + (Z_2 - Z_1)^2\right]^{1/2}$$

The precision was found in terms of the variances of X, Y, Z These followed directly from the estimated variances of x, y, z and the transformation of x, y, z. Covariance between X and Z was ignored Then

$$\mathrm{Var}(d_{12}) = \left\{(X_1 - X_2)^2\left(\mathrm{Var}(X_1) + \mathrm{Var}(X_2)\right) + (Y_1 - Y_2)^2(\quad \right\}/d_{12}^2$$

Values of the interatomic distances of greatest interest are tabulated in Table XVI

Table XVI

Interatomic Distances and Estimated Precision Oxalic Acid Dihydrate

Atoms	Distance (A)	Standard Error (A)
C - C	1 533	0 011
C - O_1	1.254	0 008
C - O_2	1.229	0 014
O_1 - O_3	2 518	0 008
O_1 - H_3	1.057	0 016
O_3 - H_1	0.968	0 029
O_3 - H_2	0.945	0.021
O_3 - O_2'	2 840	0 008
O_3 - O_2''	2 856	0 008

Bond angles were calculated from the relationship

$$\cos \theta = (\underline{A} \quad \underline{B})/(|A||B|)$$

where $\underline{A}$ and $\underline{B}$ are vectors and θ is the angle between them Then the angle defined by the two bonds from an origin atom, 1, to two other atoms, 2 and 3 may thus be found from

$$\cos\angle 213 = \left[(X_2-X_1)(X_3-X_1) + (Y_2-Y_1)(Y_3-Y_1) + (Z_2-Z_1)(Z_3-Z_1)\right]/(d_{12}d_{13})$$

For angles not near 0° or 180° it can be shown that

$$Var(\cos \theta) = 2Var(X)(A^2+B^2+\underline{A}\ \underline{B})/A^2B^2$$

where A and B are the interatomic vectors defining the angle θ and with the simplifying assumption that the variances of all the parameters of each of the three atoms are equal to Var(x). In calculating precisions, the largest individual uncertainty was substituted for Var(x) Then $Var(\theta) = Var(\cos \theta)/\sin 2\ \theta$, and $\sigma\theta = Var(\theta)^{1/2}$, in radians

For angles near 0° or 180°, $\cos\theta$ is not a normally distributed function and the treatment preceding does not apply The procedure followed was to calculate the precision of the normal distance of one atom from the line joining the other two. If atom 1 is located nearly on a line joining atoms 2 and 3, a distance h away from it, and vectors $\underline{12}$, $\underline{13}$, and $\underline{23}$ are designated $\underline{a}$, $\underline{b}$ and $\underline{c}$, respectively,

$$\mathrm{Var}(h) = (h^2/c^2)\left\{\left[\mathrm{Var}(N)/h^2\right] + \mathrm{Var}(\underline{c})\right\}$$

where $N = |\underline{a} \times \underline{c}|$ and

$$\begin{aligned}\mathrm{Var}(N) &= (4N^2)^{-1}\mathrm{Var}(N^2)\\ &= N^{-2}\Big\{\mathrm{Var}(X_1)\left[(\underline{a} \times \underline{c}) \times \underline{c}\right]_X^2 + \mathrm{Var}(Y_1)\left[(\underline{a} \times \underline{c}) \times \underline{c}\right]_Y^2 + \\ &\quad + \mathrm{Var}(X_2)\left[(\underline{a} \times \underline{c}) \times \underline{b}\right]_X^2 + \\ &\quad + \mathrm{Var}(X_3)\left[(\underline{a} \times \underline{c}) \times \underline{a}\right]_X^2 + \quad \Big\}\end{aligned}$$

The values of $h + \sigma(h)$ and $h - \sigma(h)$ thus obtained define the limits of variation of θ so that

$$1/2\left[\theta_{(h+\sigma(h)} - \theta_{(h-\sigma(h)}\right] = \sigma(\theta)$$

approximately.

The following bond angles were calculated and precisions estimated

Table XVII

Bond Angles and Estimated Precisions

Bonds	Angle	Std Error
$C-C-O_1$	112°22'	0°41'
$C-C-O_2$	120°54'	0°50'
O_1-C-O_2	126°43'	0°57'
$O_1-H_3-O_3$	175°21'	2°0'
$C-O_1-H_3$	112°56'	1°40'
$H_1-O_3-H_2$	105°41'	3°0'
$O_3-H_2-O_2'$	167°2'	2°30'
$O_3-H_1-O_2''$	156°6'	3°0'

As might have been anticipated, angles and distances involving hydrogen atoms were found to be considerably less precisely known than those involving only carbon and oxygen atoms because of the greater uncertainty of the hydrogen parameters.

An interesting aspect of the acid molecule was the confirmation of the previously noted planarity of the carbon and oxygen skeleton, and the observation that the hydrogen atoms in the carboxyl group were less than 0 02 A out of the plane of the molecule, which is not significant displacement The sum of the bond angles around carbon was found to be 359°59', which with the presence of a center of symmetry between carbons, requires the molecule to be planar

I. Compatibility of X-ray and Neutron Diffraction Data

During the process of refining the (0kl) data an attempt was made to eliminate the resolution problem in the carbonyl group by combining

x-ray and neutron data The objective was to prepare a Fourier synthesis from combined neutron and x-ray data in which one atom of the unresolved pair was absent That this can be done in principle is shown from a consideration of the x-ray and neutron structure factors

The neutron structure factor is

$$F_N = \sum_i f_i T_i(h) \cos 2\pi(\underline{h}\ \underline{r_i}) + f_j T_j(h) \cos 2\pi(\underline{h}\ \underline{r_j})$$

and that for x-rays is

$$F_x = \sum_i \phi(h) T_i(h) \cos 2\pi(\underline{h}\ \underline{r_i}) + \phi_j(h) T_j(h) \cos 2\pi(\underline{h}\ \underline{r_j})$$

where f is a neutron scattering amplitude, $\phi(h)$ an x-ray atomic form factor, $\underline{h}$ the reciprocal lattice vector of a plane, T(h) the value of the exponential expression for the temperature factor, and $\underline{r}$ is the position vector of an atom One atom, the jth, has been segregated from the usual sum The linear combination

$$F_h = (F_N \phi_j(h)/f_j) - F_x$$

is seen to depend on contributions from all atoms except j, and a Fourier synthesis in which these quantities are the coefficients will consist of peaks centered in all atomic positions except that of atom j, with shapes characteristic of the combination form factor

$$(f_i/f_j)\phi_j(h) - \phi_i(h)$$

Combination syntheses were made in which first carbon and then oxygen peaks were removed The x-ray form factors calculated by McWeeny[32] were used, and two sets of (0kl) data were tried These were the data of Robertson and Woodward[10] alone and their data combined

with those of Brill et al[11], normalized by the procedure described by Ahmed and Cruickshank[13]. Unfortunately the method did not give satisfactory results, the oxygen combination peak appearing in two quite different locations for the two sets of x-ray data Since the neutron data were common to the two syntheses, it was believed that the x-ray data themselves were not wholly concordant and the method was not pursued further

Further consideration of the x-ray data tended to support this conclusion Ahmed and Cruickshank multiplied the structure factors of Robertson and Woodward by a so called temperature factor to normalize them to the structure factors of Brill et al This procedure seems to have little physical significance and is in fact of questionable empirical value A plot (Figure 8) of the logarithm of the ratios of Robertson and Woodward's structure factors to those of Brill et al versus $(\sin \theta/\lambda)^2$ does not show a linear trend, as it must if the "temperature factor" of Ahmed and Cruickshank could effect a normalization In Figure 9 the same ratio is plotted against the logarithm of the intensity measured by Brill et al Although the scattering of the points is considerable, there is much more evidence of a trend Apparently Brill et al consistently obtained higher values of F for small intensities than did Robertson and Woodward This can easily be a consequence of photographic estimation of intensity if the relation between blackening and intensity is not completely established

When refinement of the (0kl) neutron data was complete, a set of

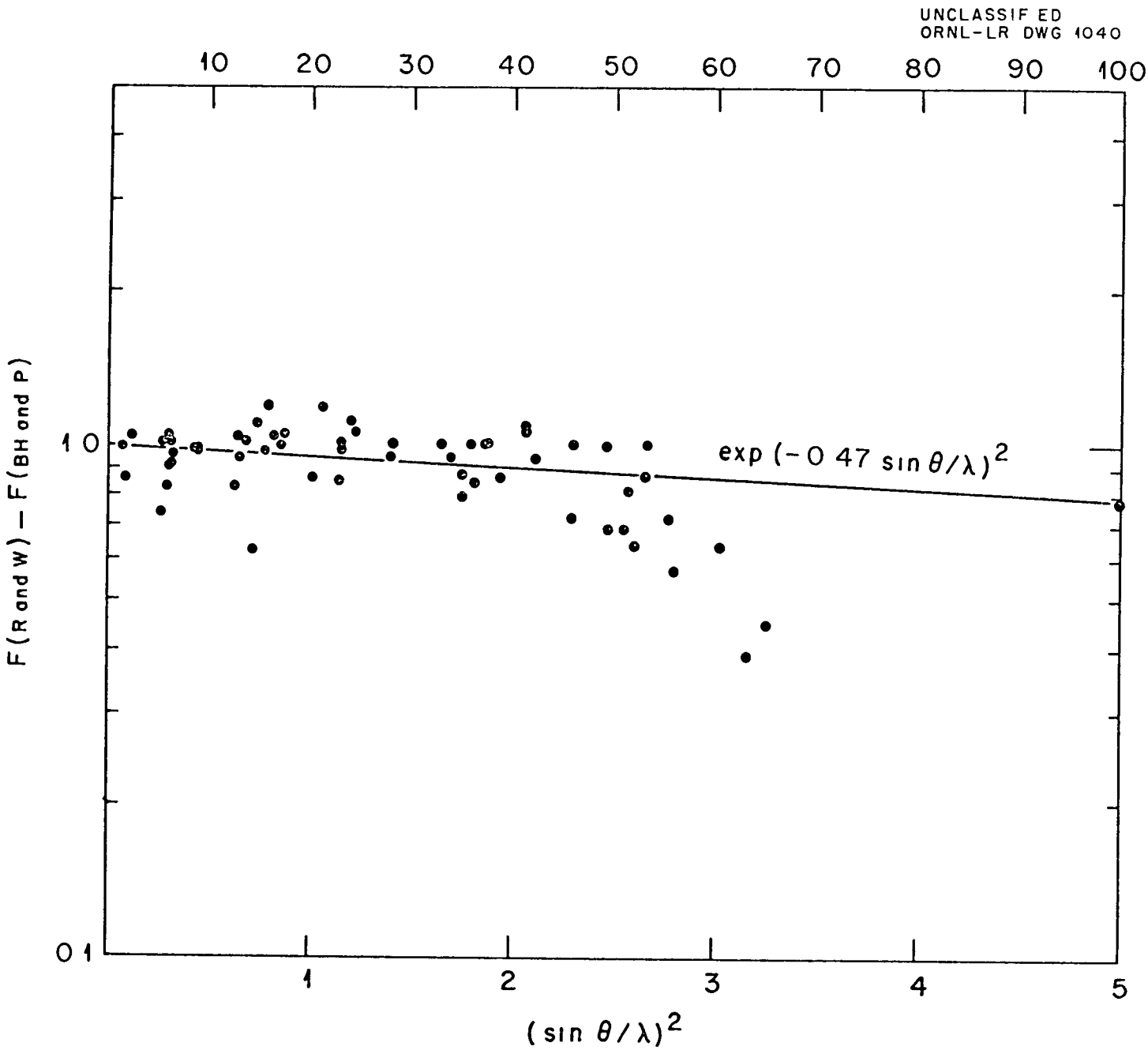

FIG 8

COMPARISON OF TWO SETS OF X-RAY DATA AS FUNCTIONS OF $(\sin \theta/\lambda)^2$

F (R and W) from Robertson and Woodward
F (B H and P) from Brill, Hermann and Peters
Line $[\exp(-0\ 47 \sin \theta/\lambda)^2]$ Is Normalizing Function of Ahmed and Cruickshank

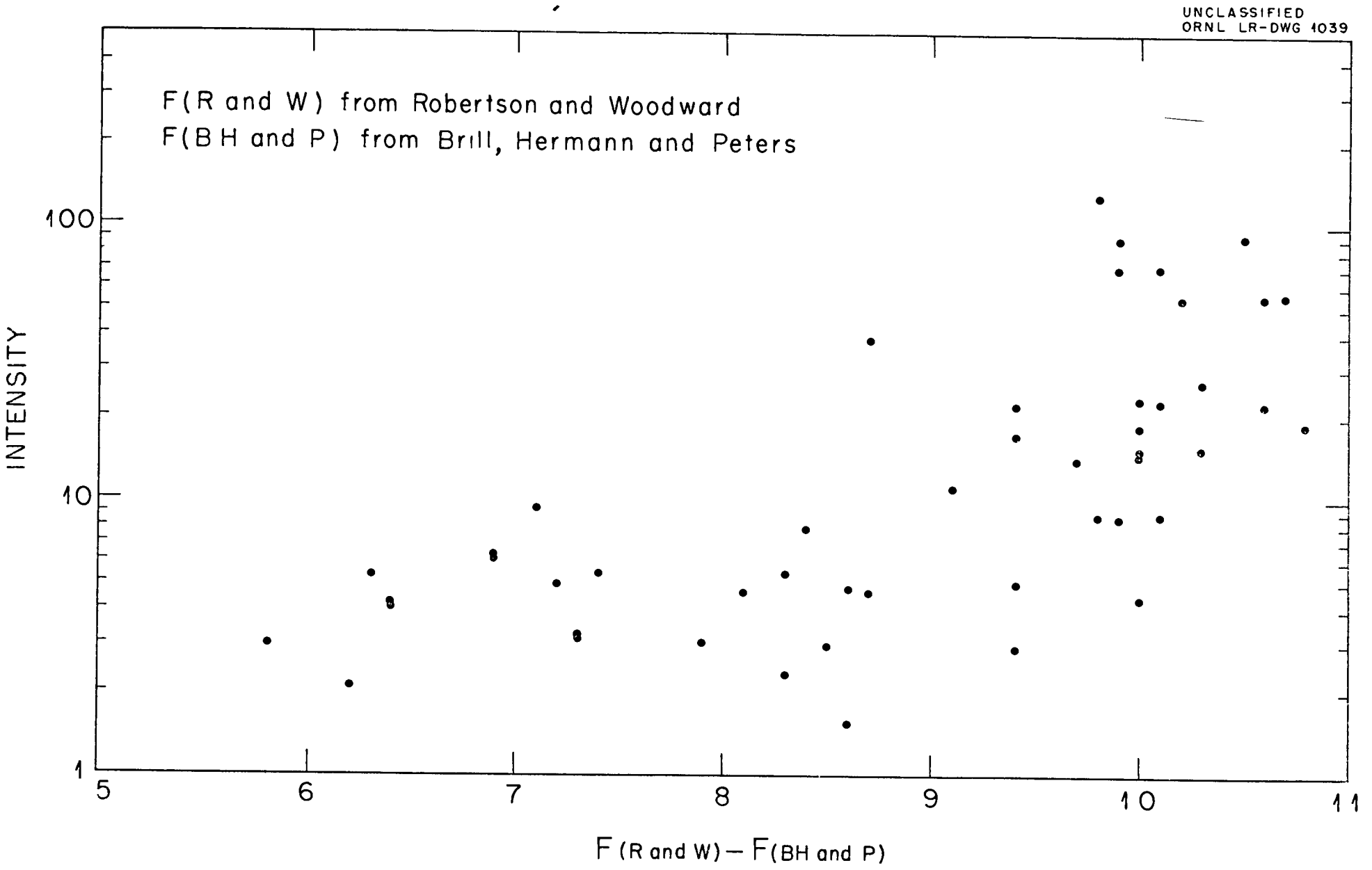

FIG 9

COMPARISON OF TWO SETS OF X-RAY DATA AS FUNCTIONS OF INTENSITY

x-ray structure factors was calculated from McWeeny's atomic form factors and the parameters and temperature factors from the neutron diffraction analysis Comparison with the combined set of x-ray structure factors gave an agreement factor of 17%, indicating the lack of concordance between neutron and x-ray analyses This undoubtedly arose in large part because of the very different temperature factors found

However, following the indication that weak reflections were estimated too high and noting that the intense reflections calculated high, it seemed sensible to seek the source of non-concordance in the x-ray data Intensities were calculated from the combined set of x-ray structure factors and for the set calculated from the neutron diffraction model A plot of the logarithms of these two quantities showed that there is a simple approximate relationship of the form

$$I_n = AI_x^B$$

where A and B are constants, I_n is the intensity calculated from the neutron model and I_x is the intensity calculated from the x-ray structure factors After graphical determination of the constants A and B, the x-ray intensities were corrected and a corrected set of structure factors was compared with the set from neutron model The agreement factor was found to be 11%, with the indication that a separate treatment of the data of Robertson and Woodward and that of Brill et al might yield still further improvement

While this agreement was better than any previously obtained for x-ray data for this zone, at least one other feature is open to some

question This is also related to the intensity measurement problem The treatments of x-ray data indicated no necessity for considering asymmetric thermal motion although it was clearly required by the neutron data The answer appears to be in over estimation of low intensities and insufficient sensitivity to many others which were observed zero It was noted that six of the eight (041) reflections were observed zero, as were five of the twelve (031) reflections Several of these reflections calculated appreciably more than zero and would have calculated even larger without asymmetric temperature factors The effect of this combination of circumstances was to destroy the detail in the map which might have led to the discovery of asymmetric thermal motion

It was concluded that a new x-ray determination of the structure factors, at least for the (0kl) zone of reflections, is desirable in order to test these hypotheses directly and to permit an adequate test of the method of combining data to resolve composite peaks

Discussion

A General Results of Structure Determination.

Determination of the structure of oxalic acid dihydrate by neutron diffraction confirmed the main features of the carbon and oxygen arrangements described by previous investigators[9,10,11,13]. The whole acid molecule, now including also the hydrogen atoms, is found to be planar. It was shown that the structure was composed of discrete water and acid molecules with no evidence of hydrogen disorder or

of OH_3^+ ions The C-C distance was found to be that of a single bond, in agreement with values reported by Brill, Hermann and Peters[11], and Ahmed and Cruickshank[13]. Values of parameters, interatomic distances and bond angles from various investigations are given in Tables XVIII, XIX and XX.

TABLE XVIII

Comparison of Atomic Parameters in Oxalic Acid Dihydrate as Determined by Several Investigators

Atom	Parameter	Investigator: Zachariasen[9]	Robertson and Woodward[10]	Brill et al [11]	Ahmed and Cruickshank[13]	This Investigation
C	x	-0 042	-0 037	-0 0465	-0 0455 ± 0 0011	-0 0450 ± 0 0013
	y	0 042	0 033	0 0615	0 0543 ± 0 009	0 054 ± 0 003
	z	0.055	0 051	0 0511	0 0507 ± 0 0005	0.0501 ± 0 0003
O_1	x	0 089	0 086	0 0828	0 0854 ± 0 0009	0 0817 ± 0 0009
	y	0 938	0 943	0 9440	0 9477 ± 0 004	0 943 ± 0 002
	z	0 150	0 148	0 1478	0 1485 ± 0 0004	0 1467 ± 0 0004
O_2	x	0 222	0 228	-0 2192	-0 2204 ± 0 0009	-0 2235 ± 0 0010
	y	0 222	0 214	0 2435	0.2156 ± 0 008	0 227 ± 0 005
	z	0 042	0 038	0 0362	0 0364 ± 0 0004	0 0375 ± 0 0005
O_3	x	0 556	0.548	0 5451	0 5473 ± 0 0009	0 5452 ± 0 0013
	y	0 626	0 608	0 6160	0 6028 ± 0 005	0 614 ± 0 006
	z	0 173	0 179	0 1780	0 1796 ± 0 0004	0 1778 ± 0 0003

Table XIX

Interatomic Distances in Oxalic Acid Dihydrate as Determined by Several Investigators

Bond	Investigator					
	Zachariasen[9]	Robertson and Woodward[10]	Brill et al.[11]	Dunitz and Robertson[12]	Ahmed and Cruickshank[13]	This Investigation
C - C	1 59 A	1 44 A	1 53 A	1.46 A	1 529 ± 0 020 A	1 533 ± 0 011 A
C - O_1	1.25	1 24	1 28	1.24	1 285 ± 0 012	1 254 ± 0 008
C - O_2	1.25	1 30	1 17	1 25	1 187 ± 0 022	1 299 ± 0.014
O_1 - O_3		2.52	2.51	2.50	2.491 ± 0 008	2 518 ± 0 008
O_3 - O_2'		2.84	2.90	2.89	2.879 ± 0 018	2.840 ± 0.008
O_3 - O_2''		2.87	2.90	2.89	2 879 ± 0 009	2 856 ± 0 008
O_1 - H_3						1 057 ± 0.016
O_3 - H_1						0 968 ± 0 029
O_3 - H_2						0 945 ± 0 021
H_1 - O_2''						1 944
H_2 - O_2'						1 911
H_3 - O_3						1 463

Table XX

Bond Angles in Oxalic Acid Dihydrate as Calculated from X-ray Diffraction Data and From Neutron Diffraction Data

Atoms Forming A B C	X-ray Determination Ahmed and Cruickshank[13]	Neutron Determination This Investigation
$C - C - O_1$	$112^\circ 34' \pm 1^\circ 3'$	$112^\circ 22' \pm 0^\circ 41'$
$C - C - O_2$	$121^\circ 38' \pm 1^\circ 4'$	$120^\circ 54' \pm 0^\circ 50'$
$O_1 - C - O_2$	$125^\circ 48' \pm 1^\circ 23'$	$126^\circ 43' \pm 0^\circ 57'$
$O_1 - H_3 - O_3$		$175^\circ 21' \pm 2^\circ 0'$
$C - O_1 - H_3$		$112^\circ 56' \pm 1^\circ 40'$
$O_3 - H_2 - O_2'$		$167^\circ 2' \pm 2^\circ 30'$
$O_3 - H_1 - O_2''$		$156^\circ 6' \pm 3^\circ 0'$
$H_1 - O_3 - H_2$		$105^\circ 41' \pm 3^\circ 0'$

B Comparison With Previous Structures

Attention is directed toward the structure of Ahmed and Cruickshank because their procedure, particularly the use of termination-of-series errors corrections, produced a more complete refinement of the data on which earlier structures were based The agreement between the atomic parameters, interatomic distances, and bond angles from their treatment with those with neutron diffraction is generally quite good In fact, considering the marked discrepancy in the isotropic temperature factors used by Ahmed and Cruickshank[13] and those used in the neutron diffraction analysis, and the complete omission of asymmetric temperature factors by them, the agreement is remarkable. It is a demonstration of the power of the Fourier syrthesis method of

determining atomic positions and the insensitivity of the atomic positions to other disturbing factors such as temperature factors and intensity scale

Several atomic parameters, x and z of O_1, x of O_2, and z of O_3 differ by amounts which are at least possibly significant, the differences being about twice the sum of the standard errors of the two determinations Since these atoms, with the exception of O_3 were all well resolved in the (h0l) projection, it is concluded that the differences result from differences in the two sets of experimental data, probably the same factors responsible for the much more serious differences in temperature factors Another atomic parameter is in less serious disagreement statistically, but is in question for other reasons The y parameter for the water oxygen, O_3, was estimated by Ahmed and Cruickshank to be 0 6028 ± 0 005, while the result from neutron diffraction is 0 614 ± 0 0006 There is some question as to the correctness of this value because the value obtained by Brill et al is 0 616 and the same value was read directly from a Fourier map prepared for comparison from Ahmed and Cruickshank's combined set of x-ray data This would indicate a termination-of-series error of 0 05 A, which seems unreasonably large to have escaped comment by Ahmed and Cruickshank With these exceptions, the part of the structure described by spatial parameters is in satisfactory agreement between the two methods

The descriptions of the thermal motion in terms of temperature factors are not concordant As already noted, the asymmetric component

of thermal motion was overlooked in the x-ray studies, probably because of the intensity measurement problem The abnormally large percentage of structure factors observed zero for $k = 3$ and $k = 4$ together with the probable overestimation of the intensities of the weakest observed reflections undoubtedly masked the systematic effect of asymmetric motion With respect to the isotropic temperature factors for carbon and oxygen, the effect of overestimating intensities of weak reflections would be expected to result in a reduced temperature factor, B, since reflections near the $\sin \theta/\lambda$ limit tend to be weak Some interesting relationships have been observed among the various values of B which have been estimated for carbon and oxygen The values used by Ahmed and Cruickshank[12] were determined by Finbank and Norman[32] by peak shape analysis, largely from the data of Brill et al [11] They were 1 42 for oxygen and 1 26 for carbon The value obtained for oxygen by dividing a Hartree form factor out of Robertson and Woodward's empirical form factor curve for oxygen is 1 8 If the normalization by Ahmed and Cruickshank had been to multiply the data of Brill et al by $e^{-0\ 47(\sin \theta/\lambda)^2}$ instead of multiplying the data of Robertson and Woodward by $e^{0\ 47(\sin \theta/\lambda)^2}$, the effective temperature factors for their combined data would have been 1.89 for oxygen and 1 73 for carbon, quite close to the values of 2 0 and 1 8, respectively, found in the neutron diffraction investigation This is probably a coincidence, however, since no physical basis for the normalization is evident (Figure 8)

In the course of attempting to resolve the (0kl) projection of

the carbonyl group by combining x-ray and neutron diffraction data directly into coefficients of a Fourier series, the question of the choice of x-ray form factor arose The form factors of McWeeny[31] were chosen because of indications from other structures that they represent an improvement over the older Hartree form factors Ahmed and Cruickshank observed that the best agreement factors were obtained using the empirical form factor curve of Robertson and Woodward The interesting observation was made that this form factor curve is approximately equivalent in shape to the product of the McWeeny form factor and a temperature factor The essential difference between the McWeeny form factor curve and a Hartree curve is in the flatness of the former below $\sin \theta/\lambda = 0\ 1$ The McWeeny curve lies above the Hartree curve out to $\sin \theta/\lambda = 0\ 5$, at which point they merge The improved agreement with an empirical form factor noted by Ahmed and Cruickshank was therefore probably not accidental.

C. Planarity of the Acid Molecule

All previous investigators have agreed that the oxalic acid molecule, or at least the two carbons and four oxygens of the acid molecule, lie in a plane (Figure 10). Because the C - C bond lies across a center of symmetry, the planes of the carboxyl groups must be parallel. The only additional requirement for planarity of the whole molecule is that the C - C bond lie in the plane of two C - O bonds That it does so is evidenced by the observation that the sum of the bond angles around a carbon atom is 359°59' The plane was found to

UNCLASSIFIED
DWG 21994

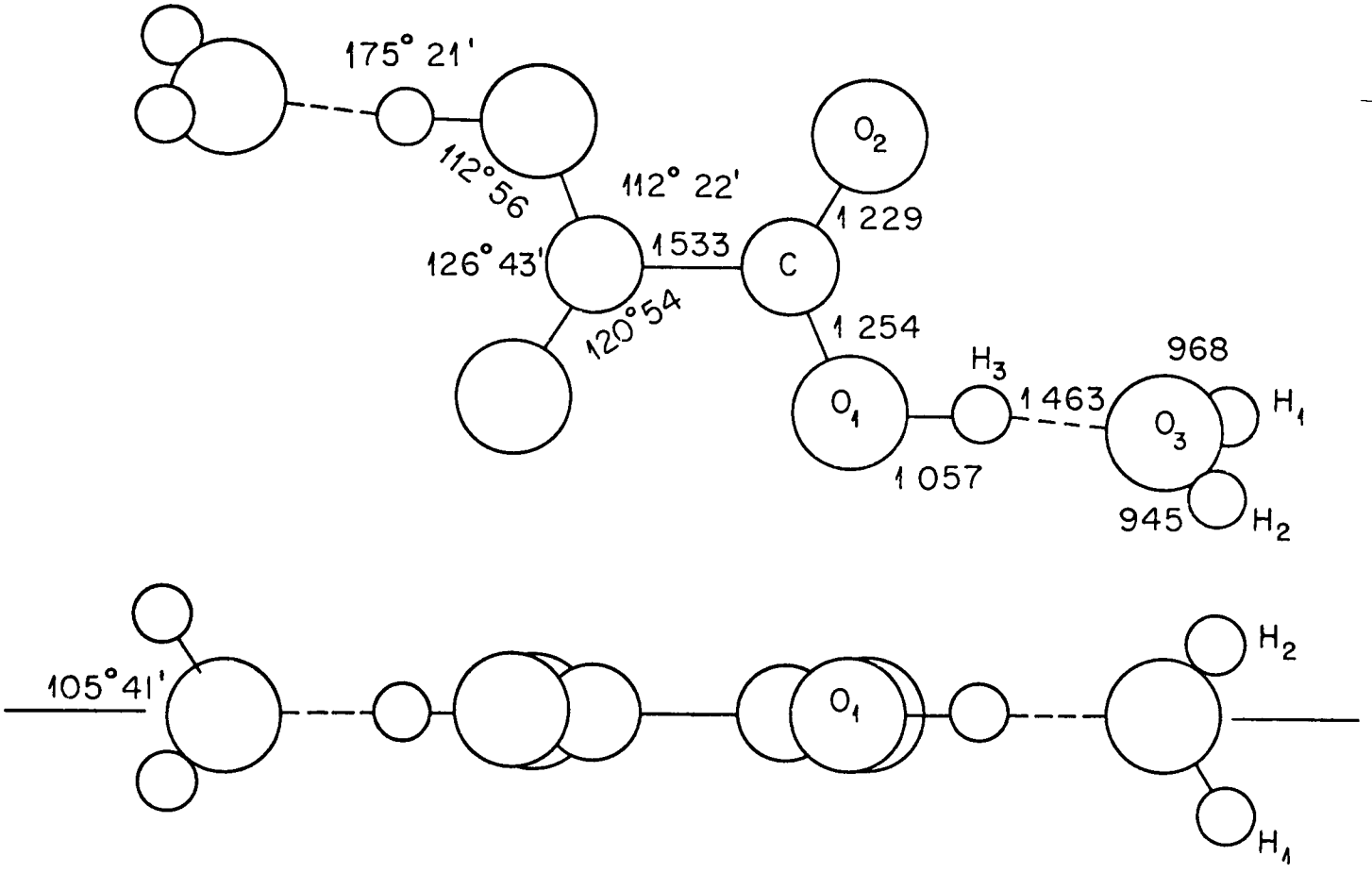

FIG 10

DIMENSIONS OF THE OXALIC ACID DIHYDRATE COMPLEX

Top View Normal to Plane of Acid Molecule
Bottom View in Plane of Acid Molecule
Distances in Angstroms (not Projected)
Angles Are Actual (not Projected)

include the carboxyl hydrogen atoms, whose distance from the plane was calculated to be less than 0 02 A, hardly a significant displacement This result was not unexpected in view of the large amount of double bond character indicated by the 1 254 A length of the C - O_1 bond.

The question of why the oxalic acid molecule should be planar in this compound and in both the α and β modifications of the anhydrous acid has been discussed in some detail by Cox, Dougill, and Jeffrey[33]. Jeffrey and Parry[34] observed that in the oxalate ion of ammonium oxalate dihydrate, the carboxyl groups are mutually rotated, the angles between planes being 28°; they pointed out that resonance across the molecule which would restrict rotation should have been greater for this compound than for the acid Cox, Dougill and Jeffrey concluded that the tendency for the acid molecule to be planar must be related to some intrinsic property of the molecule, discounting the probability that packing could be responsible, because of the widely different arrangements of the two anhydrous acid forms and the dihydrate

This investigation sheds no new light on the problem. If the results obtained on ammonium oxalate dihydrate are taken as conclusive evidence that rotation about the C - C bond in the acid is possible, and if the argument that C - O bonds with double bond character require the C - C and O - C - O links to be coplanar, is accepted, the problem in simplest form is to explain why the molecule has a center of symmetry in various environments The converse problem would be to explain why rotation about the C - C link is free in the ion and restricted in

the acid Both questions depend on evaluating quantitatively the factors favoring planarity, such as charge separation in the acid, possible small amount of π bonding across the C - C bond, packing effects and the opposing factors, including packing effects again, charge separation in the ion and many others Such a calculation probably could not be carried out in detail in a reasonable time

It may be noted that if both halves of the molecule are to be crystallographically equivalent they must be related by either a diad axis or a center of inversion, either constrains the molecule to planarity It is felt that packing, even in widely different structures, may be more efficient when both ends of the molecule are crystallographically equivalent The proof of this statement is not at hand, so it must remain a speculation

D Dimensions of the Acid Molecule

The central C - C bond does not differ significantly in length from the C - C bond in diamond, 1 5445 A The π bonding must be quite small or be opposed by a stretching force, such as Coulomb repulsion Essentially single bond lengths have also been observed in the anhydrous acid by Cox, Dougill and Jeffrey[33] and in ammonium oxalate dihydrate by Jeffrey and Parry[34]

The dimensions of the carboxyl group are in general agreement with those reported by Ahmed and Cruickshank[13], except that less difference was found between the C - O_1 and C - O_2 bond lengths by neutron diffraction The angles corresponding to C - C - O and C - C - O_2, respectively have been tabulated by Ahmed and Cruickshank

for several amino acids and the anhydrous α oxalic acid The angle $C - C - O_1$ ranges from $109^\circ 13'$ for anhydrous α oxalic acid to 117° for serine, angle $C - C - O_2$ from 117° for serine and 124° for N-acetylglycine The angles determined for oxalic acid dihydrate of $112^\circ 22'$ for $C - C - O_1$ and $120^\circ 54'$ for $C - C - O_2$ are typical of these ranges

The near equivalence in length of the two C - O bonds may be taken to indicate considerable resonance within a carboxyl group. If the two bonds were equivalent, the C - C - O angles might be expected to be equal, but they are found to differ by 9° This may not be of great significance because it was observed in the ion[34] that there are two C - C - O angles, differing by 2° where the distinction between the C - O bonds is crystallographic and not chemical It is probable that an assignment of bond orbitals could be made which would be consistent with the observed bond lengths and angles, taking into account the considerable effect of environment

The hydroxyl O - H bond was found to be 1 057 A in length and to lie in the plane of the molecule The large increase in O - H distance over the 0.96 A distance in H_2O gas may be largely attributed to the close (2.51 A) approach of the water oxygen, although the other bond in which the carboxyl O atom is involved may have some influence on the length of its O - H bond

E Dimensions of the Water Molecule

The (OH_3^+) ion suggested by Zachariasen[9] and Finbank and Norman[31] to be present in oxalic acid dihydrate has been conclusively ruled out

The water oxygen is close to only two hydrogens at distances of 0 968 and 0 945 A while the third hydrogen is 1 463 A away The dimensions of the water molecule in oxalic acid dihydrate are remarkably close to those of H_2O gas for which O - H = 0 96 A[35] and the H - O - H angle = 104°31'. The strong hydrogen bond in which the water oxygen is involved and the weak ones in which the water hydrogens participate seem to have little effect on the size or shape of the H_2O group

F Hydrogen Bonding

The hydrogen bond connecting the hydroxyl oxygen atom with the water oxygen atom must be quite strong The O - O approach of 2 52 A is among the shortest reported, and the O - H stretching (compared to gaseous water) of almost 0 1 A must correspond to a considerable attractive force from the water oxygen The bond is nearly linear, as might be expected for such a strong bond of electrostatic nature On the other hand, the hydrogen is definitely associated with the carboxyl hydroxyl group, with no indication of centering between oxygen atoms of the carboxyl group or between the water oxygen and a carboxyl oxygen There is no evidence of disorder in the hydrogen location

The hydrogen atoms of the water molecule are engaged in much weaker hydrogen bonds which tie together adjacent molecules of oxalic acid dihydrate The bonds extend from the water molecule of one oxalic acid dihydrate complex to the carbonyl oxygen atoms of adjacent oppositely tilted complexes (Figures 11 and 12) The bonds extend in opposite senses along the a and b axes of the crystal and in the same sense along c Four principal strings of hydrogen bonds can be

UNCLASSIFIED
DWG 21822

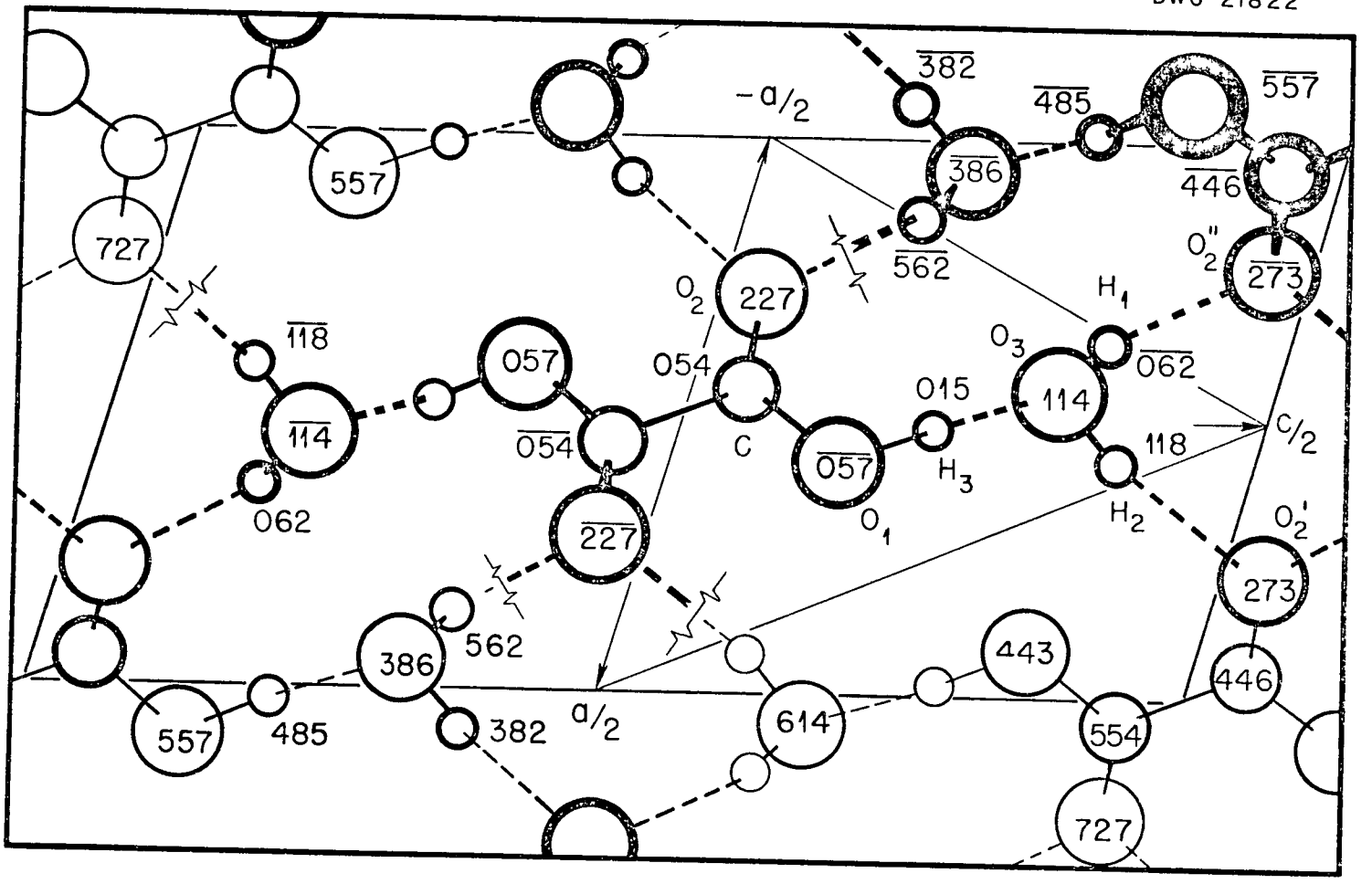

FIG 11

ILLUSTRATIVE DRAWING OF THE (hOl) PROJECTION OF OXALIC ACID DIHYDRATE

Dashed Lines Are Hydrogen Bonds
Solid Lines Connect Atoms Within a Molecule
Triangle Outlines Asymetric Unit Corresponding to Fourier Map (Fig 5)
Numerals at Atomic Positions Indicate Elevations in Fractions of the Cell Edges
Positive Direction of b Axis Is into the Drawing

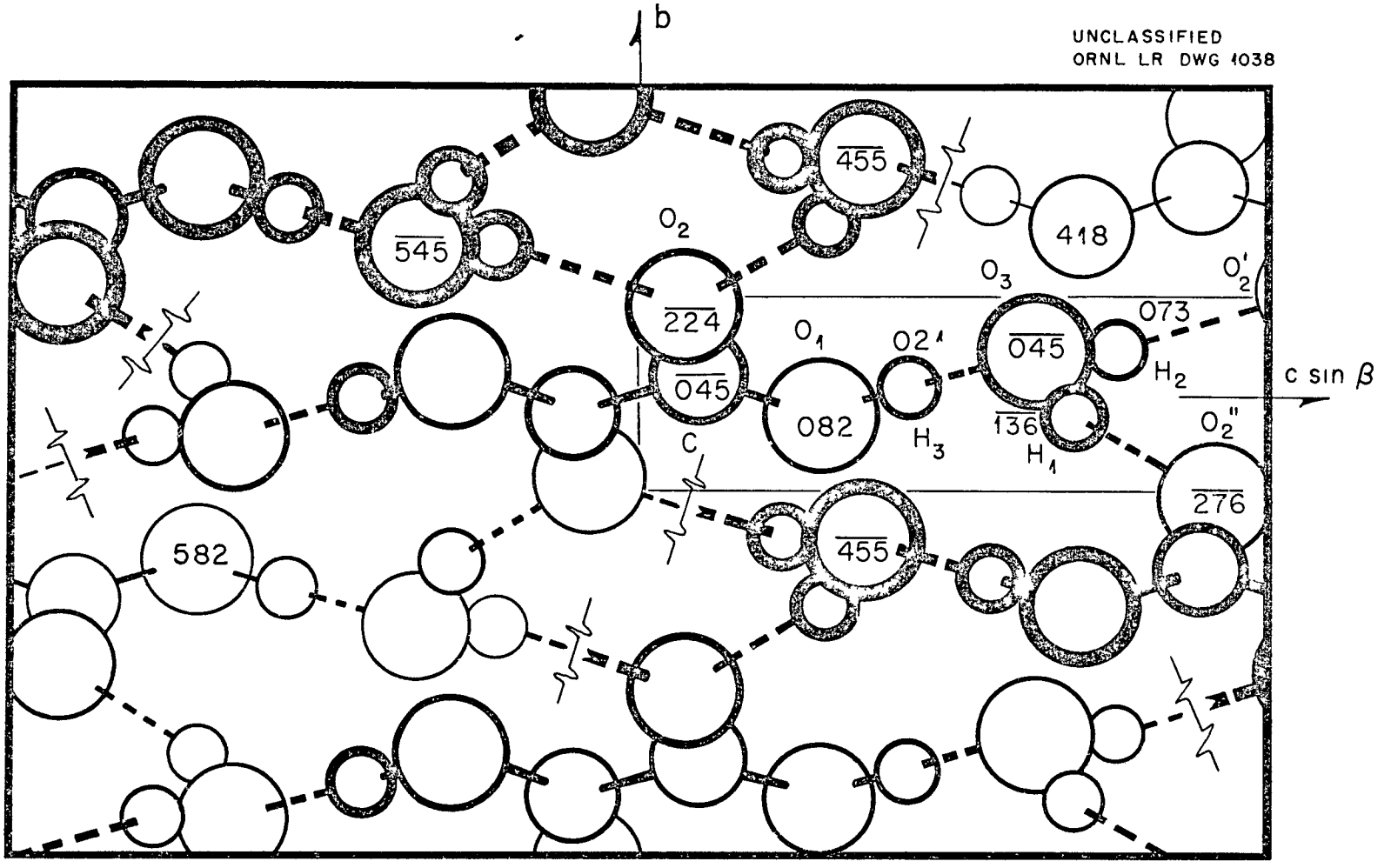

FIG 12

ILLUSTRATIVE DRAWING OF THE (Okl) PROJECTION OF OXALIC ACID DIHYDRATE

Dashed Lines Are Hydrogen Bonds
Solid Lines Connect Atoms Within a Molecule
Small Rectangle Outlines Asymmetric Unit Corresponding to Fourier Map (Fig 7)
Numerals at Atomic Position Indicate Elevations in Fractions of the Cell Edge
Positive Direction of the 'a' Axis Is into the Drawing

discerned in Figures 11 and 12 In Figure 11, beginning with O_3 and proceeding through H_1 to O_2'', thence across the carboxyl group to O_1'' and back to O_3'', it is seen that the $O_3'' - H_1''$ bond connects with a carboxyl group displaced one unit cell along b from the starting point, thus forming a helical chain parallel to the b axis Another helical chain parallel to b is formed by following from O_3 through H_2 to O_2', thence through the carbon - carbon bond of the acid to the water molecule at the other end of the acid molecule This water molecule connects through its H_2 atom with an acid molecule displaced one unit cell along b in the opposite direction from the starting point If a path is designated by specifying the links to be through H_1 atoms and the carbon - carbon bonds, a chain parallel to the long diagonal of the a - c plane is defined A path through H_2 atoms and across the carboxyl group from O_2 to O_1 defines a chain parallel to the short diagonal of the a - c plane

The weakness of these bonds is attested by several observations. The lengths of 2.84 A and 2 86 A are only slightly shorter than a normal O - O van der Waals contact of about 3 0 A The facts that the H - O - H angle was found to be near the 105° value for H_2O gas and that the O - H - O bonds are far from linear also suggest that the attractive forces involved in these bonds are considerably weaker than that between water oxygen and oxalic acid hydroxyl Comparison of the $O_3 - H_2 - O_2$ angle of 167° with the $O_3 - H_1 - O_2''$ angle of 156° suggests that the $O_3 - H_2 - O_2'$ hydrogen bond is somewhat stronger This is also consistent with the lengths of the $H_2 - O_2'$ and $H_1 - O_2''$

approaches of 1 911 A and 1 944 A respectively and with the greater amplitude of thermal motion observed for H_1

G Thermal Motion

The neutron diffraction data, particularly the (0k1) zone, gave clear indication of unusual thermal motion which was taken into account in the analysis by the approximation that there was an asymmetric component for certain atoms in the b direction Consideration of the values of the asymmetric temperature factors assigned to the atoms within the acid molecule strongly suggests that the motion involved is actually a libration about the C - C bond This follows from observation that the asymmetric temperature factors of the atoms O_1 and O_2 are equal while that of the C atom is zero The approximation that the asymmetric motion was directly along b, while not completely satisfactory, is seen to be the best simple assumption that could be made, since the acid molecule is only about 30° out of the a - c plane

It is not possible to obtain information about the modes of vibration involved from values of B, which are proportional to the mean square amplitude, an average quantity Speculation as to the modes of libration about the C - C bond favors contra-oscillation of the carboxyl groups rather than co-oscillation because the former preserves the symmetry of the crystal Such motion would be opposed by any stiffening of the C - C bond resulting from double bond character and consequently tends to confirm the essential single-bond character of this link The motion of the water molecule is apparently quite complex The outstanding features are the large motion of the

molecule as a whole and the relatively violent motion of H_1. The reason for the large motion of the molecule is not completely clear, but it undoubtedly is coupled through the three hydrogen bonds to the oscillating carboxyl groups of the acid molecules The large motion of H_1 probably results from the combination of several factors; the normally large isotropic thermal motion of hydrogen, the large anisotropic motion of the oxygen to which it is bonded, and the lack of restriction by the weak hydrogen bond it forms are all possible contributors

PART TWO

STRUCTURE OF ALPHA IODIC ACID

Introduction

The crystal structure of alpha iodic acid was originally investigated by Rogers and Helmholz[36], who used x-ray diffraction techniques They determined the symmetry and dimensions of the unit cell and carried out Fourier and Patterson analyses of the three axial projections, from which they estimated parameters for the iodine atom and the oxygen atoms

They found that the IO_3 group within each molecule forms a pyramid with I at the apex There are also three close approaches to each iodine atom by oxygen atoms of other molecules, completing an irregular octahedron around each iodine They found that one of three crystallographic kinds of oxygen made two equal approaches to oxygen atoms in other molecules They postulated that this oxygen atom is the hydrogen donor in a bifurcated hydrogen bond. They assigned parameters to hydrogen, assuming that the hydrogen is 1 01 A from the donor oxygen and is equidistant from the two acceptor atoms of the bifurcated bond

The structure proposed by Rogers and Helmholz may be described as composed of irregular IO_3 pyramids bound together by secondary I - O intermolecular bonds and by strings of hydrogen bonds along the b and c axes respectively

Wells[37] has criticized this interpretation in the following manner He postulated that, if close intermolecular I - O approaches are interpreted as evidence of weak bond formation, the short length of O - O distances within the coordination octahedron about a parti-

cular iodine is not evidence for hydrogen bonding. He observed that one of the acceptor oxygens in the proposed bifurcated hydrogen bond was in the same coordination octahedron as the donor oxygen, while the other acceptor was not He concluded, therefore, that the hydrogen bond was between the pair of oxygen atoms which were not in the same octahedron, the hydrogen bonds linking the molecules in chains parallel to the b axis.

The first objective of this investigation was to use the ability of neutron diffraction to locate hydrogen atoms directly in order to make a direct choice between the two suggested hydrogen bond arrangements Secondly, it was hoped that more precise determinations of the oxygen parameters might be made, since the neutron scattering amplitudes of iodine and oxygen are nearly equal. This information was desired in order to confirm the unusually close I - O approaches, which are significantly less than the conventional van der Waals contact distance of 3 5 A

Simultaneously with this investigation, a study of the nuclear quadrupole spectroscopy, including Zeeman effects, of alpha iodic acid was undertaken by Dr R Livingston and Dr H Zeldes of the Oak Ridge National Laboratory. This presented an opportunity to attempt to correlate structural information with information about the electric field gradient at the iodine nucleus, with the objective of describing the I - O bonds The quadrupole spectroscopy investigation is only partially complete at this time

The apparatus and equipment used in this investigation were the

same as described in Part One

Procedure and Results

A Crystallographic Description of Alpha Iodic Acid

The chemical formula of alpha iodic acid is HIO_3 The solid is a hard, nearly colorless crystal; The morphological properties are reported by Groth The unit cell is orthorhombic with space group symmetry $D_2^4 - P_{2_1}P_{2_1}P_{2_1}$, L aue symmetry D_{2h} The axial lengths are: $a_o = 5\ 536$ A, $b_o = 5\ 869$ A, $c_o = 7\ 731$ A, the unit cell has a volume of 251 2 A^3 There are four molecules per unit cell, and the calculated density is 4 651 g cm^{-3}, the observed density 4 63 g cm^{-3} The crystal is non-centrosymmetric, as evidenced by a positive test for piezo-electricity

The atoms ($4I$, $4O_1$, $4O_2$, $4O_3$) are in the general fourfold positions (x, y, z), $(1/2 - x, \bar{y}, 1/2 + z)$, $(1/2 + x, 1/2 - y, \bar{z})$, $(\bar{x}, 1/2 + y, 1/2 - z)$

B Procedure

1. Preparation of Specimens

Large crystals of iodic acid were supplied by Dr A N Holden of Bell Telephone Laboratories of Murray Hill, N J After morphological examination following Groth[38] to identify the faces and axes, specimens were cut from one large crystal, using the same general procedure as described above in Part One It was found that the crystal could be satisfactorily sawed with a wetted jeweler's saw Final reduction and polishing was accomplished by rubbing with a warm damp cloth

Two specimens for the (h0l) and (0kl) zones, respectively, were prepared, a small specimen of about 0.5 mm radius, and a larger one of about 1 5 mm radius. The specimens were thinly coated with Duco cement and immersed in liquid nitrogen to reduce extinction effects

Considerable difficulty was experienced in preparing the larger (h0l) specimen The crystal exhibits a perfect cleavage along (101), with the result that immersion in liquid nitrogen usually caused the larger specimens to split into two or more partially mis-oriented segments The specimen which was used was originally the lower third of a larger specimen which split along its axis for two thirds of its length. Careful examination of the unsplit fragment indicated that it had retained its identity as a single crystal, and that it was acceptable as a diffraction specimen.

2 Alignment of the Specimens and Preliminary Examination on the Neutron Spectrometer

The crystal specimens were cemented to a glass fiber and mounted on a two circle goniometer head, which was then set on a spindle on the spectrometer table After confirming the identity of the rotation axis of the crystal by observation of several reflections at the proper scattering angles and crystal settings, alignment of the crystal was undertaken. Following physical centering of the specimen in the neutron beam, the first step in the procedure consisted of rotating the crystal about the vertical axis of the goniometer until the two sets of basal planes of the zone were each parallel to the direction of motion of a goniometer circle. By setting the spectrometer counter

at the proper scattering angle and maximizing the intensity of a given basal reflection by adjusting the goniometer circle perpendicular to this plane, then repeating alternately for reflections in each of the two sets of basal planes, a procedure which converged on the proper alignment was established

After alignment, the equivalence of the intensities of 0kl and 0k$\bar{l}$ and h0l and h0$\bar{l}$ was verified, as was the occurrence of the space group absences of $P2_12_12_1$, which are: h00, $h \neq 2n$, 0k0, $k \neq 2n$; 00l, $l \neq 2n$.

3. Standardization and Calibration

The method of calculating structure factor magnitudes from experimental intensities was the same as described for oxalic acid dihydrate in Part One above No resolved powder peaks could be measured The only resolved peak (002) was quite weak. The neutron scattering amplitudes used were $f_H = -0.38$, $f_O = 0\ 58$ and $f_I = 0.52$.

4. Absorption Corrections

Before specimens were cut from the large single crystal, which was in the form of a slab, transmission measurements were made to determine the absorption coefficient The slab thickness was 0 742 cm, I/I_0 was 0 53; μ_ℓ was determined to be 0 837 cm^{-1}.

5. Secondary Extinction.

When no intense powder reflections are resolved, no direct check of extinction effects can be made If most of the structure is already known with fairly good precision, however, indirect methods of checking are believed to be applicable The problem of estimating

and correcting for extinction has the effect of adding one to the number of parameters to be determined, provided that the simplifying assumption is made that extinction is isotropic with respect to directions in the crystal.

After experimental structure factor magnitudes have been determined, the first step is to compare them with those calculated from the approximate structure Particular attention is paid to low index intense reflections, because their intensities are relatively insensitive to variations in atomic parameters and temperature factors. If extinction is important, the experimental structure factors will average smaller than the calculated structure factors, the deviation increasing with intensity. The problem then becomes one of finding the correct function with which to correct experimentally observed intensities

The effect of not too severe extinction on intensity measurements can be approximately expressed analytically as that of a variable absorption coefficient which is proportional to intensity. The combined effect of normal absorption and extinction can be written

$$E_{obs} = AE^{o}$$

where E_{obs} is the observed integrated intensity, E^{o} is the integrated intensity corrected for absorption and secondary extinction, and A is a function of μR which is no longer a constant for the specimen. If μ_e is the effective absorption coefficient

$$\mu_e R = (\mu_\ell + hE^{o})R$$

where h is a constant which determines the dependence of μ_e on

intensity, that is, the effect of secondary extinction The procedure for determining the best value of h depends on finding values of A for several intensities This is done by comparing observed with calculated intensities for the least sensitive intense reflections From the corresponding values of $\mu_e R$, the constant μ_ℓ is subtracted, giving hE^oR Since E^o has been calculated and R is known, h is determined A plot of A versus E_{obs} is constructed from the values of hR and $\mu_\ell R$ determined for the specimen, and structure factor magnitudes, corrected for extinction, are calculated using the variable absorption correction A

The question of the validity of the extinction correction cannot be answered directly when no standard of reference is available It is possible to apply tests of internal consistency to the data, in many cases, however When an extinction correction has been made, the results must be compared with some set of data in which extinction is not believed to be important As a rule, extinction is less important in small specimens Hence, if constant values of structure factors are obtained over a range of crystal sizes, it is taken as an indication that extinction is probably not present If the comparison of observed structure factors with those calculated from an approximate structure shows a random correlation, with the observed structure factor magnitudes exceeding the calculated ones as often as not, extinction is probably not important

Comparison among specimens can be done only within a single zone of reflections It is probably necessary to have data on several

specimens in a zone in order to make with confidence the assumptions that extinction is absent in the smaller specimens and that the correction applied to the largest one is valid

A less direct, but possibly more conclusive, method of comparison is between Fourier maps of different zones. If one set of zonal data appears to require an extinction correction and another does not the peak shapes of a particular atom should be the same in both projections, provided that the amplitudes of thermal motion are not too different Inequality between zones indicates inconsistency which is not necessarily a result of incorrect extinction correction, equality between zones would seem to require rather great coincidence, if accidental, and is taken as an indication that the correction is correctly made

6 (0kl) Data

The dimensions of the two (0kl) specimens are given in Table XXI

Table XXI

Dimensions of the (0kl) Specimens of Alpha Iodic Acid

Specimen	Large	Small
Ht (mm)	7 0	6 0
Wt (mg)	175.2	46.1
Radius (mm)	1.30	0 73
$\mu_\ell R$	0 11	0 061
A (%)	83	90

Nine of the most intense reflections were measured on the small specimen; all seventy-six reflections which were within the range of spectrometer at λ = 1 062 A were measured on the larger specimen

The magnitudes of the structure factors were calculated from the experimental intensities in the same way as described for oxalic acid dihydrate in Part One above The magnitudes of the structure factors for the nine reflections measured on both specimens are given in Table XXII

Table XXII

Comparison of Structure Factors from Large and Small (0kl) Specimens of Alpha Iodic Acid

Reflection	|F| large	|F| small
004	1.27	1.30
006	2.55	2 71
011	1.21	1 33
012	1 65	1 97
015	1.39	1.39
022	2.65	3 05
036	1.94	2 04
043	3 61	3 67
053	1.30	1 23

The values obtained on the large specimen were generally smaller There appeared to be a trend with intensity, indicating possible extinction effects in the data from the large specimen. Because of the lack of a comparison with a powder peak it was not possible at this time to determine the extent of extinction in either specimen

7. (h0l) Data

The dimensions of the h0l specimens are given in Table XXIII.

Table XXIII

Dimensions of the (h0l) Specimens of Alpha Iodic Acid

Specimen	Large	Small
Ht. (mm)	3 6	7.0
Wt (mg)	134 0	45.9
Radius (mm)	1.60	0 67
$\mu_{\ell}R$	0.134	0 056
A (%)	80	91

Seven of the most intense reflections were measured on the small specimen and all seventy-two reflections within the sin θ/λ limit of the spectrometer at λ = 1.062 A were measured on the larger specimen the magnitudes of the structure factors measured on both specimens are given in Table XXIV

Table XXIV

Comparison of Structure Factors from Large and Small (h0l) Specimens of Alpha Iodic Acid

Reflection	|F| large	|F| small
004	1 29	1 35
102	1.43	1.38
103	4.53	3.02
204	2.08	1.97
305	2.98	2.77
400	2.62	2.46
503	1.73	1.54

The rather surprising observation was made that extinction in the small specimen appeared to be more serious than in the larger one An explanation for this may lie in the different histories of the specimens after they were formed from the slab The larger specimen suffered violent mechanical as well as thermal shock, and had the appearance of being more completely reduced to small oriented fragments than did the smaller specimen, which remained relatively transparent optically

Analysis of Diffraction Data

A Methods

The overall scheme of analysis of the data from both zones was similar to that used in the analysis of oxalic acid dihydrate data. With the exception of the extinction correction problem the procedure was simpler and more straightforward Determination of signs of the structure factors was less involved because the contributions of hydrogen were relatively less important

In the (0kl) projection, after an extinction correction (described below) was made, the procedure consisted of obtaining a final experimental Fourier map and correcting the parameters by the backshift method In the (h0l) projection the backshift correction could be made to only two atoms, and final refinement of the x-parameters of the other three atoms was done by the method of least squares.

In general the structure factors of a non-centrosymmetric structure, such as this one, are complex, and the determination of the structure factors is a difficult problem Fortunately, however,

the projections of space group $P2_12_12_1$ are centrosymmetric, and the problem was again one of sign determination

B The (0kl) Zone

Most of the signs of the structure factors were determined by the iodine and oxygen contributions These were estimated by applying an approximate temperature factor correction to contributions calculated from the atomic parameters of Rogers and Helmholz[36] The approximate average temperature factor for iodine and oxygen was estimated from the fifteen reflections of highest $\sin \theta/\lambda$ from the relation

$$\exp\left\{-B_{av}\overline{(\sin \theta/\lambda)^2}\right\} \sim \frac{\Sigma(F_{obs})}{\Sigma(F_{calc})},$$

ignoring the hydrogen contributions An average B equal to 1 7 was estimated in this way

Most of the remaining signs were determined by assignment of approximate parameters to hydrogen The z parameter was determined to be near $(2n + 1)/8$ in accord with the observation that the hydrogen contribution was nearly zero for (002) and near a maximum for (004) and (008) Extension of this argument to include other reflections led to the assignment of $z = 1/8$ for hydrogen Observation that hydrogen contributions were large but not maximal for (020) and (060) and nearly zero for (040) led to the assignment $y = 5/16$ for hydrogen Signs for all reflections except (002), (013), (035), (040), (051), and (063) were determined, assuming B_H equal to 2.5 A Fourier series was prepared using these signs and the modification function

illustrated in Figure 13 This modification function has the form of an exponential, $e^{-1\ 4(\sin\theta/\lambda)^2}$ out to $\sin\theta/\lambda$ equal to 0 625, from this point out to $\sin\theta/\lambda$ equal to 0 780 additional convergence is added by multiplying the exponential by a parabolic function. Parameters were read by Gaussian interpolation of the atomic peaks After calculation of a new set of structure factors, the signs of (002), (040), and (063) remained undetermined

At this time it was observed that the Fourier peaks of three oxygen atoms were not equal and were all lower than those in a concurrently prepared projection of the (h0l) zone After a peak shape analysis indicated a change in B of iodine to 1 0, a new set of (0kl) structure factors was compared with the sets from the large and small specimens The presence of extinction was clearly evident and an effort was made to effect a systematic correction Since extinction was less serious in the small specimen, a correction was first estimated for it

Because the calculated value of (022) appeared to be relatively insensitive to atomic parameters, a value of hR for the small crystal was calculated in the manner described above, assuming the calculated value of F (022) to correspond to the true integrated intensity, E^o The value $hR = 7\ 9 \times 10^{-4}$ and the observed $\mu_\ell R$ of 0 061 were used to construct a plot of E_{obs} versus A, and the remaining eight reflections were corrected.

Extinction in the large crystal was more severe and apparently not perfectly isotropic Approximate values of hR for the large

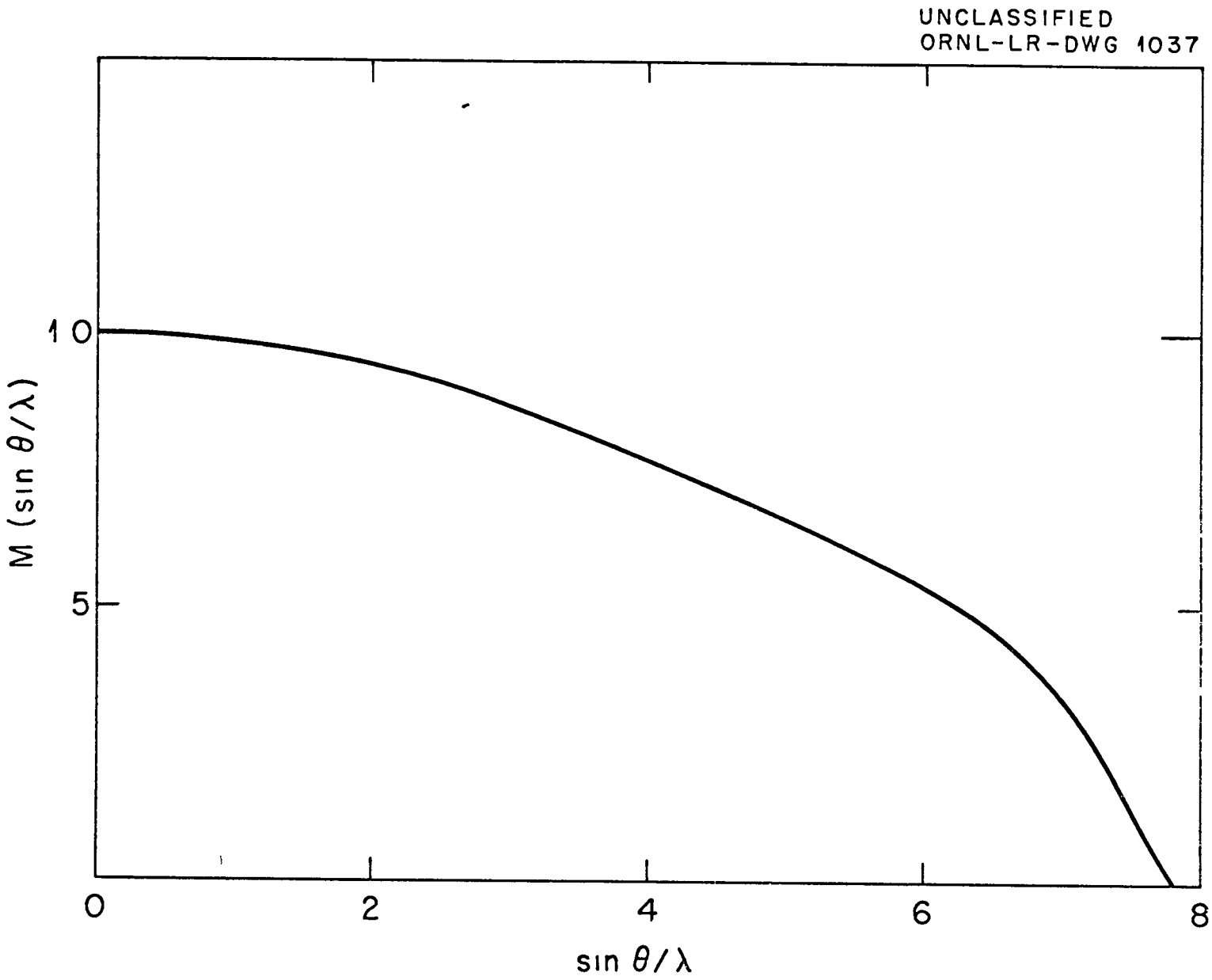

FIG 13
MODIFICATION FUNCTION USED TO INTRODUCE ADDITIONAL CONVERGENCE INTO ALPHA IODIC ACID DATA

crystal were calculated for several reflections and the average used to correct all of the thirty-four reflections which seemed to show extinction Several values of hR near this average value were evaluated, the value of 7 0 x 10^{-4} being chosen on the basis of giving the best all around fit between the two specimens and between calculated and corrected observed structure factors for the large crystal.

A Fourier map (Figure 14) was prepared with the corrected coefficients in which the oxygen peak heights were equal and also equal to the resolved oxygen peaks of the (h0l) projection within ± 1 5% Peak shape analysis of this final map indicated the best values of B to be 0 5 to 1 0 for iodine, 1 3 for oxygen, and 2 5 for hydrogen A value of 0 75 for iodine was finally chosen on the basis of the agreement factor, R, which was 9 9% A backshift map was prepared and termination-of-series corrections were made With the exception of a correction of 0 027 A to y of hydrogen all of the termination-of-series corrections were less than 0 010 A The final agreement factor was 9 3% The final y and z parameters obtained for alpha HIO_3 are given in Table XXV

Table XXV

Final y and z Parameters from (0kl) Projection of Alpha Iodic Acid

Atom	y	z
H	0.3220	0 1350
I	0 0861	0 1580
O_1	0 5225	0 2429
O_2	0.1978	0 0864
O_3	0.1566	0 4481

UNCLASSIFIED
DWG 21996

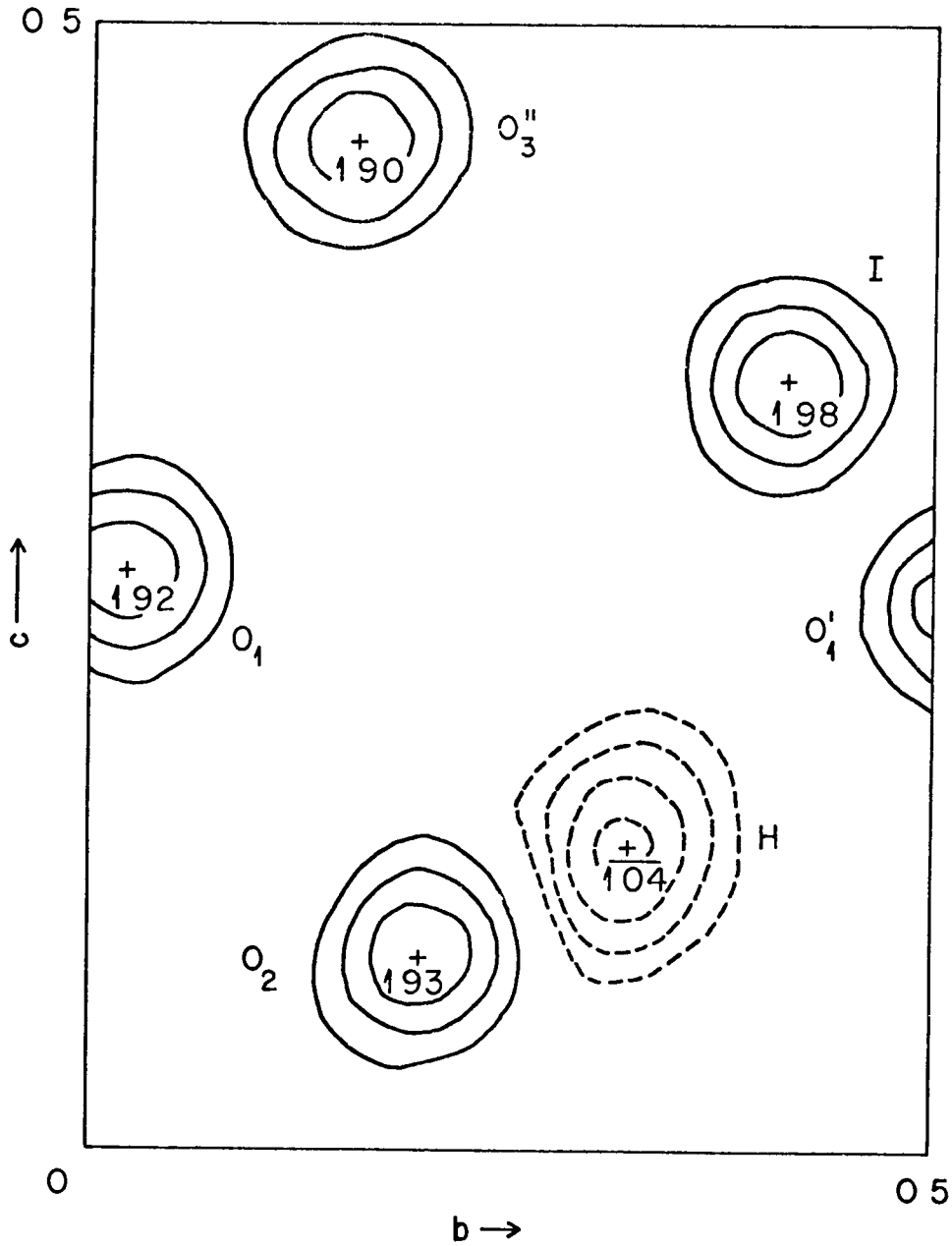

FIG 14

FOURIER MAP OF THE (0kl) PROJECTION
OF ALPHA IODIC ACID

Solid Lines Are Positive Contours at
Intervals of 0 50 x 10^{-12} cm/A^2
Dashed Lines Are Negative Contours at
Intervals of 0 25 x 10^{-12} cm/A^2
Zero Contour Omitted
Crosses Locate Positions of Atoms
Numbers (x 10^{-12}) Indicate Maximum
Values of the Scattering Density

The final parameters for hydrogen are seen to be reasonably close to the estimated parameters, y = 0 312 and z = 0 125. No signs changed as a result of the more precise estimation of the hydrogen position

Experimental structure factors, before and after extinction correction, are listed for comparison with calculated structure factors Where two values are given in the list of uncorrected experimental structure factors, the second refers to the smaller specimen The reported corrected value is an average of the two corrected values.

Table XXVI

Comparison of (0kl) Structure Factors of Alpha Iodic Acid Observed Values Before and After Extinction Corrections and Calculated Values

Reflection hkl	$\lvert F_{obs} \rvert$	$\lvert F_{corr} \rvert$	F_{calc}
002	24	24	- 04
004	1 27, 1 30	1 31	+1 37
006	2 55, 2.71	2 97	-3 08
008	1 49	1.49	-1 32
0 0 10	2.97	3.43	-2 71
011	1.21, 1 33	1 34	-1 42
012	1 65, 1 97	1 88	+1 91
013	1.00	1.00	+ 96
014	1.59	1.63	-1.59
015	1 39, 1 39	1 44	-1.46
016	2 22	2 44	-2 44

Reflection hkl	$\lvert F_{obs} \rvert$	$\lvert F_{corr} \rvert$	F_{calc}
017	1.61	1 67	-1 78
018	1.27	1.27	+1 23
019	2.02	2 02	+1 93
0 1 10	1 26	1 26	-1 24
0 1 11	2 16	2 31	+2.36
020	1.26	1.36	+1 33
021	1 32	1.42	-1.28
022	2.65, 3 05	3 95	-4 08
023	2 21	2.59	-2.62
024	1 18	1 18	+1.32
025	3 09	4 40	-3 66
026	1.18	1 18	+1 05
027	.99	99	+1 04
028	2.48	2.74	+2 75
029	57	.57	+ 42
0 2 10	1.77	1 85	-2 07
031	2.02	2 27	-2 31
032	1.66	1.78	-1 74
033	1.72	1.84	+1 65
034	1.10	1 10	+1.16
035	.35	.34	+ .24
036	1.94, 2 04	2.17	+2 14
037	0	0	- 05

Reflection hkl	$\lvert F_{obs} \rvert$	$\lvert F_{corr} \rvert$	F_{calc}
038	1 98	2 09	+1 98
039	1 38	1 38	+1 33
0 3 10	.44	44	- 18
040	25	.25	+ 04
041	2 24	2.52	+2.54
042	1.97	2.14	-2.10
043	3.61, 3 67	4 50	+4 77
044	1.25	1 25	+1.39
045	1.12	1 12	-1 10
046	1.98	2 07	-2 17
047	1.63	1 63	+1.33
048	2 02	2.13	+1 72
049	.66	66	- 62
0 4 10	91	.91	+ 73
051	1 48	1.48	+1 50
052	.57	.57	+ .52
053	1.30, 1 23	1 27	+1.38
054	2.19	2 37	+2.25
055	.83	.83	- 63
056	.81	81	- .76
057	.58	.58	- 73
058	2.15	2 29	-2.15
059	.63	.63	- 84

Reflection hkl	F_{obs}	F_{corr}	F_{calc}
060	.76	.76	+ .87
061	1 63	2 37	-2 19
062	.97	.97	+1.15
063	.30	.30	- .01
064	2 64	2.96	+2.74
065	0	0	- .72
066	3.11	3.64	-3 49
067	1.95	1 95	+1 91
068	.71	71	- .57
071	0	0	+ 08
072	2.47	2.73	-2.87
073	.67	.67	- .80
074	.98	.98	- 86
075	.73	73	- .51
076	.28	.28	- 63
080	1.09	1.09	- 71
081	2.69	3.02	-2 49
082	1.13	1.13	- 89
083	.71	.71	+ .36

C The (h0l) Zone

Signs were determined in the same way as in the (0kl) zone. Hydrogen was assigned an x parameter of 1/4 on the basis of the magnitude of its contribution to (200), (404) and (208) An experimental Fourier map was prepared using the same modification function, (Figure 13) Structure factors from the larger crystal were used since it showed less extinction Reflections (002), (404), (408) and (705) were omitted Only the oxygen atoms were sufficiently well resolved that parameters could be read directly, the hydrogen and iodine atoms were almost completely overlapped In order to obtain an approximate x parameter for hydrogen, a graphical method of removing the iodine peak was employed Assuming that the iodine peak had the same shape in both projections and that its x-ray parameters were correct, the values of the scattering density ascribable to iodine at the various points in the compound peak were subtracted A negative peak of poor quality having approximately the expected size for hydrogen remained The x parameter of this peak was estimated to be 0 225

A set of structure factors was calculated from the oxygen x parameters read from the map, with a hydrogen x parameter of 0 225, and Rogers and Helmholz' value for x of iodine The z parameters were those obtained from the (0kl) projection An agreement factor of 12 3% was obtained Comparison of calculated and observed structure factor magnitudes disclosed no systematic correlation

with intensity, and it was concluded that extinction was negligible. The data from the small crystal were discarded Signs for (408) and (705) were determined and the final experimental map (Figure 15) was prepared.

The graphical method of removing the iodine peak was not a satisfactory one Trial values indicated substantial improvement in agreement for x of hydrogen equal to 0.229 In order to resolve the H, I and O_2 atoms more systematically, a least squares treatment of the x parameters of those atoms and the temperature factor of hydrogen was carried out The value of x for hydrogen was increased to 0 233 and B_H to 3 5 by the least squares analysis and the agreement factor dropped to 10 0%. A backshift to correct termination-of-series errors in the O_1 and O_3 peaks was carried out, followed by a final least squares on the unresolved trio of atoms The only backshift correction was 0 006 A to x of atom O_1 The final hydrogen x parameter was 0.234

The least squares treatment indicated a further increase in B_H to 4 3, but this result is viewed with some suspicion. The meaning of the result is not clear If it is accepted literally as a large isotropic temperature factor, it must be observed as a large anisotropic component in the hydrogen peak in the (0kl) projection Unfortunately the interpretation of the hydrogen peak in the (0kl) projection is not straightforward because of overlap and poor general definition If the result is not interpreted literally,

UNCLASSIFIED
DWG 21991

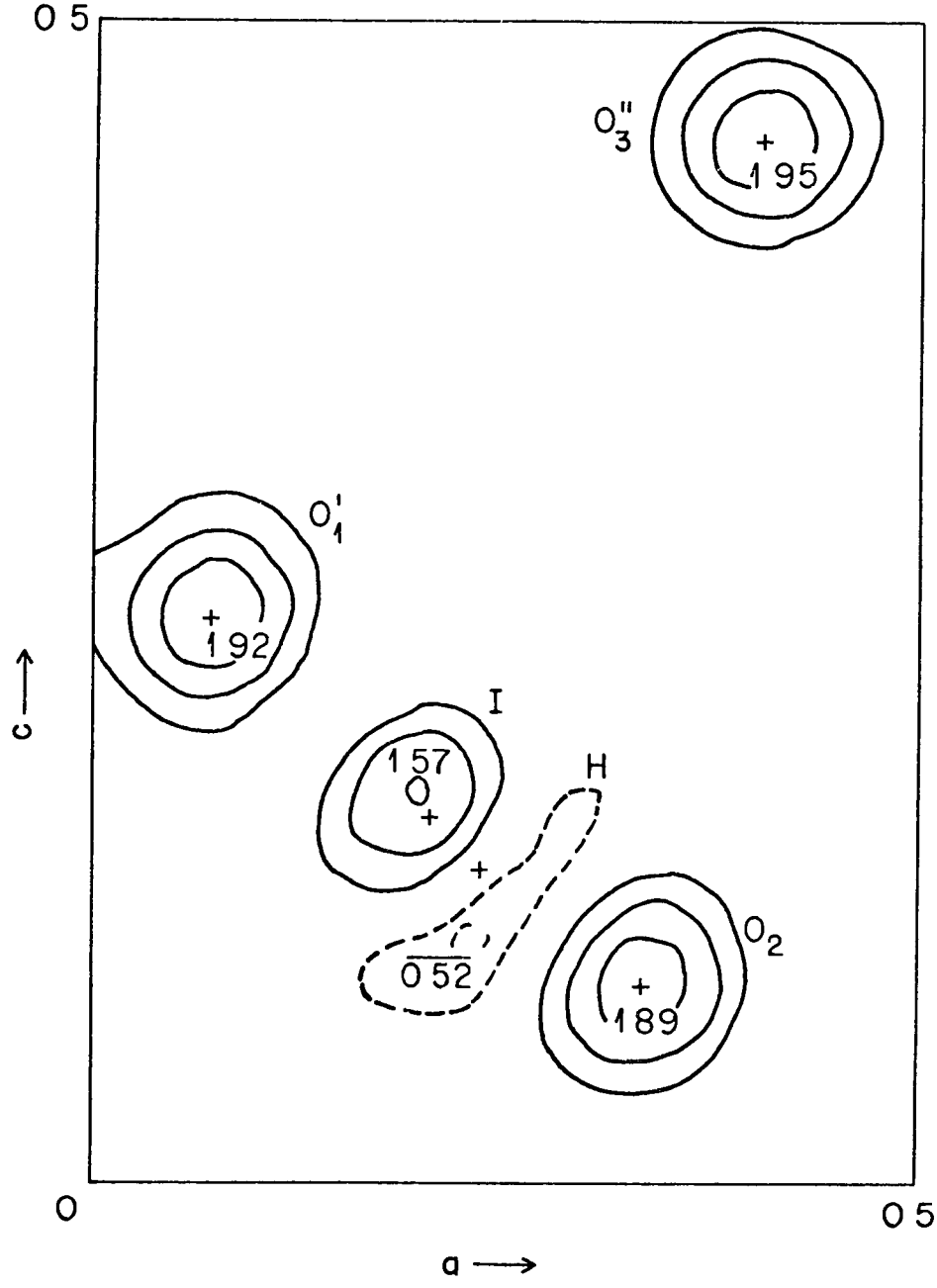

FIG 15

FOURIER MAP OF THE (hOl) PROJECTION
OF ALPHA IODIC ACID

Solid Lines Are Positive Contours at
Intervals of 0 50 x 10^{-12} cm/A^2
Dashed Lines Are Negative Contours at
Intervals of 0 25 x 10^{-12} cm/A^2
Zero Contour Omitted
Crosses Locate Positions of Atoms
Numbers (x 10^{-12}, Indicate Maximum
Values of the Scattering Density

it must be taken to mean that some variable, such as an asymmetric temperature factor for one of the atoms, which was omitted from the least squares, has a strong interaction with the hydrogen temperature factor The final agreement factor was 9 9% with a final x parameter for hydrogen equal to 0 234 and the hydrogen temperature factor of 3 5 or 4 3 The agreement factor was quite insensitive to the change in hydrogen temperature factor

The final x parameters are listed in Table XXVII

Table XXVII

Final x Parameters from (h0l) Projection of Alpha Iodic Acid

Atom	x
H	0.2340
I	0.2036
O_1	0 0712
O_2	0.3340
O_3	0 4043

Calculated and observed structure factors are listed for comparison in Table XXVIII

Table XXVIII

Comparison of (h0l) Structure Factors of Alpha Iodic Acid.

Observed and Calculated Values

Reflections hkl	$\lvert F_{obs} \rvert$	F_{calc}
002	35	- 04
004	1 22	+1 29
006	2.84	-3 01
008	1.27	-1 18
0 0 10	2 69	-2 78
101	1.34	+1 25
102	1.45	-1.43
103	3.90	-4 53
104	.91	+ .91
105	.86	- .75
106	.67	+ 70
107	1.84	-1.73
108	55	+ 65
109	1 78	+1.90
1 0 10	1.58	+1 52
1 0 11	47	- 72
200	.82	+ 72
201	.88	+ 81
202	.78	- 73
203	.34	+ 11

Reflections hkl	$\lvert F_{obs} \rvert$	F_{calc}
204	2.09	+2.08
205	2 07	+2 08
206	1.84	-1 62
207	66	+ .37
208	1 36	+1 32
209	2 18	-1 85
2 0 10	61	- .69
2 0 11	2.37	-2 31
301	.71	+ .73
302	1 13	+1 12
303	1.77	+1 89
304	1.56	+1.46
305	2.98	+2.72
306	1.11	+1.37
307	1.96	-1 89
308	2.30	+2 07
309	1.57	-1 43
3 0 10	1.33	-1.31
400	2.62	-3 01
401	1.94	+2.05
402	1.44	-1 39
403	2.10	+1.76
404	.43	- .01

Reflection hkl	$\lvert F_{obs} \rvert$	F_{calc}
405	1 53	-1 56
406	2 03	+2 05
407	3 25	-3 12
408	.38	+ 53
409	.89	+1 03
501	43	+ 26
502	1 74	+2 00
503	1 73	+1 71
504	1.71	+1 64
505	1 06	-1 21
506	.79	- 56
507	3 13	+3 33
508	0	- 65
600	46	- .52
601	0	+ 07
602	70	+ .86
603	1.83	-1.83
604	2 68	-2 94
605	.66	+ 71
606	86	+ .60
607	1.15	+1 14
701	2.38	-2 51
702	2 51	-2.64

Reflection hkl	|Fobs|	Fcalc
703	1 12	+1 02
704	.96	-1.39
705	38	+ 19
800	2.44	-2 61
801	2.12	-2 43
802	1.11	+1 29

D. Reliability of the Structure

For the reasons discussed in Part One, the average error inherent in the measurements was expected to be two or three per cent, at most The results of the structure analysis showed an average error three or four times this amount, indicating that the analysis had not been carried to the maximum degree of refinement consistent with the reliability of the data

There are at least two factors which were not taken into account in the analysis which may have contributed to the final errors. There is an indication in the slight ellipticity of the contours of the oxygen Fourier peaks that there is some anisotropy in the oxygen thermal motion The same possibility exists for the thermal motion of hydrogen, particularly in the (0kl) projection Omission of consideration of asymmetric motion would have contributed to the lack of agreement in both zones The assumption that extinction was isotropic was probably only partially valid, which would have affected the agreement in the (0kl) zone directly and in the (h0l) zone

indirectly through the z parameters derived from the (0kl) zone

The lack of resolution of the iodine, hydrogen and hydroxyl oxygen atoms made direct analysis of the (h0l) Fourier map impossible The results from the least squares method which was used would have been affected by incorrect assignments of temperature factors, including asymmetric factors, to all three atoms The complexity of handling the computations involved in a multiparameter least squares treatment of this problem precluded a complete analysis

Indications that the extinction correction was not isotropic were found in the large over-corrections of (0 0 10) and (081). The reflection (0 0 10) appeared to show no extinction at all, comparing closely before correction with the calculated value and the value determined in the (h0l) zone

The explanation for the observation of a value of about 0 30 for (002) in both zones, while the calculated value was nearly zero, is not known The structure factor is not sensitive to parameter or temperature variation, and, while weak, was definitely observed in both zones The only suggested explanation available is that the coherent scattering amplitude of iodine is not accurately known This should probably be redetermined with data not involving extinction corrections, however

The effect of the incompleteness of the treatment should have had a nearly random effect on the distribution of errors in the analysis, since there is no obvious direct correlation between

parameters and these sources of error For this reason the statistical estimates of the reliability of the parameters, interatomic distances, and bond angles are believed to be reasonable estimates of their actual reliabilities.

E Precision of Parameters, Interatomic Distances and Bond Angles

Calculations of the precision of parameters and of interatomic distances and bond angles and their precisions were made by the same procedures as described for oxalic acid dihydrate in Part One The standard errors of the x parameters of H, I and O_1 were estimated from the least squares treatment, all others were estimated from the curvatures of the Fourier atomic peaks.

Parameters, interatomic distances and bond angles with estimates of their standard errors are presented in Tables XXIX, XXX, and XXXI respectively

Table XXIX

Final Parameters of Atoms in Alpha Iodic Acid.

Atom	x	y	z
H	0 2340 ± 0 0043	0 3220 ± 0 0015	0 1350 ± 0 0020
I	0.2036 ± 0 0011	0 0861 ± 0 0015	0 1580 ± 0 0010
O_1	0 0712 ± 0 0016	0 5225 ± 0 0011	0 2429 ± 0 0010
O_2	0 3340 ± 0 0014	0 1978 ± 0 0012	0 0864 ± 0 0010
O_3	0 4043 ± 0 0010	0 1566 ± 0 0014	0 4481 ± 0 0010

Table XXX

Interatomic Distances in Alpha Iodic Acid

Atoms	Distance (A)
$H - O_2$	0 990 ± 0 017
$H - O_1'$	1 700 ± 0 018
$H - I$	2 407 ± 0 013
$I - O_1$	1 816 ± 0 010
$I - O_2$	1 899 ± 0 011
$I - O_3$	1 780 ± 0 010
$O_1 - O_2$	2.800 ± 0 010
$O_1 - O_3$	2 769 ± 0 009
$O_2 - O_3$	2 686 ± 0 010
$O_2 - O_1'$	2 685 ± 0 010
$I - O_1'$	2 503 ± 0 011
$I - O_3''$	2 879 ± 0 010
$I - O_3'''$	2 767 ± 0 009

Table XXXI

Bond Angles in Alpha Iodic Acid

Atoms	Angles
$O_1 - I - O_2$	$97^\circ 45' \pm 0^\circ 35'$
$O_1 - I - O_3$	$100^\circ 38' \pm 0^\circ 36'$
$O_2 - I - O_3$	$93^\circ 45' \pm 0^\circ 37'$
$I - O_2 - H$	$108^\circ 15' \pm 1^\circ 33'$
$O_1' - H - O_2$	$172^\circ 56' \pm 3^\circ 0'$

Discussion

A Description of the Structure

The arrangement of the iodine and oxygen atoms deduced by Rogers and Helmholz has been confirmed Their determination of the oxygen parameters in the presence of iodine was remarkably accurate However, their suggestion that the hydrogen bond is bifurcated wasfound to be erroneous; in fact, the suggestion of Wells that there are strings of hydrogen bonds along the b axis was confirmed The three close intermolecular I - O approaches were also confirmed.

The molecule achieves efficient packing with an unusual unit of structure There are chains of rings, sharing a side, along b (Figures 16 and 17), above and below which one kind of oxygen (O_3) projects alternately as the molecule in the chain translates along the two fold screw axis The ring is an approximately planar pentagon, if the hydrogen bond is counted as only one side The ring is composed of the two sides of the O_1 - I - O_2 angle in an HIO_3 molecule, the hydrogen bond between O_2 and O_1'', the I' - O_1'' bond and the 2.50 A approach between O_1 and I' Adjacent rings share one edge and are in the same plane Each O_3 atom above and below the chain approaches two iodine atoms in neighboring chains within 2 77 and 2 88 A, respectively. Neighboring chains are oppositely tilted with respect to the a and c axes. The acute angle between the planes containing the iodine atoms of each chain is $64°25'$.

The cross linking of the chains through iodine-oxygen approaches

UNCLASSIFIED
DWG 21993

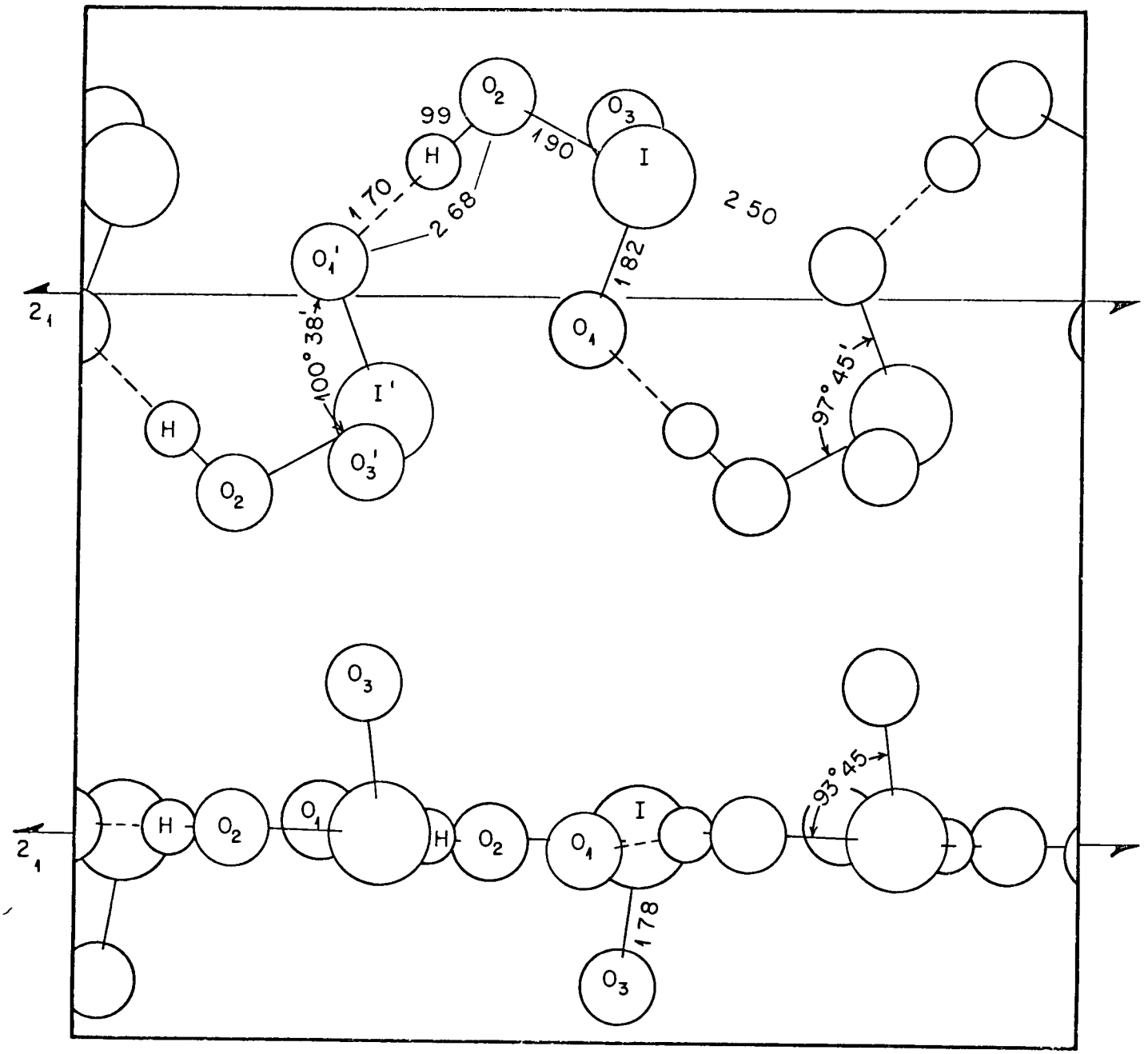

FIG 16

VIEWS OF THE CHAIN OF RINGS IN ALPHA IODIC ACID

Top View Normal to Plane of Iodine Atoms in the Chain
Bottom View in Plane of Iodine Atoms in the Chain
Distances in Angstroms (not Projected)
Dashed Lines Are Hydrogen Bonds
Solid Lines Are Intramolecular Bonds
Dotted Lines Are Close Iodine-Oxygen Approaches
Angles Are Actual (not Projected)

UNCLASSIFIED
DWG 21821

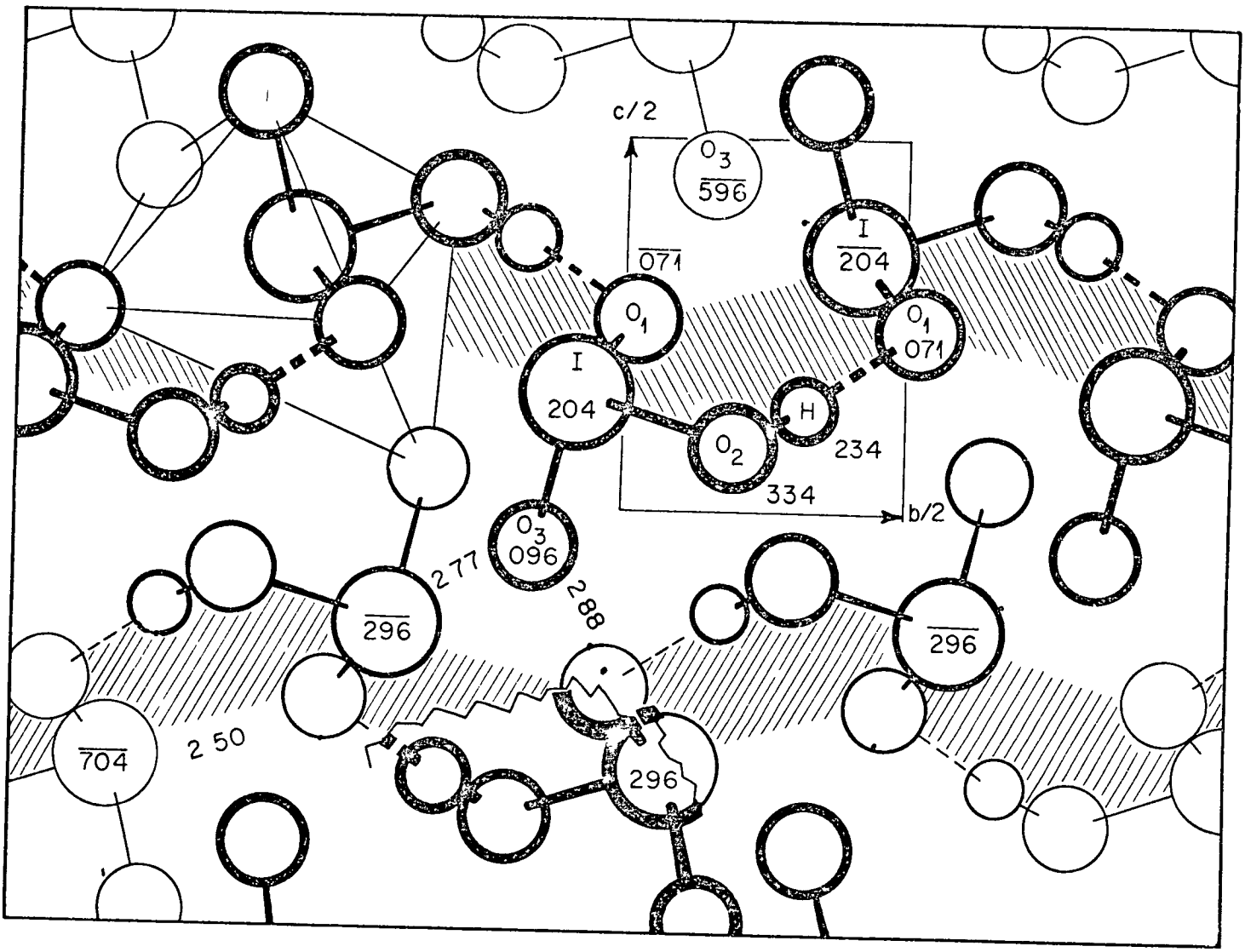

FIG 17

ILLUSTRATIVE DRAWING OF THE (0kl) PROJECTION OF ALPHA IODIC ACID

Shaded Areas Are Planes of Pentagonal Rings Forming Chains
Figure Outlined at Upper Left is Coordination Octahedron Around Iodine (Rogers and Helmholz)
Dashed Lines Are Hydrogen Bonds
Dotted Lines Are Intermolecular Iodine–Oxygen Contacts (Numerals Indicate Interatomic Distances in A)
Heavy Solid Lines Are Intramolecular Bonds
Numerals at Atomic Positions Indicate Elevations in Fractions of the Cell Edge
Positive Direction of a Axis Is out from the Drawing

(Figure 18) is the only apparent important source of cohesion between individual chains The relative weakness of this bonding compared to bonding within the chains is indicated by the pronounced tendency of the crystal to cleave parallel to the b axis

The original description of the structure by Rogers and Helmholz[36] as consisting of IO_3 pyramids of a single HIO_3 molecule, with three intermolecular I - O approaches completing an irregular octahedron about iodine is, of course, correct This octahedron is illustrated in the upper left of Figure 17 It is believed that the structure is more aptly described in terms of the pentagonal linked chains, also illustrated in Figure 17 In this description, the natures of the 2 50 A I - O contact within the chain and the longer I - O contacts between chains are clearly distinguished (Figure 17)

The high density of the material and the absence of other binding forces between chains strongly suggest that the forces between the iodine and oxygen atoms in these approaches are at least weakly attractive The nearly planar arrangement of the pentagonal ring suggests that the forces in the short I - O approach are also attractive, or at least not repulsive The hydrogen bond is the only other important stabilizing element, and it is effective in only one dimension.

In Figure 18 it can be seen that the plane of a chain also nearly includes an O_3 atom from an adjacent chain, hence two planes at an angle of $64^{\circ}25'$ include, to a close approximation, all the

UNCLASSIFIED
DWG 21820

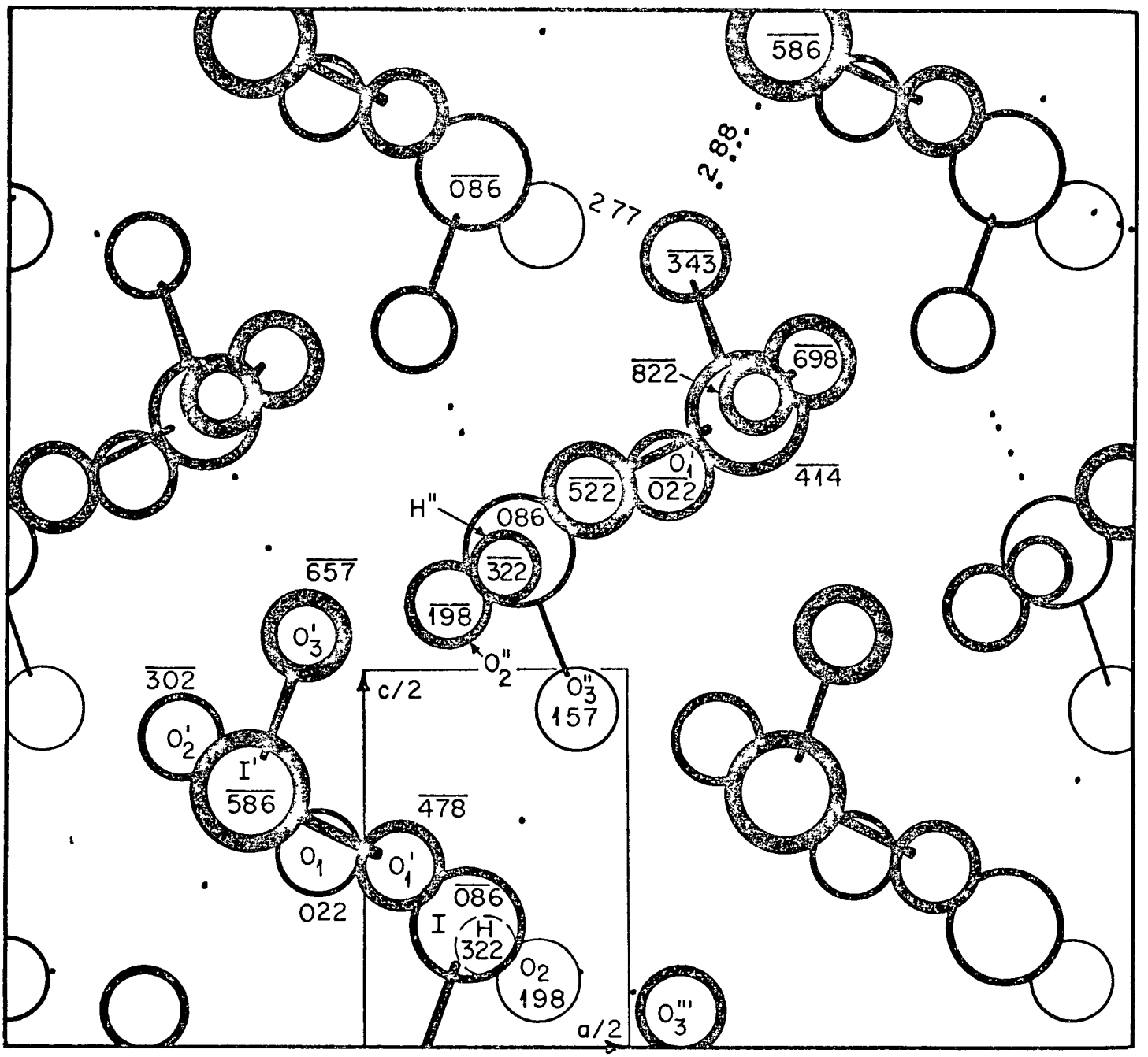

FIG 18

ILLUSTRATIVE DRAWING OF THE (hOl) PROJECTION OF ALPHA IODIC ACID

Dashed Lines Are Hydrogen Bonds
Dotted Lines Are Intermolecular Iodine-Oxygen Contacts
(Numerals Indicate Interatomic Distances in A)
Heavy Solid Lines Are Intramolecular Bonds
Numerals at Atomic Positions Indicate Elevations in Fractions of the Cell Edge
Positive Direction of the b' Axis Is into the Drawing

atoms in the structure This suggests that the crystal should be very strongly birefringent

B Comparison with X-ray Structure

In Table XXXII the values of the parameters obtained by Rogers and Helmholz are compared with those obtained in this investigation.

Table XXXII

Comparison of Parameters of Atoms in Alpha Iodic Acid as Determined by X-ray and Neutron Diffraction

Atom	Parameters	Rogers and Helmholz*	This Investigation
H	x	(0.340)	0.2340 ± 0 0043
	y	(0 300)	0 3220 ± 0 0015
	z	(0 197)	0.1350 ± 0 0020
I	x	0.204 ± 0 002	0 2036 ± 0 0011
	y	-0 088 ± 0 002	-0 0861 ± 0 0015
	z	0 156 ± 0 002	0 158 ± 0 0010
O_1	x	0 068 ± 0 005	0 0712 ± 0 0016
	y	0 534 ± 0 005	0 5225 ± 0 0011
	z	0 250 ± 0 005	0 2429 ± 0 0010
O_2	x	0 340 ± 0 005	0.3340 ± 0 0014
	y	0.195 ± 0 005	0 1978 ± 0 0012
	z	0 090 ± 0 005	0 0864 ± 0 0010
O_3	x	0 407 ± 0 005	0 4043 ± 0 0010
	y	0 170 ± 0 005	0.1566 ± 0 0014
	z	0 447 ± 0 005	0 4481 ± 0 0010

* The significance of the limits of reliability was not given

Only the y and z parameters for O_1 and the v parameter of O_3 differ between the two sets by amounts greater than the estimates of the limits of reliability The two analyses of the structure are otherwise concordant The average temperature factor coefficient found by Rogers and Helmholz, B = 1 0, was intermediate between the values of B_I = 0 75, B_O = 1 3 found in this investigation The non-concordance of the oxygen parameters probably arises from overlap or termination-of-series errors in the x-ray data The oxygen Fourier peaks were generally poorly resolved in the x-ray Fourier maps On the whole the accuracy of the x-ray determination of the oxygen parameters was surprisingly good in view of the dominance of iodine in the x-ray scattering The parameters assigned to hydrogen on the assumption of a bifurcated bond were completely erroneous, however

In Tables XXXIII and XXXIV comparisons of interatomic distances and angles are given

Table XXXIII

Comparison of Interatomic Distances in Alpha Iodic Acid as Determined by X-ray and Neutron Diffraction

Atoms	Rogers and Helmholz*	This Investigation
$I - O_1$	1.81 ± 0.04	1.816 ± 0.010
$I - O_2$	1.89 ± 0.04	1.899 ± 0.011
$I - O_3$	1.80 ± 0.04	1.780 ± 0.010
$O_1 - O_3$	2.78 ± 0.04	2.769 ± 0.004
$O_2 - O_3$	2.78 ± 0.04	2.686 ± 0.009
$O_1 - O_2$	2.75 ± 0.04	2.800 ± 0.010
$I - O_1'$	2.45 ± 0.04	2.503 ± 0.011
$I - O_3''$	2.90 ± 0.04	2.874 ± 0.011
$I - O_3'''$	2.70 ± 0.04	2.767 ± 0.010
$O_2 - O_1'$	2.76 ± 0.04	2.685 ± 0.010

* See footnote to Table XXXII.

Table XXXIV

Comparison of Bond Angles in Alpha Iodic Acid as Determined by X-ray and Neutron Diffraction

Atoms	Rogers and Helmholz	This Investigation
$O_1 - I - O_2$	98°10'	97°45'
$O_1 - I - O_3$	101°25'	100°38'
$O_2 - I - O_3$	95°40'	93°45'

The general agreement between values of interatomic distances and of bond angles was excellent. The difference in values for the

$O_2 - O_3$ distance was a result of the previously noted discrepancy in y parameters found for O_3

C The Iodic Acid Molecule

1 General Description

The original description of the HIO_3 molecule given by Rogers and Helmholz was essentially correct except for the part pertaining to the hydroxyl group The IO_3 group was described as composed of two kinds of I - O bonds, one bond having a small amount of double bond character and two bonds having much greater double bond character The oxygen in the longer bond was correctly presumed to be the hydroxyl oxygen On the basis of the observed O - I - O angles, which were near 100°, the iodine bond orbitals were described as probably having mostly p character with some s character

Their interpretation of the bond lengths is now susceptible to some refinement because of the increased precision with which the oxygen parameters have been determined The conclusion that the $I - O_2$ bond has only a small amount of double bond character is probably correct The observed distance, 1 899 A is only 0 04 A shorter than the sum of the tetrahedral radii of iodine and oxygen[39]. It is not possible to distinguish between shortening because of double bond character or because of ionic character in this case The two shorter I - O bonds, with greater double bond character are now clearly distinguished The length of the $I - O_3$ bond, 1.780 A, is equal to that given by Pauling[39] for a pure double bond

The I - O_1 bond is intermediate in length, 1 816 A Discussion of its bond order is probably not highly significant because of the perturbing influences of the two intermolecular contacts, with hydrogen and iodine, in which O_1 is involved

The hydrogen atom was found to be located 0 989 A from O_2 in the direction of O_1' of an adjacent molecule The short O_2 - O_1' distance, 2 865 A, and the near linearity of the O_2 - H - O_1' links identify this to be the hydrogen bond The relatively small increase in the hydroxyl O - H distance above that in gaseous water, 0 96 A, contrasts with the large increase observed in the carboxyl O - H distance in oxalic acid dihydrate This subject is discussed separately below The I - O - H angle of $108^{\circ}15'$ is in the usual range of oxygen bond angles The observation that the H atom is about 0 06 A out of the plane of I - O_2 - O_1' is in the probably significant range If the I - O_2 bond were a pure single bond, the hydrogen atom would be free to make the nearest approach to O_1' by rotating about the single bond, which would lie in the plane This deviation from planarity is not sufficiently outside the range of insignificance to support arguments as to its cause

2 Electronic Configuration of Iodine

Rogers and Helmholz original conclusion was that the iodine bonding orbitals were of mostly p character, with some s character to explain the increase in observed angles to about 100° A preliminary attempt has been made to correlate information about the electric field gradient at the iodine nucleus, obtained by nuclear

quadrupole spectroscopy, with structural information in order to describe the bonding orbitals more fully.

The nuclear quadrupole spectroscopy experiment furnishes two pieces of information which are directly related to the electronic environment of the iodine nucleus These are the quadrupole coupling and the asymmetry of the field gradient tensor The meanings and relationships of these and related quantities are discussed in detail by Townes and Dailey[40,41], and by Livingston[42]

If placed in the neighborhood of other electric charges, a nucleus having a nuclear electric quadrupole moment, Q, will give rise to an interaction energy which depends on the relative orientation of the nuclear and extranuclear charge systems This interaction is described in terms of the set of second partial derivatives with respect to the coordinates, q_{ij}, of the electric potential at the location of the nucleus The quadrupolar nucleus can take a number of allowed orientations in the q_{ij} system, each with different energies Measurement of the energy of allowed transitions among these energy levels gives the nuclear electric quadrupole coupling, which is essentially determined by the nuclear quadrupole moment, a constant, and the electric field gradient at the quadrupolar nucleus, which is a characteristic of the chemical state of the atom

The electric field gradient produced by a charge distribution $\rho(r)$ is given by the equation

$$\partial^2\phi/\partial s^2 = \int (e\rho(r)/r^3\left[3\cos^2(\underline{r}, \underline{s})-1\right]d\tau$$

where ϕ is the electric potential, $\underline{s}$ is the direction in which the electric field gradient, $\partial^2\phi/\partial s^2$, is measured, e is the electronic charge and $\rho(r)$ the charge density in the element $d\tau$ at the position denoted by $\underline{r}$ The electric field gradient will have large values when $\rho(r)$ is large at small values of $\underline{r}$ It is a tensor quantity which is determined by five independent components Townes and Dailey have shown that the gradient from orbitals for which the electronic distribution probabilities are high near the nucleus, and which are not spherically symmetric, will be large The contributions from p orbitals are usually the most important in determining the total gradient at a nucleus Townes and Dailey[41] have found that a 5d electron is equivalent to only 0.14 5p electrons in its contribution to the field gradient

The electric field gradient arising from any hybridized orbital can be calculated from the linear combination of the contributions of each of the atomic p and d orbitals used This electric field gradient is resolved in the principal axis system of the orbital, with its major axis in the direction of the maximum extension of the orbital in space. When more than one bond to the quadrupolar atom involves orbitals which contribute to the total electric field gradient, which is a tensor quantity, the gradients from each bond must be resolved in a single axis system so that the tensor elements may be added The resulting tensor may then be diagonalized to the principal axis system of the total gradient, with only components

$\phi_{xx}, \phi_{yy}, \phi_{zz}$

The second quantity measured by nuclear quadrupole spectroscopy is the asymmetry of the electric field gradient By convention

$$\phi_{yy} \leq \phi_{xx} \leq \phi_{zz}$$

and the asymmetry, η, is defined as

$$(\phi_{xx} - \phi_{yy}) / \phi_{zz}.$$

The asymmetry is a measure of the departure from cylindrical symmetry on the electric field gradient

The problem at hand was to determine whether or not a set of orbitals could be found which would be consistent with the observed values of bond angle and lengths, and observed values of the quadrupole coupling was found to be equivalent to a net unbalance of about one-half a 5p electron by comparison with atomic iodine[43] The asymmetry was found to be 0 4505, the largest yet observed

Calculations were carried out for a model involving some simplifying assumptions The model assumed was an IO_3 group consisting of one single I - O bond at an angle of 96° to two equivalent double bonds The angle between double bonds was taken to be the $O_1 - I - O_3$ angle observed experimentally, 100°38' The three Σ bonds were assumed to be s-p hybrids and the two π bonds to have pure d character.

A set of sp hybrid Σ orbitals was found for which the angle between the single and double bonds was 96°4' and that between double bonds was 102°15'. The net unused 5p orbital was equal to

0 40 electrons

The π bonds were assumed to be best d orbitals, which make a mutual angle of $54^{\circ}44'$, and to be each perpendicular to one of the bonds of the double bonds This defined their orientation with respect to the three Σ bonds

The quadrupole coupling in units of p electrons was calculated for each bond in its own principal axis system For the Σ bonds it was proportional to the p character of the bond The coupling for each π bond was equal to 0 14 p electrons. The five tensors were resolved into a single axis system The direction of the single bond was taken as the z axis, the x axis was perpendicular to and the y axis was in the plane of symmetry between the double bonds. The individual tensors were resolved in this axis system by application of the rules for transforming the second derivatives of a scalar quantity The individual elements of the five tensors were added to give a non-diagonal tensor expression for the resultant quadrupole coupling This tensor was diagonalized by rotation of axes to the principal axis system of the electric field gradient The resulting components relative to a 5p electron contribution as unity, are:

$$\phi_{zz} = 493, \quad \phi_{xx} = -247, \quad \phi_{yy} = -246$$

and the asymmetry, η, is close to zero

The value of 0 493 5p electrons for ϕ_{zz} corresponds to the observed value of about one half, but the calculated asymmetry is

clearly in disagreement with the observed value of 0 4505 This solution was apparently unique for the model chosen, since no other choices could be made which were consistent with the assumptions made and the observed structural features

The effects of types of bonds other than purely covalent were then considered Qualitative considerations indicated that ionic character in the single bond might affect the asymmetry considerably without appreciably changing the magnitude of the quadrupole coupling A calculation was carried out in which the single bond was assumed to have 20% ionic character in addition to the previous assumptions. The resulting components relative to a 5p electron are

$$\phi_{zz} = 0\ 526, \quad \phi = -0.346, \quad \phi = -0\ 180$$

and the asymmetry = 0 32

These two calculations are sufficient to show that a set of hybridized bond orbitals can be found which is consistent with the observed quantities, the electric field gradient, the asymmetry of the electric field gradient tensor, and the bond lengths and angle However, it is probable that a unique assignment of bond orbitals cannot be made with the information available because it is not possible to take into account all of the important independent variables Some of these, in addition to ionic character in the single bond, include ionic character in the double bonds and the actual non-equivalence of the double bonds, which was ignored in the model.

It is also probable that other assumptions about the types of hybridization involved in the Σ and π bonds would lead to a consistent set of hybridized orbitals Qualitatively it appears that a model with Σ bonds of spd hybridized orbitals and π bonds of pure p character might be such an alternative starting point It is possible, however, that experimental determination of the directions of the principal axes of the electric field gradient tensor would permit a choice between different models such as these two.

D Hydrogen Bond Lengths

Rundle and Parasol[44] noted a strong correlation between OH stretching frequencies and the distance of the O - O approach in a number of hydrogen bonded compounds They observed that the stretching frequency was quite sensitive to the O - O distance below about 2 7 A, varying from 3600 cm^{-1} for the 2 9 A, approach in oxalic acid dihydrate to 1775 cm^{-1} for the 2 44 A approach in nickel dimethylglyoxime On the basis of finding only one N - O stretching frequency they concluded that the hydrogen atom in nickel dimethylglyoxime was centered.

The O - H and O - O distances and O - H stretching frequencies for several compounds are given in Table XXXV

Table XXXV

O - H and O - O Distances in Hydrogen Bonds

Compound	Distance (A) O-H	O-O	O-H Stretching Freq (cm^{-1})
H_2O (gas)	0.96[35]		3650 (sym) 3755 (unsym)
Ice (D_2O)	1 01[45]	2.76	
KH_2PO_4	1.08[46]	2 48	2400
KH_2AsO_4	1 06[47]	2 52	
KD_2AsO_4	1.03[47]	2 52	
$(COOH)_2$ $2H_2O$			
1 carboxyl-water	1 06	2.52	
2 water-carboxyl	0 96	2 85	3600
Alpha HIO_3	0 99	2.68	
Ni-dimethyl glyoxime	1 22[48]*	2 44	1775

* One half of O - O distance, based on proposed certered hydrogen

It is observed that there is a regular increase in the O - H distance as the O - O distance decreases This is correlated with the observed decrease in O - H stretching frequency. The observed stretching frequency for the H_2O molecule in oxalic acid dihydrate is very close to those in gaseous water, confirming the conclusion from the diffraction data that the molecule is essentially unperturbed in the crystal The O - H and O - O distances in KH_2PO_4 are close to those in the hydrogen bond between the water oxygen and carboxyl hydrogen in oxalic acid dihydrate, indicating that a stretching frequency near 2400 cm^{-1} would be expected for the carboxyl O - H

The O - H distance in alpha iodic acid is abnormally short according to these criteria If the O - O distance were the only parameter, an O - H distance between 1 06 A observed in KH_2AsO_4 and the 1 01 A in deutero-ice would be expected On the basis of the isotopic substitution effect observed in the two arsenate compounds, the lower limit would probably be nearer 1 03 A than 1 01 A It is suggested that participation in other bonds by the acceptor oxygen in a hydrogen bond may influence the relationship between O - H and O - O distances, particularly in cases where the two oxygens are chemically non-equivalent In particular it is believed that the close involvement of the acceptor oxygen in iodic acid with a neighboring iodine atom reduces its effectiveness as a hydrogen acceptor It is predicted that the O - H stretching frequency in alpha iodic acid should be greater than predicted by the relationship of Rundle and Parasol, probably in the vicinity of 3000 cm^{-1}.

Bibliography

1 Elsasser, W M , Compt rend 202, 1029-30 (1936).

2. Halban, H , Jr , and Preiswerk, P , J Phys Radium 8, 29-40 (1937).

3 Mitchell, D P and Powers, P N , Phys Rev 50, 486-7 (1936)

4. Halpern, O and Johnson, M H , Jr , Phys Rev 55, 898-923 (1939).

5 Breit, G , and Wigner, E , Phys Rev 49, 519-31 (1936)

6 Breit, G , Phys Rev 58, 506-37 (1940).

7 Weinstock, R , Phys Rev 65, 1-20 (1944)

8 Shull, C G and Siegel, S , Phys Rev 75, 1008-10 (1949).

9 Zachariasen, W H , Z Krist A89, 442-7 (1934).

10 Robertson, J M , and Woodward, J , J Chem Soc 1936, 1817-24 (1936)

11. Brill, R , Hermann, C , and Peters, C , Ann Physik 42, 357-77 (1942)

12. Dunitz, J D , and Robertson, J M , J Chem Soc 1947, 142-147 (1947)

13. Ahmed, F R and Cruickshank, D W J , Acta Cryst 6, 385-392, (1953)

14. Booth, A D , Nature, London, 156, 51-2 (1945)

15 Cruickshank, D W J , Acta Cryst 5, 511-18 (1952).

16. Richards, R E and Smith, J A S , Trans Faraday Soc 47, 1261-74 (1951)

17. Marignan, R , Bull Soc Chim Fr., 352 (1948).

18 Groth, P , "Chemische Kristallographie", Leipzig, (1917), Vol III, p 138

19 Wollan, E O and Shull, C G , Phys Rev 73, 830-41 (1948)

20 Levy, H A and Peterson, S W , to be published

21 Peterson, S W and Levy, H A , J Chem Phys 19, 1416-18 (1951)

22 "International Tables for the Determination of Crystal Structures", Gebruder Borntrager, Berlin, (1935), Vol II, p 584

23 Bacon, G E , and Lowde, R D , Acta Cryst , 1, 303-14 (1948)

24 Wilson, A J C , Acta Cryst 2, 318-21 (1949)

25. Waser, J and Schomaker, V , Rev Mod Phys 25, 671-90 (1953)

26 Carpenter, G B and Donohue, J , J Am Chem Soc 72, 2315-28, (1950)

27. Harker, D and Kasper, J S , Acta Cryst 1, 70-5 (1948)

28. Grison, E , Acta Cryst 4, 489-90 (1951)

29 Hughes, E W , J Am Chem Soc 63, 1737-52 (1941)

30 Cruickshank, D W J , Acta Cryst 2, 154-7 (1949).

31. Finbank, C , and Norman, N , Acta Chem. Scand 2, 813-27 (1948)

32. McWeeny, R , Acta Cryst 4, 513-9 (1951)

33 Cox, E G , Dougill, M W and Jeffrey, G A , J Chem Soc 1952, 4854-63 (1952).

34 Jeffrey, G A , and Parry, G S , J Chem Soc 1952, 4863-67 (1952)

35. Dennison, D M , Rev Mod Phys 12, 175 (1940).

36 Rogers, M T , and Helmholz, L., J Am Chem Soc 63, 278-84 (1941)

37 Wells, A F , Acta Cryst 2, 128-9 (1949)

38. Groth, P , "Chemische Kristallographie", Vol I, p 125, Leipzig (1917).

39. Pauling, L "The Nature of the Chemical Bond", 2nd ed , Ithaca, N Y , Cornell Univ Press (1944).

40. Townes, C H, and Dailey, B P, J Chem Phys 17, 783-96 (1949)

41. Townes, C H, and Dailey, B P, J Chem Phys 20, 35-40 (1950).

42 Livingston, R, Science 118, 61-66 (1953)

43. Livingston, R, and Zeldes, H, to be published

44 Rundle, R E, and Parasol, M, J Chem Phys 20, 1487-8 (1952)

45 Peterson, S W, and Levy, H A, Bull Am Phys Soc 28, No. 5, p 10 (1953)

46. Levy, H A, Peterson, S W, and Simonson, S H, J Chem Phys. 21, in press

47. Levy, H A, and Peterson, S W, to be published

48 Godycki, L E, and Rundle, R E, Acta Cryst 6, 487-95 (1953)

Acknowledgement

The author gratefully acknowledges the guidance and inspiration given him by Dr R R Edwards of the University of Arkansas and by Dr H A Levy of the Oak Ridge National Laboratory He also wishes to express his appreciation for the financial and other assistance afforded him by the Oak Ridge Institute of Nuclear Studies through their Graduate Fellowship Program